UNIVERSIDADE FEDERAL DE PERNAMBUCO
CENTRO DE CIÊNCIAS DA SAÚDE
PROGRAMA DE PÓS-GRADUAÇÃO EM ODONTOLOGIA

LUANA OSÓRIO FERNANDES

TOMOGRAFIA POR COERENCIA OPTICA NA AVALIAÇÃO DE TECIDOS PERIODONTAIS E DE RESTAURAÇÕES LAMINADAS

Recife
2019

LUANA OSÓRIO FERNANDES

TOMOGRAFIA POR COERENCIA OPTICA NA AVALIAÇÃO DE TECIDOS PERIODONTAIS E DE RESTAURAÇÕES LAMINADAS

Tese apresentada ao Programa de Pós-Graduação em Odontologia da Universidade Federal de Pernambuco, como requisito parcial para obtenção do título de Doutorado em Odontologia.

Área de concentração: Clínica Integrada.

Orientador: Prof. Dr. Anderson Stevens Leônidas Gomes

Recife

2019

Catalogação na Fonte
Bibliotecária: Mônica Uchôa, CRB4-1010

F363t Fernandes, Luana Osório.
Tomografia por coerência óptica na avaliação de tecidos periodontais e de restaurações laminadas / Luana Osório Fernandes. – 2019.
138 f.: il.; 30 cm.

Orientador: Anderson Stevens Leônidas Gomes.
Tese (Doutorado) – Universidade Federal de Pernambuco, CCS. Pós-graduação em Odontologia. Recife, 2019.

Inclui referências, apêndices e anexos.

1. Diagnóstico por imagem. 2. Tomografia de coerência óptica. 3. Gengiva. 4. Doenças periodontais. 5. Facetas dentárias. I. Gomes, Anderson Stevens Leônidas (Orientador). II. Titulo.

617.6 CDD (20.ed.) UFPE (CCS2019-177)

LUANA OSÓRIO FERNANDES

TOMOGRAFIA POR COERENCIA OPTICA NA AVALIAÇÃO DE TECIDOS PERIODONTAIS E DE RESTAURAÇÕES LAMINADAS

Tese apresentada ao Programa de Pós-Graduação em Odontologia da Universidade Federal de Pernambuco, como requisito parcial para obtenção do título de Doutorado em Odontologia.

Aprovado em: 18 /02 /2019

BANCA EXAMINADORA

_____
Profa. Dra. Renata Cimões Jovino Silveira (Examinador Interno)
Universidade Federal de Pernambuco

_____
Prof. Dr. Luiz Alcino Gueiros (Examinador Interno)
Universidade Federal de Pernambuco

_____
Prof. Dr. Alexandre Batista Lopes do Nascimento (Examinador Externo)
Universidade Federal de Pernambuco

_____
Prof. Dr. Emery Lins (Examinador Externo)
Universidade Federal de Pernambuco

_____
Prof. Dr. Sergio de Lemos Campello (Examinador Externo)
Universidade Federal de Pernambuco

À minha mãe, minhas irmãs e meu esposo por todo o amor e cumplicidade.

AGRADECIMENTOS

A **Deus**, por sempre estar presente na minha vida.

A meus pais **Antonio Lucas** e **Maria dos Anjos,** especialmente a minha mãe por ser um exemplo de pessoa, superando todas as intempéries da vida sem perder a luz, a bondade e dedicando tanto amor as suas filhas.

As minhas irmãs **Lana, Liana e Priscila**, pelo profundo amor, carinho, amizade e respeito que compartilhamos.

A meu esposo **Rodrigo Brito,** por todo amor e apoio incondicional nas minhas aventuras, que em todos os momentos acreditou no meu sucesso e comigo viveu e suportou todas as incertezas. Te amo muito.

Aos meus sogros **Sidinha e Ribamar**, por me adotarem como filha e incentivarem meu crescimento tanto pessoal quanto profissional.

Aos meus cunhados **Daniele, Gustavo, Lilian, Romulo, Batista e Rubens**, minha eterna gratidão por todos os momentos que me permitiram viver com vocês como irmãos que se tornaram.

Aos meus sobrinhos **Olívia, Gustavo e Lucas**, pela luz que vocês promovem na minha vida.

A toda minha família, em especial a **Tia Elza,** minha segunda mãe, e **Vovó Mazé**, por serem tão importantes e presentes na minha vida.

Ao meu orientador **Prof. Anderson Gomes**, pela atenção, dedicação e paciência, por ter aceitado ser meu orientador. Seu amor à docência é contagiante, e me fez tomá-lo como um exemplo a ser seguido.

As amigas **Claudia Brainer** e **Luciana Afonso**, sempre solícitas a me ajudar. Vocês foram fundamentais para elaboração deste trabalho. Tenho gratidão eterna a vocês, obrigada por tudo.

A Família **Labfoton** que me acolheu de forma muito especial, fortalecendo amizades antigas e cativando novas. Em especial à **Tereza, Vanda, Daniela, Mariana, Cecília, Monica, Gisele Camboim, Ana Michele, Evair, Audrey, Emery e Bismarck**, pelo apoio e amizade.

As amigas **Patricia Fernandes** pela amizade que perdura por todos esses anos e **Ana Paula** pelo apoio incondicional e trabalho conjunto em busca do mesmo ideal. Toda a minha gratidão.

Aos **colegas de turma**, em especial a **Rafaella Maria e Monica** pela amizade e companheirismo. Foi muito satisfatório poder conviver com vocês.

Aos **professores da pós-graduação** pelos ensinamentos.

Ao **Prof. Claudio Heliomar** e a **Profa. Renata Pedrosa,** pelas parcerias e por proporcionar a minha participação na formação dos alunos da Clínica Integral 1 (noturno). Vocês foram fundamentais para meu crescimento profissional e pessoal.

Aos amigos **Cynthia, Diogo, Natalia, Camille, Caio, Anderson, Camylla, Soriano, Patricia, Michelle, Fabricia, Pamella**. Obrigada pelos anos de amizade e carinho, de maneira tão particular! O tempo passa e nossos laços de amizade são renovados e fortalecidos.

As minhas irmãs de farda, **Glaucyane, Ludmilla, Marcella, Samantha, Paula, Amélia, Thassia, Livia,** pela amizade, apoio, conselhos e torcida. Nunca imaginei que poderia formar um elo tão forte numa situação tão desafiadora.

Aos **voluntários** que contribuíram de forma significativa para a execução do trabalho.

A todos vocês MUITO OBRIGADA!

RESUMO

A Tomografia por Coerência Óptica (OCT) é uma técnica de geração de imagens, com alta resolução espacial, utilizada na avaliação da microestrutura interna de materiais e tecidos biológicos, medindo a luz que é refletida e retroespalhada em tempo real, de modo não invasivo e sem emitir radiação ionizante. As suas características podem apresentá-la como uma estratégia alternativa ou complementar ao diagnóstico. Apesar de suas vantagens, a técnica ainda não é utilizada clinicamente na Odontologia. O objetivo deste trabalho foi aplicar a ténica de OCT em situações distintas nas especialidades de Periodontia e Dentística, analisando as possibilidades de aplicação da técnica no âmbito clínico. Foi realizada a avaliação do comportamento do tecido gingival *in vivo e ex vivo*. Outro ponto abordado, foi a perspectiva de inclusão do OCT como uma nova categoria de sondas periodontais, as sondas biofotônicas. Foi realizado o monitoramento de restaurações laminadas investigando sua adaptação e integridade através de captura de imagens *in vivo*. Os artigos contidos na tese abordam os resultados promissores obtidos e reforçam a relevância e a contribuição para obtenção de um diagnóstico precoce e preciso. Os resultados permitiram concluir que a Tomografia por Coerência Óptica é um método eficaz para a análise dos tecidos periodontais e de tratamentos restauradores, permitindo o diagnóstico preciso, de maneira não invasiva. Porém, algumas limitações precisam ser superadas para sua utilização na clínica odontológica, tais como o custo de equipamento, aumento no poder de penetração, melhoria do contraste e o desenvolvimento de software para permitir processamento das imagens em tempo real.

Palavras-chave: Diagnóstico por imagem. Tomografia de Coerência Óptica. Gengiva. Doenças Periodontais. Facetas Dentárias.

ABSTRACT

Optical Coherence Tomography (OCT) is a high spatial resolution imaging technique used to evaluate the internal microstructure of biological materials and tissues, measuring light that is reflected and backscattered in real time, in a non-invasive manner and without emitting ionizing radiation. Its characteristics can present it as an alternative strategy or complementary to the diagnosis. Despite its advantages, the technique is still not used clinically in dentistry. The objective of this work was to apply the technique of OCT in different situations in the specialties of Periodontics and Dentistry, analyzing the possibilities of application of the technique in the clinical scope. The evaluation of gingival tissue behavior in vivo and ex vivo was performed. Another point addressed was the prospect of including OCT as a new category of periodontal probes, the biophotonic probes. Monitoring of laminated restorations was performed investigating their adaptation and integrity through in vivo imaging. The articles in the thesis address the promising results obtained and reinforce the relevance and contribution to obtain an early and accurate diagnosis. The results allowed to conclude that Optical Coherence Tomography is an effective method for the analysis of periodontal tissues and restorative treatments, allowing a precise diagnosis, in a noninvasive way. However, some limitations need to be overcome for use in the dental clinic, such as equipment costs, increased penetration power, contrast enhancement, and software development to enable real-time image processing.

Keywords: Diagnostic Imaging. Tomography, Optical Coherence. Gingiva. Periodontal Diseases. Dental Veneers.

LISTA DE ILUSTRAÇÕES

SUMÁRIO

1 INTRODUÇÃO

O exame clínico odontológico é considerado como padrão para avaliação da saúde oral, e quando necessário é associado a radiografias no intuito de auxiliar o clínico na tomada de decisão. Na periodontia, o diagnóstico é realizado a partir da avaliação clínica periodontal, podendo ser associada à tomada radiográfica para verificação do osso de suporte[1]. Na dentística, a inspeção visual e as imagens radiológicas são rotineiramente utilizadas como ferramentas de diagnóstico para a detecção de alterações com sinais e/ou sintomas clínicos. As técnicas de imagem empregadas na clínica odontológica seguem a linha tradicional da utilização de radiação X que, apesar de suas vantagens, não fornecem resolução, sensibilidade e contraste suficientes para detectar alterações em estágios inicias nos tecidos orais[2]. A especificidade e a sensibilidade desses métodos ainda são insatisfatórias e a detecção de defeitos é geralmente afetada por um atraso de tempo, uma vez que o diagnóstico só é possivel após a visualização de manifestação clínica[3,4].

A necessidade de realização de tratamentos mais simples e minimamente invasivos alavancam a busca por métodos alternativos de diagnóstico. As técnicas ópticas despertam interesse por propiciarem uma análise com poucos efeitos adversos e por permitir avaliação de áreas não contempladas pelos exames tradicionais, identificando alterações de forma precoce[5].

Os métodos ópticos de diagnóstico tem o intuito de capturar imagens de forma não invasiva empregando radiação não ionizante. As pesquisas na área têm como objetivo tentar extrapolar para o âmbito clínico a utilização de dispositivos ópticos ou acústicos, tais como: ultrassom[6], sonda óptica baseada em LED[7], microscopia confocal[8], espectroscopia de infravermelho e a tomografia por coerência ótica[9].

A tomografia por coerência ótica (OCT, acrônimo inglês de Optical Coherence Tomography) é um dos métodos mais promissores na investigação de alterações teciduais nas ciências da saúde[10]. OCT permite a formação de imagens dos tecidos biológicos com alta resolução espacial, sensibilidade, precisão de detalhes anatômicos e preservação da integridade da região avaliada, sem exposição à radiação ionizante[11]. A técnica possibilita a realização de biópsia óptica, podendo detectar precocemente alterações e patologias[12], como câncer[13], cáries[14] e doenças periodontais[15]. A simplicidade na aquisição das imagens, o monitoramento em tempo

real e a reprodutibilidade da técnica indicam a provável viabilidade clínica para exame e quantificação dos tecidos orais[16].

Na clínica odontológica, o exame tátil e o visual dependem da sensibilidade do examinador, além de ser difícil o acompanhamento da evolução entre as sessões[17]. Por isso especialidades odontológicas necessitam de alternativas na identificação de alterações e o OCT desponta como um método promissor no diagnóstico de modificações antes do surgimento de sinais clínicos[18-20]. Nos últimos anos, inúmeras pesquisas foram realizadas aplicando OCT na identificação e evolução de alterações em tecidos orais moles e duros e no comportamento de materiais restauradores[21-24]. As imagens obtidas podem orientar a escolha da melhor intervenção clínica, viabilizando ainda mais a aplicação dos preceitos de uma Odontologia minimamente invasiva.

Esta tese aborda uma revisão de literatura sobre a Tomografia por Coerência Ótica e sua utilização como método diagnóstico *in vivo* em Periodontia e Dentística. Segue como parte integrante do trabalho os artigos publicados no Journal of Biophotonics (apêndice A), nos Proceedings of SPIE (apêndices B, C e D) e submetido na Journal of Dentistry (apêndice E), contendo metodologia, resultados e discussão acerca do tema abordado.

1.1 TOMOGRAFIA POR COERÊNCIA ÓPTICA

A Tomografia por Coerência Óptica é uma técnica de imagem óptica não destrutiva de alta resolução para a criação de imagens transversais de tecidos duros e moles em tempo real[25]. O método utiliza as propriedades de espalhamento e reflexão associado a uma fonte emissora de luz para transmitir informações de diferenças estruturais a um detector coleta dos dados[26].

A tecnologia foi utilizada pela primeira vez em 1991 para aquisição de imagens transversais não invasivas em sistemas biológicos[11], e desde então, o sistema evoluiu e se tornou bem estabelecido na medicina, especialmente no campo da Oftalmologia[27,28]. Na Odontologia, há muitos relatos sobre o uso do OCT principalmente no diagnóstico de alterações teciduais, como em regiões de dentes e do periodonto[16,20,21,29,30].

OCT usa interferometria de baixa coerência para produzir uma imagem bidimensional de espalhamento óptico a partir de microestruturas internas do tecido

avaliado, de forma análoga à imagem ultrassônica de eco de pulso[11]. O método consegue alcançar resoluções espaciais longitudinais e laterais em escala micrométrica e tem a capacidade de detectar frações extremamente pequenas dos sinais refletidos[31,32], no qual é possível identificar e diferenciar detalhes e particularidades estruturais de tecidos, pois sua capacidade vai além do alcance dos microscópios ópticos confocais tradicionais[11, 33].

O OCT pode produzir imagens com uma resolução de até 20 μm, uma ordem de magnitude maior em comparação com o ultrassom e sua profundidade de penetração normalmente varia entre 1 e 3 mm, dependendo do tipo de tecido[34]. Nos tecidos biológicos, a técnica permite construir imagens das estruturas numa faixa de até 3mm abaixo da superfície, a depender do índice de refração do meio analisado e consequentemente da estrutura da matriz extracelular e da morfologia celular[35]. As imagens obtidas são mapas topográficos apresentadas em esquemas de falsas cores, no qual observa-se áreas de alto sinal de retroespalhamento (cores claras) e de baixo sinal de retroespalhamento (cores escuras).

OCT apresenta vantagens quanto ao baixo custo em relação a outras técnicas de imagem da mesma categoria, a alta resolução espacial e a profundidade de penetração[36]. As imagens obtidas de forma não invasiva e a ausência de radiação ionizante permitem sua utilização *in vivo*. Porém, existem algumas barreiras que precisam ser superadas pela técnica, tais como a melhoria do contraste das imagens e a não compensação entre resolução transversal e profundidade do foco[37,38,39].

1.1.1 Mecanismo de Funcionamento

A interferência é um fenômeno físico no qual há sobreposição de duas ou mais ondas resultando em uma onda de maior ou menor amplitude. A interferometria óptica é gerada por ondas de luz que se propagam num dado meio e apresentam alguma correlação entre si, através da identificação do maior comprimento de coerência da fonte óptica em relação a diferença de percurso óptico entre dois feixes de luz[26].

Existem vários tipos de interferômetros, porém o mais utilizado é o Interferômetro de Michelson devido à sua versatilidade e facilidade de construção. Esse dispositivo foi desenvolvido em 1881, com o objetivo de identificar a existência do éter e já foi aplicado na verificação do efeito do éter na velocidade da luz, detecção

de ondas gravitacionais, identificação de planetas em torno de estrelas próximas e na espectroscopia de transformada de Fourier[40].

Para o seu funcionamento, um feixe de luz incidente atravessa um espelho semitransparente (divisor de feixes), e será desmembrado em duas partes iguais e independentes. Cada parte irá em direção a um espelho plano específico, isto é, um feixe segue para um espelho fixo (objeto) e o outro para um móvel (amostra)[41]. Ao encontrar os devidos espelhos, os feixes são refletidos e tornam a se recombinar no divisor de feixes. As informações são captadas por um fotodetector permitindo a identificação de diferenças de fase entre eles, já que percorreram caminhos ópticos diferentes, decorrentes de um atraso temporal entre as ondas de referência e do objeto[42].

O interferômetro de Michelson permite identificar a diferença entre os caminhos ópticos dos feixes, o índice de refração, variações no caminho geométrico e a aferição de comprimentos de onda com grande precisão. O sinal captado pelo fotodetector é resultado da sobreposição da reflectividade da amostra biológica. Com a associação do seccionamento óptico longitudinal e o transversal, há a construção de mapas tridimensionais com resoluções longitudinais e transversais micrométricas. Nesse contexto, surge a nomenclatura tomografia[10,43].

A coerência é uma característica primordial para identificar a existência de interferência entre duas ondas, detectado pela invariabilidade da relação entre as fases das ondas e o tempo[26]. OCT é um método de aquisição de imagem que utiliza a interferometria de baixa coerência produzida por feixes de luz coerentes, através da coleta de informações advindas das medidas das franjas de interferência (claras e escuras) para determinar precisamente distâncias e espessuras muito pequenas[41]. A luz de baixa coerência é produzida por uma fonte de banda larga, gealmente próximo da faixa de luz infravermelho (~800nm - 1300nm), que é acoplada ao interferômetro de Michelson. O próprio feixe óptico de baixa coerência, ilumina a amostra e executa o seccionamento óptico transversal do objeto, através do deslocamento do espelho de referência do interferômetro, resultando na formação de imagens de forma não invasiva, com elevada resolução espacial e em tempo real. Assim, o OCT é extremamente sensível à luz que sofreu um ou poucos eventos de dispersão, durante o retroespalhamento[41,44]. O fracionamento óptico é semelhante à biópsia tradicional de tecidos biológicos, porém de modo virtual, sem invasividade, por isso o OCT é considerado uma biópsia óptica[28,45].

1.1.2 Formação das imagens

O tempo de atraso da onda refletida é usado pelo OCT para medir a profundidade da estrutura-alvo, princípio semelhante ao do ultrasom[46]. Os espalhamentos causados pelas diferenças estruturais nos tecidos analisados interferem na intensidade da interferência observada, ou seja, a luz é retroespalhada de maneira diferente frente a índices de refração distintos[47]. As maiores interferências são observadas em áreas com maior poder de reflexão, não ocorrendo interferência se o feixe luminoso possuir um atraso maior que o comprimento de coerência.

A terminologia em imagens segue a mesma da ultrassonografia. Porém, no OCT um perfil de profundidade traz informações sobre a variação do índice de refração óptica dentro do tecido[48]. A varredura em profundidade de um único ponto, ou seja, a variação na medida de espalhamento em relação à profundidade, é chamada de “A-scan” (Amplitude Scan). Também conhecido como varredura axial, contém informação unidimensional da posição axial das estruturas dentro da amostra[49,50]. Os dados de cada A-scan são apresentados em um gráfico de refletividade em função da profundidade. A terminologia e o sistema de coordenadas dos planos de imagem de Tomografia por Coerência Óptica pode ser observada na figura 1. O eixo z corresponde à coordenada axial (profundidade), enquanto que os eixos x e y correspondem a coordenadas laterais (transversais).

Figura 1 - Terminologia de planos de imagem de Tomografia por Coerência Óptica.

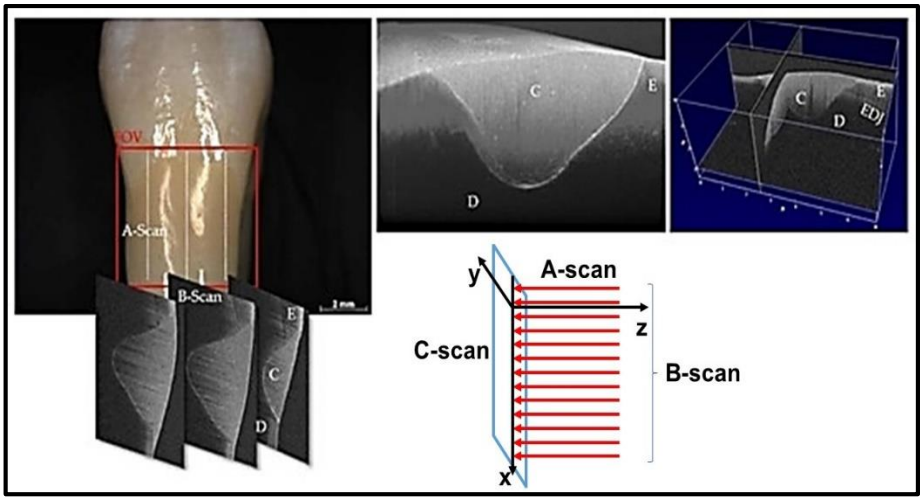

Fonte: Adaptado de SCHNEIDER *et al*, 2017.

O B-scan (Brilho Scan) é composto por uma coleção de A-scans adjacentes, tomadas linearmente em uma direção transversal. A varredura transversal produz informações de uma ‘fatia’ de tecido dentário, que é o tomograma[51]. As imagens transversais são bidimensionais e correspondem ao plano de imagem xz, permitindo a avaliação tanto da profundidade quanto do aspecto lateral do objeto[52].

Para imagens volumétricas são utilizados múltiplos B-scans sequenciais formando um vetor de valores de refletância. T-Scan ou varredura en-face é produzido por um feixe que varre o objeto transversalmente, mantendo um ponto de referência fixo. A varredura coronária ou C-Scan se dá após uma varredura em uma direção transversal do plano xy, ou seja, é uma coleção de muitas varreduras T transversais[48,52]. Diferentes cortes transversais são captados para diferentes profundidades, quer avançando a diferença de trajeto óptico em etapas após cada varrimento transversal completo, ou continuamente a uma velocidade muito mais lenta[49].

1.1.3 Resolução das imagens

Para a formação das imagens utilizando o OCT, são formados mapas de reflexão da amostra através da realização de múltiplas varreduras. A coerência da luz emitida pela fonte é o fator primordial para determinação da resolução axial, mantendo alta resolução de profundidade. A resolução axial é a propriedade que permite distinguir os limites e os diferentes tipos celulares de acordo com o comprimento de coerência da fonte de luz[10]. Em geral quanto menor for a coerência da luz utilizada, maior é a resolução longitudinal do OCT[11].

A Figura 2 mostra a representação esquemática da resolução espacial e profundidade de penetração e velocidade de aquisição de imagens da técnica de Tomografia por Coerência Óptica em comparação com outras modalidades de imagem. O OCT possui uma maior resolução para a mesma profundidade de penetração quando comparado ao ultrassom e as imagens obtidas apresentam uma similaridade com cortes histológicos.

Figura 2- Comparação do OCT com outros métodos de diagnóstico por imagem.

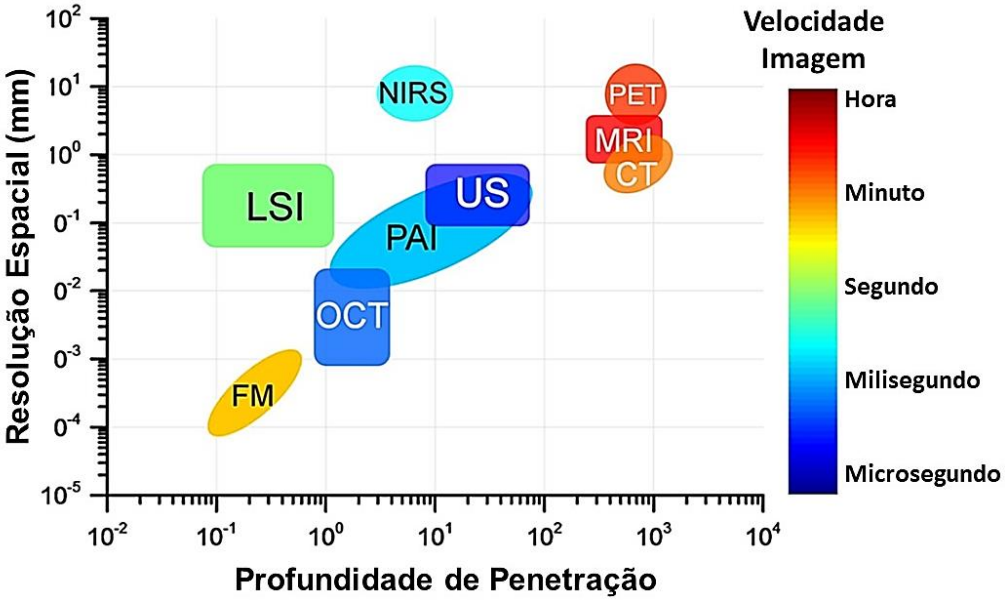

Fonte: Adaptado de ZHU *et al*[53].

As características da imagem de OCT dependem do comprimento de onda utilizado[54]. A profundidade da imagem é determinada pelas especificações de iluminação e detecção, mas é geralmente limitada pelo espalhamento e dependente do comprimento de onda da amostra[41]. Com isso, elevados comprimentos de onda, entre 800 a 1325nm, proporcionam aquisição de imagens de regiões mais profundas, por estarem dentro da janela óptica de tecidos vivos[55].

OCT possui uma capacidade de penetração em profundidade de até 3 mm, limitada principalmente pelo espalhamento óptico[26], resultando numa imagem com resolução espacial de até 20 μm[31,32]. A resolução axial é determinada pelo comprimento de coerência da fonte de luz, e quanto maior a largura de banda espectral, maior a resolução axial. Uma alta resolução axial no tecido é alcançada ao utilizar uma fonte de alta potência[54].

A dispersão de luz pelo tecido é determinada pela variação espacial do índice de refração que, por sua vez, é resultado da estrutura e organização do tecido. Sabe-se que a variação do índice de refração no tecido exibe propriedades fractais devido à grande variedade de tamanhos de dispersores presentes no tecido, alterando a resolução das imagens[56-59]. Quando a luz é focada no tecido, as não homogeneidades dos índices de refração fazem com que a luz se espalhe em ângulos diferentes.

Devido a sua alta resolução, capacidade de imagem não invasiva e livre de contato, o OCT é adequado para uso clínico e intraoperatório[60].

Autores como Liu *et al*[61] reforçam a importância de aumentar a resolução dos sistemas de OCT para a aquisição de imagens em áreas de difícil manejo, para a detecção, diagnóstico e monitoramento de doenças em órgãos luminais. Para isso é necessário utilizar fontes de luz com comprimentos de onda mais curtos e com larguras de banda mais amplas para melhorar a resolução axial e a lateral. Porém, essa manipulação aumenta o grau de espalhamento em comprimentos de onda mais curtos, limitando a penetração da luz e, consequentemente, diminui bastante a profundidade da imagem.

1.1.4 Tipos de OCT

Os primeiros sistemas de OCT foram baseados na tecnologia do domínio do tempo (TD-OCT), que empregavam um braço de referência móvel, operavam em velocidades bastante baixas de até 400 A-scan/s e possuíam resolução limitada de até 10 µm. Esses fatos dificultaram seu emprego, limitando sua utilização clínica e aceitação geral[41]. O TD-OCT utiliza uma fonte de luz de baixa coerência de banda larga e o atraso no percurso de referência é medido de forma repetitiva, alterando a posição do braço de referência para detectar a interferência entre o caminho de referência e os sucessivos locais de difusão na amostra[26,34]. No sistema TD-OCT apenas um único ponto de volume da estrutura de retroespalhamento da amostra é registrado por vez[48].

A técnica evoluiu após a implementação do domínio de Fourier (FD-OCT, do inglês Fourier Domain Optical Coherence Tomography)[62,63] que utiliza um espectrômetro ou um filtro de frequência sintonizável no lugar do detetor para análise espectral do sinal interferométrico, medindo a luz interferida do domínio de Fourier[63]. Esse fato proporcionou o aumento da velocidade de acquisição da imagem, uma melhoria na sua qualidade decorrente da maior densidade de pixels, além de possibilitar a aquisição de imagens tridimensionais[64].

O FD-OCT utiliza a transformação de Fourier, uma operação matemática, para converter as medições da luz interferida em atrasos físicos ou distâncias[34]. O FD-OCT é capaz de medir toda a luz decorrente de diferentes atrasos, atingindo resoluções

axiais próximas de 2 μm (com fontes de luz avançadas) e velocidade de aquisição de imagem entre 26.000 e 1.700.000 Ascans/s[64,65].

Sistemas FD-OCT subdividem-se em duas categorias distintas: OCT de fonte de varredura (Swept-source OCT, SS-OCT) e OCT de domínio espectral (SD-OCT). Os dois modos são baseados na interferometria de baixa coerência, porém o SS-OCT usa uma fonte laser de banda estreita e de varredura sintonizável, enquanto que o SD-OCT utiliza um diodo superluminescente (fonte de luz contínua e banda larga)[26].

A fonte luminosa utilizada no SD-OCT emite uma ampla gama de comprimentos de onda. Nesse sistema utiliza-se um espectrômetro e uma CCD (acrônimo em inglês para “Charge-coupled Device) linear para detecção da luz difusa que é lida digitalmente em alta velocidade[64]. A taxa de A-scan é determinada pela exposição e pelo tempo de leitura da câmera de varredura linear. No entanto, a resolução das imagens é limitada pela resolução espectral do detector[66].

O laser utilizado no SS-OCT emite um único comprimento de onda e varre uma ampla faixa de comprimentos de onda em função do tempo. O espectro de interferência é detectado por um único fotodetector cuja saída é digitalizada à medida que o comprimento de onda é varrido, gerando A-scan de acordo com o fluxo de varredura da fonte de luz[63]. SS-OCT utiliza fontes de luz com comprimento de onda acima de 1000 nm, operando em velocidades iguais ou maiores que 100 kHz[67], permitindo a visualização simultânea de diferentes estruturas e em tempo real[60].

A melhoria das características ópticas e a evolução do sistema aumentou o potencial de uso do OCT na área da saúde[23] e, novas alterações funcionais foram desenvolvidas, tais como o Doppler OCT (D-OCT) [68], sistemas de OCT sensíveis à polarização OCT (PS-OCT) [69], OCT endoscópico[38] e OCT acústico[70], visando promover um aumento na eficiência de diagnóstico pelo OCT.

1.1.5 Biópsia Óptica

Uma biópsia convencional é um processo em que uma amostra de tecido é removida do corpo, passa por um processamento químico, e uma fina fatia de tecido é seccionada e lida ao microscópio óptico por um patologista. A imagem fornecida na avaliação histológica do tecido é invasiva, pois há necessidade de cortá-lo para que possa ser realizada a avaliação.

As imagens obtidas com OCT são semelhantes ao corte histológico-padrão, o que facilita sua interpretação[71,72]. A ferramenta possui a capacidade de obter imagens em reconstrução de alta resolução de uma amostra de tecido com qualidade idêntica a uma “amostra viva” que é colocada sob o microscópio, porém sem a necessidade de preparo do espécime[12].

Evidências experimentais mostram que mudanças sutis entre células de câncer pré-invasivas comparadas às células normais[73], e entre células apoptóticas comparadas a células necróticas[74], podem ser detectadas pela técnica através da medição das propriedades de espalhamento da amostra [73,74].

O conceito de biópsia óptica partiu de experimentos realizados por Fujimoto e equipe, após o uso do OCT para obtenção de imagens da retina ocular[11, 75]. Iniciou-se uma verdadeira revolucão no diagnóstico de retinopatias, permitindo a detecção prematura de problemas estruturais nas camadas retinais, *in vivo*, em tempo real, de forma não invasiva, por seccionamento óptico de finas fatias da retina[31].

Em 2013, Abignano *et al*[76] publicaram um estudo no qual realizam a validação e comparação de imagens histológicas com as de OCT, visando avaliar o potencial clínico da técnica na identificação de alterações cutâneas decorrentes da esclerodermia. A figura 3 mostra a comparação de imagem histológica (a) da pele de paciente saudável com B-scan (b) e A-scan (linha verde) obtidos com o OCT. Em seu estudo, os pesquisadores usaram um dispositivo capaz de produzir imagens de alto contraste de pele com até 2 mm de profundidade e resoluções de 4 a 10 µm. Os autores concluíram que a imaginilogia da pele com o OCT poderia oferecer uma medida de resultado quantitativa viável e confiável da esclerodermia, podendo funcionar como um valioso biomarcador da patologia. Pode-se observar no A-scan médio das imagens de OCT um ponto mais baixo do vale no que corresponde à junção dermo-epidérmica claramente visível em ambas as imagens. Observou-se um segundo pico no A-Scan médio, que correspondeu à região mais superficial da derme papilar.

Figura 3 - Comparação de imagem histológica (a) da pele de paciente saudável com B-scan (b) e A-scan (linha verde) obtidos com o OCT.

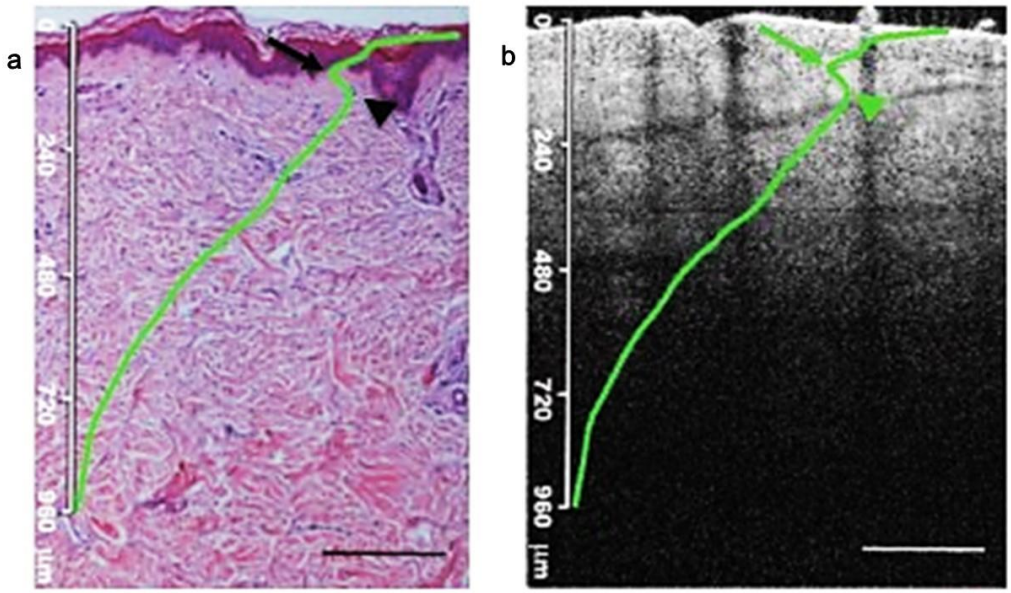

Fonte: Adaptado de ABIGNANO *et al*[76]

Um estudo prospectivo para diagnósico de tumor cerebral, utilizou amostras neurocirúrgicas de 18 pacientes na avaliação de imagens 3D obtidas por OCT de campo total (FF-OCT), com resolução de 1 μm e com profundidade de penetração de cerca de 200 μm. Foi possível identificar o parênquima epiléptico crônico temporal e tumores cerebrais, além de uma subpopulação de neurônios, fibras mielínicas e vasculatura do SNC. O estudo relatou o potencial da técnica como uma ferramenta intraoperatória para determinar a arquitetura e o conteúdo do tecido em poucos minutos, viabilizando a identificação de características de tecidos não tumorais e tumorais, com boa correspondência com as lâminas histológicas[77].

Alguns estudos relatam o uso do OCT na avaliação do perfil de refletividade do tecido, em tempo real, e a capacidade de diferenciar tecido saudável de doente[78], bem como a celularidade tecidual[79,80]. Para facilitar a sua utilização, podem ser implementados no OCT, peças de mão, fibra ótica, cateteres para avaliação da microestrutura do tecido intersticial em escala micrométrica e determinar sua celularidade. A técnica pode ainda ser utilizada para orientação de biópsias excisionais, em que a sonda OCT é incorporada dentro de uma pistola de biópsia feita sob medida, que permite a digitalização da área através do orifício da agulha de biópsia para avaliar a composição do tecido na ponta da agulha antes de sua retirada.

Esta tecnologia tem o potencial de melhorar a taxa de sucesso dos procedimentos de biópsia[81]. Iftimia *et al*[81] testaram uma tecnologia baseada em OCT para avaliar a celularidade tecidual na ponta da agulha durante a biópsia, alcançou precisão geral de 85% na diferenciação entre três tipos de tecido (tumor homogêneo, tecido heterogêneo e tecido muscular normal). A presença de regiões tumorais heterogêneas foi detectada com sucesso em todos os casos e confirmada pelos resultados histopatológicos. Entretanto, mais pesquisas precisam ser realizadas para que haja melhoraria da precisão da diferenciação tecidual.

Outro ponto de relevância clínica para realização da biópsia óptica com OCT está na sua dependência de fatores, tais como alta resolução, alta velocidade de obtenção da imagens e contraste adequado para discriminar as diferenças teciduais[82].

1.1.6 Aplicações de OCT na Odontologia

Os tecidos da cavidade oral são passíveis de escaneamento por OCT, pois possuem diferentes níveis de transparência, característica primordial para a interação da luz e captura de informação das estruturas[11]. O OCT foi inicialmente utilizado na odontotologia em 1998[21], com o desenvolvimento de um protótipo e para adquisição de imagens de tecidos dentários *in vivo*, demonstrando o potencial da técnica no diagnóstico da doença periodontal, detecção de cáries e avaliação de restaurações dentárias. A evolução da técnica permitiu investigação de potenciais áreas de aplicação do OCT na Odontologia.

O desafio do diagnóstico da cárie em fases muito precoces promoveu a busca por métodos mais eficazes e o OCT se destaca por apresentar imagens com fácil identificação da extensão axial e lateral de diferentes zonas desmineralizadas nas lesões cariosas, mesmo em estágio subclínico[24]. Wijesinghe *et al*[83] avaliaram quantitativamente o volume, a espessura e a profundidade de lesões cariosas para quantificar o esmalte residual utilizando o SD-OCT de 1,3 μm e observaram que é possivel monitorar a perda mineral e sua progressão. Os autores verificaram que havia uma diminuição da reflexibilidade na região da lesão cariosa relacionada à perda mineral.

A técnica OCT tem o potencial de caracterizar morfologicamente e monitorar cáries, inclusive cáries de radiação, além de parece ser um método mais confiável e

preciso que as radiografias interproximais na detecção e estimativa da profundidade das lesões proximais no ambiente clínico[14].

OCT também pode ajudar a diferenciar cárie radicular de lesões cervicais não cariosas[84], além de permitir a detecção de fissuras em esmalte[85]. Marcauteanu *et al*[86] utilizaram imagens 2D e 3D para avaliar o potencial do SS-OCT como uma ferramenta para monitorar a evolução dinâmica do desgaste dentário patológico em lesões cervicais não cariosas artificiais. Foi observada a alta capacidade técnica da ferramenta para mensurar a perda de tecido dentário com um volume de 2352 μm^3 a 32.352 μm^3, adquirido com 25,000 A-scans em 2,5 segundos.

A adaptação das restaurações cerâmicas são o fator mais importante para avaliar o sucesso das coroas. Li *et al*[87] utilizaram o SD-OCT como método de identificação de gap marginal em coroas de dissilicato de lítio, e comprovaram sua eficácia no diagnóstico não invasivo de restaurações cerâmicas. Turk *et al*[88] utilizaram o método para investigar as adaptações marginais e internas de restaurações inlays de cerâmica cimentadas em cavidades classe I de pré-molares superiores humanos e concluíram que a técnica pode ser utilizada para avaliar quantitativamente a adaptação de restaurações cerâmicas.

As imagens podem ser empregadas para monitorar o processo de falha em interface adesiva, analisar o crescimento de microfissuras por fadiga dinâmica[89], bem como identificar e avaliar dos estratos que compõem a restauração[90,91]. De acordo com Shimada *et al*[92], ainda é possível detectar defeitos dentro das restaurações a partir da análise das imagens tomográficas, sintetizadas com base no sinal de retroespalhamento no interior da restauração. Todor *et al.*[93] avaliaram o comportamento de cerâmicas odontológicas em próteses metalocerâmicas sinterizadas com diferentes temperaturas com OCT e identificaram, de maneira rápida, que alterações decorrentes de temperaturas acima da ideal são prejudiciais à integridade da prótese, pois promovem o estresse da cerâmica, defeitos no corpo do material e fraturas no interior das camadas cerâmicas das próteses fabricadas e inseridas na cavidade bucal.

OCT pode ser utilizado na identificação de alterações na mucosa bucal e poderia ser um método de identificação de alterações epiteilais e subepiteiais ao longo da carcinogênese[69]. Heidari *et al.* [13] avaliaram de forma cega a performance de um sistema de OCT móvel na identificação de áreas de mucosa bucal saudável, com displasia e malignidade em imagens bidimensionais de 20 pacientes com lesões orais

suspeitas e 10 indivíduos saudáveis. Os autores observaram o melhor desempenho do OCT em relação à análise realizada por inspeção visual. Tsai *et al.*[94] utilizaram um SS-OCT para observar diferentes estágios de carcinogênese oral e concluiram ser possível diagnosticar e diferenciar as fases displásicas e de carcinoma da mucosa oral normal.

Imagens de OCT podem fornecer uma avaliação dos tecidos adjacentes implante, podendo identificar os primeiros sinais de inflamação, mesmo antes de as alterações clínicas se tornarem evidentes[95]. Ajuda na visualização do sulco do implante em duas e três dimensões e também fornece informações valiosas sobre a interrelação do tecido mole do implante[52]. Bordin *et al* (2017) avaliaram alterações perimplantares através de avaliação histológia e de imagens obtidas com um protótipo de OCT para odontologia. Os autores observaram que tanto nas imagens de OCT quanto nas histológicas, foi possível visualizar um desarranjo interno no tecido perimplantar, mesmo na ausência de sinais clínicos de inflamação e perda de osso alveolar. A tecnologia pode ajudar na detecção e monitoramento de alterações estruturais dos tecidos periodontais moles, fornecendo imagens da microarquitetura tecidual.

Gladkova *et al.* [96] analisaram a capacidade de polarização cruzada do OCT (CP-OCT) no diagnóstico dos tecidos moles bucais em 35 indivíduos com implantes dentários e 30 indivíduos com doenças inflamatórias intestinais, mostraram a boa capacidade da técnica no diagnóstico de patologias dos tecidos moles da cavidade oral, uma vez que foi possivel detectar precocemente doenças inflamatórias do intestino pelo estado da mucosa oral e a visualização precoce da gengivite em indivíduos com fenótipo gengival fino que possuiam implante.

Características como a boa profundidade de penetração e a alta resolução das imagens tornam o OCT uma boa boa ferramenta para o diagnóstico periodontal, permitindo uma rápida visualização da estrutura superficial do tecido gengival, reproduzindo suas características específicas em diferentes seções da cavidade oral e morfologia das bolsas[18]. Medições quantitativas em imagens de OCT podem ser amplamente aplicadas para diagnosticar o estado periodontal, o nível de inserção gengival[15], determinar a espessura gingival[29], características do tecido epitelial e conjuntivo, a posição da crista óssea alveolar[97] e a presença de calculo dental[98], bem como para avaliar o grau de regeneração gengival[99]. Fernandes *et al*[30] avaliaram a performance do OCT na identificação de estruturas periodontais *in vivo*, após

avaliação de 23 individuos saudavéis, comparativamente com dois tipos de sondagem (manual e computadorizada). A análise das imagens permitiu identificar regiões anatômicas periodontais relevantes e determinar uma profundidade média do sulco gengival. Os autores reforçam o potencial do OCT ser uma ferramenta confiável para avaliação de tecidos periodontais *in vivo* e para medidas de profundidade de sulcos reprodutíveis em locais saudáveis.

Em um estudo preliminar, Baek *et al.*[100] estimaram a utilidade da técnica para avaliar o comportamento do ligamento periodontal durante o movimento dentário sob tração e compressão leves, ao utilizar forças de distração ortodôntica (0, 5, e 10 g) aplicadas aos incisivos inferiores de 6 ratos brancos (10 semanas de idade), durante 5 dias, usando molas de loop individualizadas. Os autores relatam que é possível avaliar com precisão as alterações do ligamento periodontal mediante forças ortodônticas utilizando o OCT, podendo medir os ligamentos alterados a partir de todas as direções, diferentemente das radiografias.

1.1.7 Outras Características Relevantes do OCT

Apesar dos pontos já mencionados, OCT apresenta algumas limitações. O alto custo dos componentes eleva o valor da máquina OCT, tornando-o caro quando produzida para comercialização. DSOUZA *et al*[36] desenvolveram e validaram um sistema portátil de SD-OCT, de baixo custo, que contém um hardware óptico associado a um espectrômetro, uma sonda portátil e um laptop. Além disso, este sistema utiliza um mosaico único em tempo real das imagens de vídeo de superfície que são sincronizadas com rápida aquisição de A-scans (10kHz), permitindo a construção de imagens transversais em distâncias laterais estendidas, utilizando lente com distancia focal de 60 mm. A resolução axial medida se deteriora com maiores profundidades de imagem (acima de 2 mm) e as melhores imagens obtidas *in vivo* foram a uma profundidade de até 1,5 mm. Todo o sistema pesa 9 kg e custa USD$ 8.000 (comparado com USD$ 40.000-60.000 para sistemas atualmente comercializados) usando componentes prontos para uso, porém ainda necessita de algumas evoluções.

É necessária a realização de mais pesquisas visando aumentar o poder de penetração óptica, melhorar o contraste entre os componentes da imagem e desenvolver um software com algoritmos para análise de imagens, visando um

processamento simultâneo em tempo real[69]. Algumas alternativas estão sendo pesquisadas, como os agentes de compensação óptica, para melhorar a visibilidade de estruturas biológicas pelo aumento da profundidade de penetração nos tecidos e diminuição da dispersão da luz. Em estudo recente Yang *et al*[101] afirmam que os agentes de compensação óptica podem aumentar o desempenho do OCT, melhorando significativamente a imagem das raízes dentárias. Braz *et al*[102] utilizaram nanoparticulas de ouro como agente de aumento de contraste para imagens de OCT em odontologia e observaram a melhoria na qualidade de imagem, elevando o grau de identificação das estruturas dentárias.

2 OBJETIVOS

2.1 GERAL

Avaliar a capacidade do OCT operando em 1325 nm, na captação de dados quantitativos e qualitativos a partir de imagens e relacionar esses dados com propriedades estruturais dos tecidos orais e de materiais restauradores.

1.2 ESPECÍFICOS

I. Avaliar o OCT como método de sondagem óptica;
II. Identificar nos tomogramas o fenótipo gengival e diferenciação entre gengiva livre e inserida;
III. Monitorar com OCT as alterações de tecidos moles decorrentes da terapia periodontal não-cirúrgica;
IV. Monitorar com OCT o reparo tecidual em pacientes submetidos à cirurgia plástica periodontal;
V. Avaliar a integridade da linha de cimentação de laminados nas imagens de OCT;
VI. Investigar a integridade e adaptação de laminados cerâmicos e pré-fabricados de resina com auxilio do OCT.

3 METODOLOGIA

3.1 ESTUDO 1 - COMPARATIVE ANALYSIS OF GINGIVAL PHENOTYPE IN ANIMAL AND HUMAN EXPERIMENTAL MODELS USING OPTICAL COHERENCE TOMOGRAPHY IN A NON-INVASIVE APPROACH.

Publicado: International Society for Optics and Photonics, 2015; doi: 10.1117/12.2180856.

Este artigo descreveu as etapas de estudos para validação do OCT na avaliação periodontal usando modelos animais (ex vivo) e pacientes.

3.1.1 Aspectos éticos

A fase ex vivo com mandíbulas suínas foi realizada após aprovação pela Comissão de Ética no Uso de Animais (Centro de Biociências da Universidade Federal de Pernambuco) sob processo número 23076057216 / 2013-91.

A fase do estudo com pacientes, por sua vez, foi conduzida após aprovação pelo Comitê de Ética e Pesquisa Envolvendo Seres Humanos da Universidade de Pernambuco, sob parecer 858.202 (ANEXO A).

3.1.2 Espécimes de animais

Para o estudo em animais, cinco mandíbulas suínas frescas obtidas de um matadouro local foram dissecadas, seccionadas e armazenadas em solução de formalina a 10% por 24 horas antes das análises, a fim de preservar a estrutura dentária e correspondentes tecidos ósseo e periodontal. Imagens foram obtidas de incisivos inferiores, pré-molares e molares e suas estruturas periodontais.

As amostras foram analisadas usando um sistema SS-OCT de domínio de Fourier operando a 1325 nm (OCS1300SS Swept Source OCT System, Thorlabs Inc, Nova Jersey, EUA) e Estereomicroscópio (Stemi 2000-C, ZEISS, Alemanha), como padrão-ouro.

O SS-OCT em 1325 nm foi escolhido devido ao comprimento de onda central mais longo que permite imagens de penetração em maior profundidade e,

principalmente, em função da maior velocidade na aquisição de imagens, um fator essencial para o cenário clínico. O comprimento de onda central da fonte de laser de varredura é de 1325 nm, com largura de banda espectral > 100 nm, largura de banda instantânea de 0,13 nm ou 0,5 GHz, taxa de varredura axial de 16 kHz, potência média de 10 mW e 100 dB de sensibilidade. As imagens geradas constituem matrizes com 2000 colunas (pixels por linha no eixo X) e 512 linhas (pixels por coluna no eixo Y), perfazendo 6 mm de varredura transversal e 1,3 mm de profundidade no ar. Foram capturadas imagens bidimensionais e tridimensionais. Após a análise das amostras com OCT, os dentes e seus tecidos periodontais e ósseos correspondentes foram seccionados ao longo do eixo sagital, da face vestibular à lingual, utilizando discos flexíveis de diamante 7075 (KG Sorensen, São Paulo, Brasil) sob refrigeração com água, para posterior análise por estereomicroscopia. As imagens foram obtidas diretamente a partir da superfície seccionada com uma lente ocular 10x fornecendo ampliação de 6,5x a 50x, com 35,4 mm a 4,6 mm de campo de visão e distância de trabalho de 92 mm, acoplada a uma câmera CCD com resolução nominal de 1,3 µm.

3.1.3 Análise de Pacientes

Para o estudo clínico observacional, um total de 30 pacientes, de ambos os sexos, com saúde periodontal e presença de dentes anteriores, foram examinados usando o mesmo sistema OCT empregado no estudo animal, SS-OCT a 1325 nm e sondagem periodontal controlada por computador (Florida Probe Corporation, Flórida, EUA).

Foram utilizados os critérios de inclusão: idade entre 18 a 65 anos; indivíduos com saúde periodontal determinada por profundidade de sondagem ≤ 3 milímetros e sangramento à sondagem < 25 %; presença de dentes anteriores. Como critérios de exclusão: mulheres gestantes; indivíduos analfabetos ou com distúrbios que comprometessem a compreensão ou a adesão aos exames e preenchimento das escalas; utilização de prótese fixa ou móvel, recessão gengival nas faces vestibular ou proximal, restaurações cervicais e utilização de aparelho ortodôntico fixo na região dos dentes anteriores.

A unidade amostral foi o sítio dental, em cada paciente, apenas 3 sítios dos dentes anteriores foram avaliados (mesiovestibular, médiovestibular, distobucal), o que resultou em 445 locais disponíveis para o estudo. Para garantir os registros de

profundidade do sulco em uma posição padronizada, foi utilizado um stent de acrílico fabricado individualmente. Três sulcos foram feitos para determinar os locais mesio-vestibular, médio-vestibular e disto-vestibular para imagem e sondagem. Para realização do exame de OCT, os pacientes permaneceram sentados, com a cabeça apoiada em posicionador específico, perpendicular ao feixe de luz emitida. Além disso, utilizou-se um afastador labial para melhor visualização da área a ser estudada.

A aquisição de imagens relacionadas aos sítios foi realizada utilizando o OCT, e as informações foram armazenadas no formato jpeg. Posteriormente, as imagens foram analisadas para cada local e as profundidades de sondagem foram obtidas por meio do ImageJ (Processamento e Análise de Imagens em Java, National Institutes of Health, Bethesda, MD). Imediatamente após o escaneamento por OCT, os pacientes foram submetidos ao exame de sondagem periodontal dos sítios vestibulares, demarcados na moldeira-guia, utilizando sonda de pressão controlada Florida Probe.

3.1.4 Análise dos Resultados

As imagens foram analisadas qualitativamente quanto à identificação das seguintes estruturas: margem gengival, gengiva livre e inserida, superfície dentária, sulco gengival, presença de cálculo/ biofilme, junção amelodentinária e amelocementária.

3.2 ESTUDO 2 - OPTICAL COHERENCE TOMOGRAPHY FOLLOW-UP OF PATIENTS TREATED FROM PERIODONTAL DISEASE

Publicado: Journal of biophotonics, 2018; doi: 10.1002/jbio.201800209

Este artigo consistiu no monitoramento de pacientes encaminhados ao Centro de Especialidades Odontológicas (CEO) para atendimento na clínica de Periodontia, previamente diagnosticados com doença periodontal crônica e presença de bosla em região vestibular dos dentes anteriores. As avaliações foram realizadas antes da primeira intervenção no CEO, e após 30, 60 e 90 dias, visando observar as alterações dos tecidos moles e deposição de cálculo e biofilme.

3.2.1 Desenho do estudo e triagem populacional

O estudo observacional *in vivo* foi aprovado pelo Comitê de Ética da ASCES-UNITA (1.235.385, Anexo B). Um total de 147 sítios vestibulares de 49 dentes em 14 pacientes com idade entre 18 e 65 anos (seis homens com média de 46 anos e oito mulheres com idade média de 36 anos) foram avaliados. Estes sítios eram referentes aos dentes anteriores, nos pontos mésio-vestibular, médio-vestibular e disto-vestibular de cada um. Os voluntários deste estudo eram pacientes encaminhados para tratamento no Centro de Especialidades Odontológicas/Periodontia da Faculdade de Odontologia, ASCES-UNITA (Centro Universitário Tabosa de Almeida), Pernambuco, Brasil. Todos os pacientes foram submetidos à terapia periodontal básica e foram avaliados em quatro momentos: dia 0 (antes da primeira intervenção clínica), dia 30, dia 60 e dia 90, utilizando a imagem de OCT, sonda manual e sonda automatizada. Excepcionalmente, um paciente foi avaliado 1 ano após o tratamento. Foram excluídos os pacientes tabagistas, grávidas, com recessão gengival, que apresentavam prótese, restaurações ou aparelho ortodôntico fixo em dentes anteriores.

3.2.2 Medição das bolsas periodontais

A profundidade da bolsa periodontal foi medida comparativamente por 3 métodos: (1) Swept Source OCT a 1325 nm (SS-OCT, Thorlabs, New Jersey, Estados Unidos); (2) sonda computadorizada (sonda da Flórida, Florida Probe Corporation, Gainsvile, Flórida, Estados Unidos); e (3) sonda manual (sonda Carolina do Norte, Golgran Millennium, São Caetano do Sul, SP, Brasil). A análise foi realizada pela interpretação visual do B-scan, para identificação das estruturas anatômicas e mensuração de espessura tecidual e profundidade de bolsa periodontal.

O sistema de OCT utilizado foi um modelo comercial, Swept Source OCT, de 1325 nm, que opera no domínio de Fourier, com resolução axial de 12 μm no ar e resolução lateral de 25 μm, largura de banda espectral> 100 nm, largura de banda instantânea de 0,13 nm (0,5 GHz), taxa de varredura axial é de 16 kHz, potência de saída média de até 10 mW e sensibilidade de 100 dB. O sistema captura 25 imagens por segundo.

Para realizar o exame de OCT, os pacientes permaneceram sentados em uma cadeira odontológica usando um afastador labial para exposição dos dentes anteriores, e o OCT foi posicionado incidindo o feixe de luz perpendicularmente à superfície dento/gengival. A fim de padronizar a localização das imagens e sondagem, placas de silicone individualizadas foram confeccionadas para cada paciente, contendo nichos realizados com uma lâmina de bisturi nº15 nos três locais da superfície vestibular dos dentes anteriores: mesio-vestibular, médio-vestibular e disto-vestibular. No momento da aquisição da imagem, o paciente foi instruído a pausar temporariamente a respiração, para que não houvesse alteração no ângulo de incidência do feixe central e da distância focal. A lente da peça de mão utilizada tem 36 mm de comprimento focal e 25,1 mm de distância de trabalho.

As profundidades de sondagem foram obtidas através de ferramentas do software do equipamento e as imagens foram armazenadas no formato BITMAP. As imagens 2D captadas para cada sítio constituem matrizes numéricas, compostas por 2000 colunas e 512 linhas, distribuídas ao longo de uma varredura transversal de 6 mm. Com o objetivo de suprimir a saturação do sinal devido a reflexões especulares, a área de interesse foi seca com ar antes da varredura e a peça de mão do OCT foi posicionada perpendicularmente à superfície durante a varredura. Todas as medidas obtidas foram corrigidas considerando o índice de refração gengival de 1,41±0,06[30].

Nas imagens de OCT, foi considerado como padrão de referência para medir a profundidade da bolsa periodontal, o valor correspondente à distância entre a junção amelodentinária como o limite superior e a região onde o retroespalhamento muda. As imagens obtidas em escala de cinza foram avaliadas por dois dentistas calibrados utilizando o software Image J (processamento e análise de imagens em Java, National Institutes of Health, Bethesda, Maryland). A captura das imagens utilizando o OCT foi sempre o primeiro exame a ser realizado, a fim de diminuir interferências decorrentes do afastamento tecidual promovido pela sondagem periodontal.

Em seguida, os registros de sondagem foram obtidos pelas sondas computadorizada e manual. Os mesmos avaliadores realizaram os registros com intervalo de 20 minutos entre o uso dos dois instrumentos. A ordem do exame foi determinada por sorteio. A profundidade da bolsa periodontal para ambos os instrumentos foi considerada como a distância entre a margem gengival ou a junção amelodentinária e a base da bolsa periodontal.

3.2.3 Análise de dados

Os dados foram analisados através da interpretação das imagens e comparação com os valores das profundidades de sondagem. Os dados de profundidade coletados na pesquisa por dois avaliadores calibrados, utilizando duas técnicas de sondagem manual, foram utilizados como referência para auxiliar na interpretação dos achados nas imagens. Esta análise qualitativa ajudou na interpretação e compreensão das imagens, proporcionando uma abordagem única. As imagens foram usadas no formato gerado pelo sistema OCT, sem qualquer tipo de tratamento digital.

3.3 ESTUDO 3 - MONITORING THE GINGIVAL REGENERATION AFTER AESTHETIC SURGERY WITH OPTICAL COHERENCE TOMOGRAPHY

Publicado: International Society for Optics and Photonics, 2016; doi: 10.1117/12.2213715.

Este artigo consistiu no acompanhamento do reparo tecidual em paciente submetido a cirurgia plástica periodontal. As avaliações foram realizadas antes da cirurgia, e após 30 e 60 dias, visando observar as alterações dos tecidos moles e o processo de cicatrização gengival.

3.3.1 História clínica do paciente

Paciente do sexo feminino compareceu à Clínica Integral do curso de Odontologia da Universidade Federal de Pernambuco (UFPE) insatisfeita com a estética de seu sorriso. Durante o exame clínico, foi possível observar diastemas generalizados nos arcos superior e inferior, associado a uma desarmonia gengival. O paciente foi submetido a exames clínicos e radiográficos. Em seguida, procedeu-se à correção estética da gengiva nos elementos superiores (14 a 24) e inferiores (33 a 43), com consentimento da paciente.

3.3.2 A cirurgia gengival

Foi realizada uma moldagem com alginato (Hydrogum, Zhermack, país) para confecção de modelo de estudo e registro de mordida para realização de enceramento diagnóstico. Foi realizada uma cirurgia no modelo para simular um aumento de coroa dos elementos. Ainda na fase laboratorial preliminar foi confeccionada uma moldeira guia em acetato para posterior fase clínica e cirúrgica.

A cirurgia periodontal a retalho foi a técnica escolhida para o arco superior. Uma placa de acetato foi usada como guia, para delimitar as novas medidas da margem gengival. Primeiramente foi executada a remoção de faixas de tecido mole queratinizado, cautelosamente desenhada para prover o contorno parabólico estético da margem gengival. Posteriormente, foi realizado o levantamento do retalho, osteotomia e osteoplastia precisas para reconfiguração do espaço biológico e suavização do arcabouço ósseo. O procedimento cirúrgico foi concluído após o reposicionamento do retalho.

3.3.3 Avaliação de Tomografia por Coerência Óptica

Imagens sagitais de OCT foram capturadas em região de terço cervical dos elementos 12 a 22 antes da cirurgia, como imagem de controle da gengiva saudável e região periodontal. Um novo escaneamento foi realizado 15 e 60 dias após a cirurgia periodontal para monitorar a recuperação dos tecidos. O sistema de OCT usado é um modelo Swept Source operando em 1325 nm (SS-OCT, Thorlabs, Nova Jersey, EUA), com 12 µm de resolução axial e 25 µm de resolução lateral. Durante o exame, a paciente foi mantida sentada com a cabeça apoiada em posicionador específico, perpendicular ao feixe emissor de luz, para padronizar a captação de imagens. Além disso, o afastador labial foi utilizado para melhor visualização da área em estudo.

3.4 ESTUDO 4 - OPTICAL COHERENCE TOMOGRAPHY INVESTIGATIONS OF CERAMIC LUMINEERS

Publicado: International Society for Optics and Photonics, 2016; doi: 10.1117/12.2213672.

Este artigo consistiu na inspeção de 14 laminados cerâmicos, cimentados em dentes anteriores. As avaliações foram realizadas antes da cimentação e após 180 dias, a fim de identificar alterações na linha de cimentação.

3.4.1 Recrutamento de pacientes

Paciente do sexo feminino, jovem, da Clínica Integral do curso de graduação em Odontologia da Universidade Federal de Pernambuco (UFPE), insatisfeita com a estética do sorriso, foi recrutada e formalmente concordou em participar do estudo.

3.4.2 Exame clínico

Durante a avaliação clínica, foi possível observar vários diastemas no arco superior e inferior da paciente. Após o exame clínico e radiográfico detalhado, foi apresentado um planejamento clínico para a fabricação dos laminados envolvendo os dentes 14 a 24 e 33 a 43.

3.4.3 Tratamento

Foi realizada uma moldagem com alginato (Hydrogum, Zhermack, Padoua, Itália) para obter um modelo de diagnóstico para o estudo do caso. Em seguida, a mordida foi registrada e os modelos foram fixados em um articulador semi-ajustável para realizar o enceramento diagnóstico. Antes de iniciar o tratamento estético, realizou-se um clareamento caseiro supervisionado utilizando Peróxido de Carbamida a 16% (White & Brite Night, 3M ESPE, São Paulo, Brasil) durante o período de 15 dias.

Após esse período, foi realizado o desgaste do esmalte com ponta diamantada 3131 (KG Sorense, São Paulo, Brasil) e discos de lixa de granulação grossa Sof-Lex Pop-On (3M ESPE, São Paulo, Brasil), visando adequar o eixo de inserção para instalação das restaurações cerâmicas. Para promover a retração gengival e proporcionar uma reprodução mais fiel dos terços cervicais, foram utilizados fios de retração gengival (000, Ultrapack, Ultradent, Rio de Janeiro, Brasil). Após a seu posicionamento, foram produzidos os moldes em silicone de adição (Express XT, 3M ESPE, São Paulo, Brasil).

Em etapa laboratorial, obteve-se o modelo de trabalho, montagem em articulador semi-ajustável e confecção das provas/microlaminados em resina e cera, para teste em boca. Foi realizada a prova dos microlaminados clinicamente, realização dos ajustes necessários em resina e cera, reenviando ao labaratório para confecção dos laminados cerâmicos.

Os laminados foram fabricados usando o sistema IPS e.max Ceramic (Ivoclar Vivadent, Schaan, Liechtenstein), seguido de caracterização. A adaptação dos laminados foi avaliada nos modelos gesso e, posteriormente, na boca com material específico para este procedimento (Variolink Veneer Try-in, Ivoclar Vivadent, Schaan, Liechtenstein). Após as etapas anteriores, os laminados de cerâmica foram fixados de acordo com as recomendações do fabricante. As superfícies internas dos laminados foram condicionadas com ácido fluorídrico (HF) a 4% (Ivoclar Vivadent, Schaan, Liechtenstein) por 30 segundos. Logo em seguida, o ácido foi completamente removido, as peças foram secas e o silano (Monobond Plus, Ivoclar Vivadent, Schaan, Liechtenstein) foi aplicado por um minuto, seguido de secagem com jato de ar. Foi então aplicada na superfície interna de cada peça um agente adesivo (Excite F, Ivoclar Vivadent, Schaan, Liechtenstein), seguido de jato de ar leve e fotoativação (LED Radii-Cal, SDI, Bayswater, Australia) por 15 segundos. O substrato dentário foi preparado usando ácido fosfórico a 37% (Total Etch, Ivoclar Vivadent, Schaan, Liechtenstein) por 15 segundos, lavando e secando em seguida. Uma camada de adesivo (Excite F, Ivoclar Vivadent) foi aplicada nas superfícies dos dentes, seguida por jato suave de ar e fotoativação por 15 segundos. Após a preparação preliminar das facetas e do dente, os laminados foram cimentados utilizando o cimento Variolink® Veener translúcido (Ivoclar Vivadent, Schaan, Liechtenstein) aplicado diretamente nas superfícies internas dos laminados com a ponta do aplicador (Variolink® veener, Ivoclar Vivadent, Schaan, Liechtenstein). Quando as facetas foram colocadas na posição correta, uma leve pressão foi exercida. Após a retirada dos excessos, seguiu-se a fotoativação por 30 segundos. O processo foi repetido até a cimentação do laminado estar completa. Os excessos foram retirados com pontas de acabamento diamantadas e discos flexíveis de polimento, nas zonas proximais foram utilizadas tiras de acabamento e polimento. Os ajustes finais foram cumpridos na máxima intercuspidação habitual, considerando os movimentos mandibulares.

3.4.4 Monitoramento do estudo clínico

Buscando examinar a região tratada, foram adquiridas imagens sagitais, antes e após 6 meses de instalação dos laminados cerâmicos. A aquisição das imagens foi realizada por meio do Swept Source OCT em 1325 nm (equipamento descrito no item 3.3.3). Para facilitar a aquisição de imagens, a paciente permaneceu sentada com a cabeça apoiada em posição específica, permitindo a focalização da luz perpendicular à área de estudo. Além disso, um afastador labial foi usado para livrar a área de estudo de qualquer anteparo. As imagens geradas foram salvas em formato JPEG.

3.5 ESTUDO 5 - *IN VIVO* EVALUATION OF THE INTEGRITY AND ADAPTATION OF LAMINATES USING OPTICAL COHERENCE TOMOGRAPHY: A PRELIMINARY STUDY

A ser submetido na Journal of Dentistry.

Este artigo verificou a capacidade de observação de alterações, no corpo de restaurações laminadas e na linha de cimentação, nas imagens obtidas *in vivo* utilizando o OCT.

3.5.1 Aspectos éticos

Todos os participantes do estudo foram informados por escrito do conteúdo da pesquisa e assinaram o termo de estudo antes de serem incluídos na avaliação. O estudo foi realizado de acordo com a Declaração de Helsinki e aprovado pelo Comitê de Ética da Universidade Federal de Pernambuco (protocolo número 49742615.0.0000.5208, parecer 1309903 – Anexo C).

3.5.2 Caracterização do estudo

Foi realizado um estudo observacional *in vivo* de 84 sítios em 28 laminados cerâmicos (IPS e.max Ceramic, Ivoclar Vivadent, Schaan, Liechtenstein) e 18 sítios em 6 facetas pré-fabricadas de resina composta nanohíbrida pré-polimerizada

(Componeer Brilliant, Coltene, Altstätten, Suíça) fixadas nos dentes superiores anteriores.

Os participantes tinham idade entre 18 e 65 anos, de ambos os sexos, atendidos na Clínica Integral I do curso de Odontologia da Universidade Federal de Pernambuco, em Pernambuco, Brasil. Foram utilizados os seguintes critérios de exclusão: má higiene bucal; ausência de dentes anterossuperiores; presença de prótese, restauração ou aparelho ortodôntico fixo na região avaliada.

Os laminados de resina foram cimentados aos dentes de acordo com as recomendações do fabricante, indicando o uso de resina composta nanohíbrida de alta carga como agente fixador (Brilliant NG, Coltene, Altstätten, Suíça) sobre o substrato dental previamente acondicionado (Magic Acid 37%, Coltene, Whaledent, Suíça) e coberto com camada adesiva (One Coat Bond SL, Coltene Whaledent, Suíça). Os dentes submetidos a esse tratamento não necessitaram de nenhum tipo de preparo dentário, apenas ajuste das bordas do laminado com discos de granulação grossa (Sof-Lex, 3M ESPE, São Paulo, Brasil).

Para laminados cerâmicos, preparações ultraconservadoras foram realizadas em todos os dentes com pontas de diamante (KG Sorense, São Paulo, Brasil), apenas para ajuste do eixo de inserção das restaurações cerâmicas. A superfície interna dos laminados foi tratada com ácido fluorídrico a 4% (Ivoclar Vivadent, Schaan, Liechtenstein) por 30s, silano (Monobond Plus, Ivoclar Vivadent, Schaan, Liechtenstein) por 1 min e adesivo (Excite F, Ivoclar Vivadent, Schaan, Liechtenstein). Os dentes foram condicionados (gel de ácido fosfórico a 37%), enxaguados, secos e tratados com agente de ligação de dentina (Excite F, Ivoclar Vivadent, Schaan, Liechtenstein). Os laminados cerâmicos foram fixados ao substrato dental com o auxílio de cimento resinoso (Variolink Veneer, Ivoclar Vivadent, Schaan, Liechtenstein) e removendo o excesso de agente cimentante com escova e fio dental. As restaurações foram polimerizadas de acordo com às recomendações do fabricante.

3.5.3 Protocolo do estudo

Todos os pacientes foram avaliados clinicamente quanto à cor, presença de gap marginal e fratura, antes da coleta de imagens[103].

O exame com OCT foi realizado para investigar a região vestibular de cada elemento, avaliando os três sítios (mesial, central e distal) nos três terços dos dentes

(cervical, médio e incisal). As imagens foram capturadas, excepcionalmente, até um ano em um único paciente. Para uma análise longitudinal padronizada, foi confeccionada uma placa guia de acetato, com marcações delimitando os locais (mesial, central e distal).

O exame com OCT, os indivíduos, que permaneceram sentados, com a cabeça apoiada em posicionador específico, perpendicular ao foco emissor de luz laser, de modo a padronizar o posicionamento do mento e da glabela para todos os sujeitos da pesquisa. Além disso, utilizou-se um afastador labial para melhor visualização da área a ser estudada.

3.5.4 Sistema OCT, imagem e análise dos dados

O sistema OCT utilizado foi o SS-OCT 1325 nm (Thorlabs Inc, Nova Jersey, Estados Unidos) com largura de banda espectral de ~ 100 nm, taxa de varredura axial de 16 kHz, captura de 25 imagens por segundo, resolução lateral ~ 25μm e resolução axial de 12 / 9 μm (ar / água, respectivamente). As superfícies vestibulares dos dentes foram varridas perpendicularmente por um feixe de luz e as imagens bidimensionais (2D) adquiridas foram armazenadas em formato BITMAP. Visando o monitoramento longitudinal de algumas regiões, imagens tridimensionais foram capturadas com um volume de 512 pixels nas direções -X, -Y, -Z, em 1 minuto.

As imagens foram avaliadas quanto à presença de alterações na superfíe e corpo do laminado, e na linha de cimentação ao substrato dentário. Além da análise qualitativa das imagens, foi realizada a mensuração dos defeitos apresentados em cada período de reavaliação, a fim de correlacionar o tamanho do defeito com a identificação de sinais clínicos de mudança na região. Todas as medidas bidimensionais (2D) foram realizadas no software do equipamento, sem qualquer outro tratamento de imagem, e a mensuração do volume de defeitos clinicamente visível foi obtida com o software ImageJ (Imaging Processing and Analysis in Java, National Institutes of Health, Bethesda, MD).

4 RESULTADOS E DISCUSSÃO

Os itens resultados e discussão do presente trabalho estão descritos nos artigos contidos nos apêndices desta tese.

5 CONCLUSÕES

As conclusões inerentes a cada um dos artigos contidos nesta tese, estão apresentações individualmente nos estudos.

Todavia, os dados obtidos para esta tese permitem concluir que o OCT apresenta um bom potencial para utilização clínica aplicada à Odontologia em um futuro relativamente próximo, visto que permite a geração de imagens de elevada resolução, adquiridas em tempo real e de forma não-invasiva, permitindo a realização de diagnóstico antes do aparecimento de sinais clínicos. O empenho para introdução da técnica na clínica alavanca as pesquisas visando superar limitações da técnica, tais como as observadas nos estudos. Entre as perspectivas para utilização clinica, relata-se o desenvolvimento de peças de mão, de sistemas portáteis com menor custo, da melhoria do contraste das imagens e o aumento na profundidade de penetração da luz.

REFERÊNCIAS

1. Lindhe J, Lang NP, Karring T. Tratado de Periodontia Clínica e Implantologia Oral. 5. ed. Rio de Janeiro: Guanabara Koogan; 2010. 1304p.

2. Seneadza V, Koob A, Kaltschmitt J, Staehle HJ, Duwenhoegger J, Eickholz P. Digital enhancement of radiographs for assessment of interproximal dental caries. Dentomaxillofacial Radiology. 2008; 37(3), 142-148.

3. Brouwer F, Askar H, Paris S, Schwendicke F. Detecting secondary caries lesions: a systematic review and meta-analysis. Journal of dental research. 2016; 95(2), 143-151.

4. Schwendicke F, Brouwer F, Paris S, Stolpe M. Detecting proximal secondary caries lesions: a cost-effectiveness analysis. Journal of dental research.2016; 95(2), 152-159.

5. Kherlopian AR, Song T, Duan Q, Neimark MA, Po MJ, Gohagan JK, Laine AF. A review of imaging techniques for systems biology. BMC systems biology. 2008; 2(1), 74.

6. Slak B, Daabous A, Bednarz W, Strumban E, Maev RG. Assessment of gingival thickness using an ultrasonic dental system prototype: A comparison to traditional methods. Annals of Anatomy-Anatomischer Anzeiger, 2015; 199, 98-103.

7. Krause F, Braun A, Jepsen S, Frentzen M. Detection of subgingival calculus with a novel LED-based optical probe. Journal of periodontology. 2005; 76(7), 1202-1206.

8. Bakhsh TA, Sadr A, Shimada Y, Tagami J, Sumi Y. Non-invasive quantification of resin–dentin interfacial gaps using optical coherence tomography: validation against confocal microscopy. Dental Materials. 2011; 27(9), 915-925.

9. Ino Y, Kubo T, Kameyama T, Shimamura K, Terada K, Matsuo Y, Kitabata H, Shiono Y, Kashiwagi M, Kuroi A, Maniwa N, Ota S, Ozaki Y, Tanaka A, Hozumi T, Akasaka T. Clinical Utility of Combined Optical Coherence Tomography and Near-Infrared Spectroscopy for Assessing the Mechanism of Very Late Stent Thrombosis. JACC. Cardiovascular imaging. 2018; 11(5), 772, 2018.

10. Tomlins PH, Wang RK. Theory, developments and applications of optical coherence tomography. Journal of Physics D: Applied Physics. 2005; 38(15), 2519.

11. Huang D, Swanson EA, Lin CP, Schuman JS, Stinson WG, Chang W *et al*. Optical coherence tomography. Science. 1991; 254(5035), 1178-1181.

12. Rosa CC. Biópsia Óptica OCT. INESC-Porto, Faculdades de Ciências, Universidade do Porto. 2010; 33(3/4).
13. Heidari AE, Sunny SP, James BL, Lam TM, Tran AV, Yu J *et al*. Optical Coherence Tomography as an Oral Cancer Screening Adjunct in a Low Resource Settings. IEEE Journal of Selected Topics in Quantum Electronics. 2019; 25(1), 1-8.
14. Shimada Y, Nakagawa H, Sadr A, Wada I, Nakajima M, Nikaido T *et al*. Noninvasive cross-sectional imaging of proximal caries using swept-source optical coherence tomography (SS-OCT) *in vivo*. Journal of biophotonics. 2014; 7(7), 506-513.
15. Kim SH, Kang SR, Park HJ, Kim JM, Yi WJ, Kim TI. Improved accuracy in periodontal pocket depth measurement using optical coherence tomography. Journal of periodontal & implant science. 2017; 47(1), 13-19.
16. Fernandes LO, Mota CCDO, Oliveira HO, Neves JK, Santiago LM, Gomes AS. Optical coherence tomography follow-up of patients treated from periodontal disease. Journal of biophotonics. 2018; e201800209.
17. Milosevic A. The problem with an epidemiological index for dental erosion. British dental journal. 2011; 211(5), 201.
18. Xiang X, Sowa MG, Iacopino AM, Maev RG, Hewko MD, Man A, Liu KZ. An update on novel non-invasive approaches for periodontal diagnosis. Journal of periodontology. 2010; 81(2), 186-198.
19. Azevedo CSD, Trung LCE, Simionato MRL, Freitas AZD, Matos AB. Evaluation of caries-affected dentin with optical coherence tomography. Brazilian oral research. 2011; 25(5), 407-413.
20. Park JY, Chung JH, Lee JS, Kim HJ, Choi SH, Jung UW. Comparisons of the diagnostic accuracies of optical coherence tomography, micro-computed tomography, and histology in periodontal disease: an ex vivo study. Journal of periodontal & implant science. 2017; 47(1), 30-40.
21. Colston BW Sathyam US, DaSilva LB, Everett MJ, Stroeve P, Otis LL Dental oct. Optics express. 1998; 3(6), 230-238.
22. Lee C, Darling CL, Fried D. Polarization-sensitive optical coherence tomographic imaging of artificial demineralization on exposed surfaces of tooth roots. Dental materials. 2009; 25(6), 721-728.
23. Hsieh YS, Ho YC, Lee SY, Chuang CC, Tsai JC, Lin KF, Sun CW. Dental optical coherence tomography. Sensors. 2013; 13(7), 8928-8949.

24. Schneider H, Park KJ, Häfer M, Rüger C, Schmalz G, Krause F, *et al*. Dental applications of optical coherence tomography (OCT) in cariology. Applied Sciences. 2017; 7(5), 472.

25. Otis LL, Everett MJ, Sathyam US, Colston Jr BW. Optical coherence tomography: a new imaging: technology for dentistry. The Journal of the American Dental Association, 131(4), 511-514.

26. Brezinski, Mark E. Optical coherence tomography: principles and applications. Elsevier, 2006.

27. Yasuno Y, Hong Y, Makita S, Yamanari M, Akiba M, Miura M, Yatagai T. *In vivo* high-contrast imaging of deep posterior eye by 1-μm swept source optical coherence tomography and scattering optical coherence angiography. Optics express.2007; 15 (10), 6121-6139.

28. Yim M, Galor A, Nanji A, Joag M, Palioura S, Feuer W, Karp CL. Ability of novice clinicians to interpret high-resolution optical coherence tomography for ocular surface lesions. Canadian Journal of Ophthalmology. 2018; 53(2): 150-154.

29. Mota CC Fernandes LO, Cimoes R, Gomes AS. Non-Invasive Periodontal Probing Through Fourier-Domain Optical Coherence Tomography. Journal of periodontology. 2015; 86(9), 1087-1094.

30. Fernandes LO, Mota CCBO, de Melo LSA, da Costa Soares M U S, da Silva Feitosa D, Gomes ASL. *In vivo* assessment of periodontal structures and measurement of gingival sulcus with optical coherence tomography: a pilot study. Journal of biophotonics.2017; 10(6-7), 862-869.

31. Fujimoto, James G. Optical coherence tomography for ultrahigh resolution *in vivo* imaging. Nature biotechnology. 2003; 21(11), 1361.

32. Wojtkowski M. High-speed optical coherence tomography: basics and applications. Applied optics. 2010; 49(16), D30-D61.

33. De Melo LSA, de Araujo RE, Freitas AZ, Zezell DM, Vieira ND, Girkin JM *et al*. Evaluation of enamel dental restoration interface by optical coherence tomography. Journal of biomedical optics. 2005; 10(6), 064027.

34. Kini A, Narula J, Vengrenyuk Y, Sharma S. Optical Coherence Tomography: Principles, Image Acquisition, and Assessment. In: Atlas of Coronary Intravascular Optical Coherence Tomography. Springer, Cham; 2018.1-13.

35. Tang H, Liu X, Chen S, Yu X, Luo Y, Wu J *et al*. Estimation of refractive index for biological tissue using micro-optical coherence tomography. IEEE Transactions on Biomedical Engineering. 2018.

36. Dsouza R, Won J, Monroy GL, Spillman DR, Boppart SA. Economical and compact briefcase spectral-domain optical coherence tomography system for primary care and point-of-care applications. Journal of biomedical optics. 2018; 23(9), 096003.

37. Kah JCY, Chow TH, Ng BK, Razul SG, Olivo, M, Sheppard CJR. Concentration dependence of gold nanoshells on the enhancement of optical coherence tomography images: a quantitative study. Applied optics. 2009; 48(10), D96-D108.

38. Pahlevaninezhad H, Khorasaninejad M, Huang YW, Shi Z, Hariri LP, Adams DC *et al*. Nano-optic endoscope for high-resolution optical coherence tomography *in vivo*. Nature Photonics. 2018; 12(9), 540.

39. TSIEN, Roger Y. Imagining imaging's future. Nature reviews. Molecular cell biology. 2003, SS16-21.

40. Nusshardt, M., Bonse Ulrich. A Michelson interferometer for X-rays capable of high-order measurement. Journal of applied crystallography. 2003; 36(2), 269-279.

41. Drexler Wolfgang, FUJIMOTO JG. Optical coherence tomography: technology and applications. Springer Science & Business Media. 2008.

42. Beddows R, James SW, Tatam RP. Improved performance interferometer designs for optical coherence tomography. In: Optical Fiber Sensors Conference Technical Digest. 2002; 527-530.

43. Farah ME. Tomografia de Coerência Óptica- OCT- Texto e Atlas. Rio de Janeiro: Cultura Médica; 2006.

44. Schmitt JM. Optical coherence tomography (OCT): a review. IEEE Journal of selected topics in quantum electronics. 1999; 5(4), 1205-1215.

45. Dhawan AP, D'alessandro B, FU Xiaolei. Optical imaging modalities for biomedical applications. IEEE reviews in biomedical engineering. 2010; 3(69-92).

46. Fercher AF, Drexler W, Hitzenberger CK, Lasser T. Optical coherence tomography-principles and applications. Reports on progress in physics. 2003; 66(2), 239.

47. Feldchtein FI, Gelikonov GV, Gelikonov VM, Iksanov RR, Kuranov RV, Sergeev AM *et al*. *In vivo* OCT imaging of hard and soft tissue of the oral cavity. Opt. Express. 1998; 3(6), 239-250.

48. Pircher M, Zawadzki RJ. Combining adaptive optics with optical coherence tomography: Unveiling the cellular structure of the human retina *in vivo*. Expert review of Ophthalmology. 2007; 2(6), 1019-1035.

49. Podoleanu AG. Optical coherence tomography. The British journal of radiology. 2005; 78(935), 976-988.

50. Schuman JS. Spectral domain optical coherence tomography for glaucoma (an AOS thesis). Transactions of the American Ophthalmological Society. 2008; 106(426).

51. Hall A, Girkin JM. A review of potential new diagnostic modalities for caries lesions. Journal of Dental Research. 2004; 83(1), 89-94.

52. Dikshit S, Grover HS, Bhardwaj A, Saini R. Optical Coherence Tomography-A Boon for Dental Diagnostics. British Biomedical Bulletin. 2015; 3(2) 239-252.

53. Zhu J, He X, Chen Z. Perspective: Current challenges and solutions of Doppler optical coherence tomography and angiography for neuroimaging. APL Photonics. 2018; 3(12), 120902.

54. Nishizawa N, Kawagoe H, Yamanaka M, Matsushima M, Mori K, Kawabe T. Wavelength dependence of ultrahigh-resolution optical coherence tomography using supercontinuum for biomedical imaging. IEEE Journal of Selected Topics in Quantum Electronics. 2019; 25(1), 1-15.

55. Schmitt JM, Knuttel A, Yadlowsky M, Eckhaus M A. Optical-coherence tomography of a dense tissue: statistics of attenuation and backscattering. Physics in Medicine & Biology. 1994; 39(10), 1705.

56. Cheong W, Prahl SA, Welch AJ. A review of the optical properties of biological tissues. IEEE journal of quantum electronics. 1990; 26(12),2166-2185.

57. Rogers JD, Radosevich AJ, YJ, Backman V. Modeling light scattering in tissue as continuous random media using a versatile refractive index correlation function. IEEE J. Sel. Top. Quantum Electron. 2014; 20(2), 173-186.

58. Schneiderheinze DHP, Hillman TR, Sampson DD. Modified discrete particle model of optical scattering in skin tissue accounting for multiparticle scattering. Optics express. 2007; 15(23), 15002-15010.

59. Jacques SL. Optical properties of biological tissues: a review. Physics in Medicine & Biology. 2013; 58(11), R37.
60. Carrasco-Zevallos OM, Viehland C, Keller B, Draelos M, Kuo AN, Toth CA, Izatt JA. Review of intraoperative optical coherence tomography: technology and applications. Biomedical optics express. 2017; 8(3), 1607-1637.
61. Liu L, Gardecki JA, Nadkarni SK, Toussaint JD, Yagi Y, Bouma BE, Tearney GJ. Imaging the subcellular structure of human coronary atherosclerosis using micro–optical coherence tomography. Nature medicine. 2011; 17(8), 1010.
62. Wojtkowski M, Bajraszewski T, Targowski P, Kowalczyk A. Real-time *in vivo* imaging by high-speed spectral optical coherence tomography. Optics letters. 2003; 28(19), 1745-1747.
63. Leitgeb R, Hitzenberger CK, Fercher AF. Performance of fourier domain vs. time domain optical coherence tomography. Optics express. 2003; 11(8), 889-894.
64. Alibhai AY, Or C, Witkin AJ. Swept Source Optical Coherence Tomography: a Review. Current Ophthalmology Reports. 2018; 6(1), 7-16.
65. Sull AC, Vuong LN, Price LL, Srinivasan VJ, Gorczynska I, Fujimoto JG *et al*. Comparison of spectral/Fourier domain optical coherence tomography instruments for assessment of normal macular thickness. Retina. 2010; 30(2), 235.
66. Li M, Landahl S, East AR, Verboven P, Terry LA. Optical coherence tomography—A review of the opportunities and challenges for postharvest quality evaluation. Postharvest Biology and Technology. 2019; 150, 9-18.
67. Potsaid B, Baumann B, Huang D, Barry S, Cable AE, Schuman JS *et al*. Ultrahigh speed 1050nm swept source/Fourier domain OCT retinal and anterior segment imaging at 100,000 to 400,000 axial scans per second. Optics express. 2010; 18(19), 20029-20048.
68. Latrive A, Teixeira LRC, Gomes ASL, Zezell DM. Characterization of skin Port-Wine Stain and Hemangioma vascular lesions using Doppler OCT. Skin Research and Technology. 2016; 22(2), 223-229.
69. Katkar RA, Tadinada SA, Bennett TA, Fried D. Optical coherence tomography. Dental Clinics of North America. 2018; 62(3), 421-434.
70. Lesaffre M, Farahi S, Boccara AC, Ramaz, F, Gross M. Theoretical study of acousto-optical coherence tomography using random phase jumps on ultrasound and light. JOSA A. 2011; 28(7), 1436-1444.

71. Schmitz L, Reinhold U, Bierhoff E, Dirschka T. Optical coherence tomography: its role in daily dermatological practice. JDDG: Journal der Deutschen Dermatologischen Gesellschaft. 2013; 11(6), 499-507.

72. Menzies SW, Westerhoff K, Rabinovitz H, Kopf AW, McCarthy WH, Katz B. Surface microscopy of pigmented basal cell carcinoma. Archives of dermatology. 2000; 136(8), 1012-1016.

73. Backman V, Wallace MB, Perelman LT, Arendt JT, Gurjar, R., Müller, M. G *et al*. Detection of preinvasive cancer cells. Nature. 2000; 406(6791), 35.

74. van der Meer FJ, Faber, DJ, Aalders M.C, Poot AA, Vermes I, van Leeuwen TG. Apoptosis-and necrosis-induced changes in light attenuation measured by optical coherence tomography. Lasers in medical science. 2010; 25(2), 259-267.

75. Fujimoto,JG, Brezinski ME, Tearney GJ, Boppart SA, Bouma B, Hee MR. Optical biopsy and imaging using optical coherence tomography. Nature medicine. 1995; 1(9), 970-972.

76. Abignano G, Aydin SZ, Castillo-Gallego C, Liakouli V, Woods D, Meekings A *et al*. Virtual skin biopsy by optical coherence tomography: the first quantitative imaging biomarker for scleroderma. Annals of the rheumatic diseases. 2013; 72(11), 1845-1851.

77. Assayag O, Grieve K, Devaux B, Harms F, Pallud J, Chretien F. Imaging of non-tumorous and tumorous human brain tissues with full-field optical coherence tomography. NeuroImage: clinical. 2013; 2, 549-557.

78. Pires NSM, Dantas AT, Duarte ALBP, Amaral MM, Fernandes, LO, Dias TJC, de Melo LSA, Gomes ASL. Optical coherence tomography as a method for quantitative skin evaluation in systemic sclerosis. Annals of the rheumatic diseases. 2018, 77(3),465-466, 2018.

79. Mujat M, Ferguson RD, Hammer DX, Gittins CM, Iftimia NV. Automated algorithm for breast tissue differentiation in optical coherence tomography. Journal of biomedical optics. 2009, 14(3), p. 034040, 2009.

80. Kuo WC, Kim J, Shemonski ND, Chaney EJ, Spillman DR, Boppart SA. Real-time three-dimensional optical coherence tomography image-guided core-needle biopsy system. Biomedical optics express. 2012; 3(6), 1149-1161.

81. Iftimia N, Park J, Maguluri G, Krishnamurthy S, McWatters A, Sabir SH. Investigation of tissue cellularity at the tip of the core biopsy needle with optical coherence tomography. Biomedical optics express. 2018; 9(2), 694-704.

82. Wessels R, De Bruin DM, Faber DJ, Van Leeuwen TG, Van Beurden M, Ruers TJ. Optical biopsy of epithelial cancers by optical coherence tomography (OCT). Lasers in medical science. 2014; 29(3), 1297-1305.

83. Wijesinghe RE, Cho NH, Park K, Jeon M, Kim J. Bio-Photonic detection and quantitative evaluation method for the progression of dental caries using optical frequency-domain imaging method. Sensors. 2016; 16(12), 2076.

84. Wada I, Shimada Y, Ikeda M, Sadr A, Nakashima S, Tagami J, Sumi Y. Clinical assessment of non carious cervical lesion using swept-source optical coherence tomography. Journal of biophotonics. 2015; 8(10), p. 846-854.

85. Zain E, Zakian CM, Chew HP. Influence of the loci of non-cavitated fissure caries on its detection with optical coherence tomography. Journal of dentistry. 2018; 71(31-37).

86. Marcauteanu C, Bradu A, Sinescu C, Topala FI, Negrutiu NL, Podoleanu AG. Quantitative evaluation of dental abfraction and attrition using a swept-source optical coherence tomography system. Journal of Biomedical Optics. 2013; 19(2), 021108.

87. Li W, Liu J, Zhang Z. Evaluation of marginal gap of lithium disilicate glass ceramic crowns with optical coherence tomography. Journal of biomedical optics. 2018; 23(3), 036001.

88. Turk AG, Sabuncu M, Ulusoy M. Evaluation of adaptation of ceramic inlays using optical coherence tomography and replica technique. Brazilian oral research, 2018, 32.

89. Lin CL, Kuo WC, Yu JJ, Huang SF. Examination of ceramic restorative material interfacial debonding using acoustic emission and optical coherence tomography. Dental Materials, 2013; 29(4), 382-388.

90. de Andrade Borges E, Cassimiro-Silva PF, Fernandes, LO, Gomes ASL. 6. In: Biophotonics South America. International Society for Optics and Photonics. 2015; 953147.

91. Fernandes LO, Graça ND, Melo LS, Silva CH, Gomes, A. S. Optical coherence tomography investigations of ceramic lumineers. In: Lasers in Dentistry XXII. International Society for Optics and Photonics, 2016, 96920P.

92. Shimada Y, Sadr A, Nazari A, Nakagawa H, Otsuki, M, Tagami, J., Sumi, Y. 3D evaluation of composite resin restoration at practical training using swept-source optical coherence tomography (SS-OCT). Dental materials journal,2012; 31(3), 409-417, 2012.

93. Todor R, Negrutiu ML, Sinescu C, Topala FI, Bradu A, Duma VF *et al*. Investigation of firing temperature variation in ovens for ceramic-fused-to-metal dental prostheses using swept source optical coherence tomography. In: 2nd Canterbury Conference on OCT with Emphasis on Broadband Optical Sources. International Society for Optics and Photonics; 2018. p. 105910I.

94. Tsai, M. T., Lee, C. K., Lee, H. C., Chen, H. M., Chiang, C. P., Wang, Y. M., & Yang, C. C. Differentiating oral lesions in different carcinogenesis stages with optical coherence tomography. Journal of Biomedical Optics. 2009;14(4), 044028.

95. Bordin S, Pino CM, Mavadia-Shukla J, Li X. Optical coherence technology detects early signs of peri-implant mucositis in the minipig model. International Journal of Dentistry and Oral Science. 2017; 3(375-379).

96. Gladkova N, Karabut M, Kiseleva E, Robakidze N, Muraev A, Fomina J. Cross polarization optical coherence tomography for diagnosis of oral soft tissues. In: Lasers in Dentistry XVII. International Society for Optics and Photonics, 2011. p. 78840V.

97. Kakizaki S, Aoki A, Tsubokawa M, Lin T, Mizutani K, Koshy G *et al*. Observation and determination of periodontal tissue profile using optical coherence tomography. Journal of periodontal research. 2018; 53(2), 188-199.

98. Tsubokawa M, Aoki A, Kakizaki S, Taniguchi Y, Ejiri K, Mizutani K *et al*. In vitro and clinical evaluation of optical coherence tomography for the detection of subgingival calculus and root cementum. Journal of Oral Science. 2018; 17-0289.

99. Fernandes LO, Graça ND, Melo LS, Silva CH, Gomes AS. Monitoring the gingival regeneration after aesthetic surgery with optical coherence tomography. In: Lasers in Dentistry XXII. International Society for Optics and Photonics, 2016. p. 96920Q.

100. Baek JH, Na J, Lee BH, Choi E, Son WS. Optical approach to the periodontal ligament under orthodontic tooth movement: a preliminary study with optical coherence tomography. American Journal of Orthodontics and Dentofacial Orthopedics. 2009; 135(2), 252-259.

101. Yang VB Curtis DA, Fried D. Use of Optical Clearing Agents for Imaging Root Surfaces With Optical Coherence Tomography. IEEE Journal of Selected Topics in Quantum Electronics. 2019; 25(1), 1-7.

102. Braz AKS, de Araujo RE, Ohulchanskyy TY, Shukla S, Bergey EJ, Gomes AS, Prasad PN. In situ gold nanoparticles formation: contrast agent for dental optical coherence tomography. Journal of biomedical optics. 2012; 17(6), 066003.
103. Gurel G, Marimoto S, Calamita MA, Coachman C, Sesma N. Clinical performance of porcelain laminate veneers: outcomes of the aesthetic pre-evaluative temporary (APT) technique. The International Journal of Periodontics & Restorative Dentistry. 2012; 32, 625-635.

APÊNDICE A – COMPARATIVE ANALYSIS OF GINGIVAL PHENOTYPE IN ANIMAL AND HUMAN EXPERIMENTAL MODELS USING OPTICAL COHERENCE TOMOGRAPHY IN A NON-INVASIVE APPROACH.

Cláudia C. B. O. Mota[a], Luana O. Fernandes[b], Luciana S. A. Melo[c], Daniela S. Feitosa[b], Renata Cimões[b], Anderson S. L. Gomes[b,c]

[a]Associação Caruaruense de Ensino Superior e Técnico, Faculty of Dentistry, Av. Portugal, 584, Bairro Universitário, 55016-400, Caruaru-PE, Brazil

[b]Universidade Federal de Pernambuco, Graduate Program in Dentistry, Av. Prof. Moraes Rego,
1235, Cidade Universitária, 50670-901, Recife-PE, Brazil.

[c]Universidade Federal de Pernambuco, Physics Department, Av. Prof. Luis Freire s/n, Cidade
Universitária, 50670-901, Recife-PE, Brazil.

Biophotonics South America, edited by Cristina Kurachi, Katarina Svanberg, Bruce J. Tromberg, Vanderlei Salvador Bagnato, Proc. of SPIE Vol. 9531, 95313S · © 2015 SPIE CCC code: 1605-7422/15/$18 · doi: 10.1117/12.2180856

ABSTRACT

Imaging methods are widely used in diagnostic and among the diversity of modalities, optical coherence tomography (OCT) is nowadays commercially available and considered the most innovative technique used for imaging applications, in both medical and non-medical applications. In this study, we exploit the OCT technique in the oral cavity for identification and differentiation between free and attached gingiva, as well as determining the gingival phenotype, an important factor to determination of periodontal prognosis in patients. For the animal studies, five porcine jaws were analyzed using a Swept Source SS-OCT system operating at 1325nm and stereomicroscope, as gold pattern. The SS- OCT at 1325nm was chosen due to the longer central wavelength, that allows to deeper penetration

imaging, and the faster image acquisition, an essential factor for clinical setting. For the patient studies, a total of 30 males and female were examined using the SS-OCT at 1325nm and computer controlled periodontal probing. 2D and 3D images of tooth/gingiva interface were performed, and quantitative measurements of the gingival sulcus could be noninvasively obtained. Through the image analysis of the animals jaws, it was possible to quantify the free gingiva and the attached gingiva, the calculus deposition over teeth surface and also the subgingival calculus. For the patient's studies, we demonstrated that the gingival phenotype could be measured without the periodontal probe introduction at the gingival sulcus, confirming that OCT can be potentially useful in clinic for direct observation and quantification of gingival phenotype in a non-invasive approach.

Keywords: Optical Coherence Tomography; Periodontal diagnostics; Gingival Sulcus; Gingival phenotype; Non- invasive periodontal probing.

1. INTRODUCTION

The periodontal probe is the main method used in the diagnosis of periodontal disease. It is used to establish the presence and severity of the disease and the effect of periodontal treatment[1]. Several factors may influence the values obtained with the probing, such as those related to the examiner, the instrument or the conditions of the tissues[2,3]. Errors during the probing may lead the clinician to the choice of an inadequate treatment plan[4].

For the evaluation of periodontal diseases, the gingival phenotype directly affects the results of periodontal therapies[5]. The gingival thickness is considered a risk factor for development of changes, such as gingival recession in the presence of low gingival thickness (thin phenotype) or less likely on patients with thick gum (thick phenotype) after surgical therapy or restorative[6]. The thin phenotype is characterized by a narrow band of keratinized gingival tissue with an average thickness of 1.5 mm, while the thick have large amounts of keratinized tissue and gingival thickness greater than 2.0 mm[7].

The identification of phenotype through the thickness of the gum to be obtained by various techniques, since there is no standard of evaluation in the literature and several methods, invasive or not, are used as drilling, cone beam tomography, histological analysis, the use of ultrasonic devices and visual inspection[7]. Another method used is probing in which a trans gingival periodontal probe is transfixed through the gum, however, this method is invasive and inconvenient for the patient, and has to be performed under local infiltration anesthesia, whose thickness can be influenced by the deposited anesthetic[8]. The most used method is the combination of visual inspection to the probing with normal periodontal probe, as a method of execution simple, inexpensive and considered very effective[5,9], but depends directly on the evaluation capacity of each examiner making the questionable method.

Diagnostic imaging methods are widely used and arouse great interest of researchers and clinicians. Among the diversity of modalities optical coherence tomography (OCT) is a noninvasive diagnostic method through image obtained by non-ionizing radiation, commercially available and considered the most innovative technique used to obtain medical and non-medical image[10].

The OCT is capable of evaluating hard and soft tissues of the oral cavity and accurately identify their structural differences by analysis of the images formed[11]. Thus, several authors have suggested the use as a promising method for the early diagnosis and for the monitoring of periodontal disease with greater accuracy and sensitivity[12].

In this study, we explored the OCT technique in the oral cavity for the identification and differentiation between free and attached gingiva and identification of gingival phenotype, an important factor for determining the prognosis periodontics.

2. MATERIALS AND METHODS

2.1 Animals specimens

For the animal study, five porcine jaws were analyzed using a Fourier Domain SS-OCT system operating at 1325 nm (Swept Source, SS-OCT, Thorlabs, New

Jersey, USA) and stereomicroscope, as gold pattern. The SS-OCT at 1325 nm was chosen due to the longer central wavelength that allows to deeper penetration imaging, and the faster image acquisition, an essential factor for clinical setting.
Fresh porcine jaws obtained from a local slaughterhouse were dissected, sectioned and stored in formalin solution at 10% for 24 hours before the analysis through OCT and stereomicroscope, in order to preserve the dental structure and corresponding bone and periodontal tissues. Images were obtained from lower incisors, premolars and molars and their periodontal structures.

The images were performed with 2000 pixels per column at X-axis and 512 pixels per column at Y-axis (6 mm scanning and to 1.3 mm depth in air) to obtain two- and three-dimensional images. After the OCT analysis of the samples, the teeth and their corresponding periodontal and bone tissues were sectioned along the sagittal axis, from buccal to lingual surface, using flexible diamond disks 7075 (KG Sorensen, São Paulo, Brazil) under water refrigeration for further stereomicroscopy analysis.

The images were performed from the buccal surface of the samples and after OCT analysis and subsequent samples sectioning, stereomicroscopic images were performed directly from the sectioned surface with a 10x eyepiece providing magnification from 6.5x to 50x, 35.4 mm to 4.6 mm field of view and 92 mm working distance, coupled to a CCD camera with nominal resolution of 1.3µm.

2.2 Analysis of Patients

For the human study, a total of 30 patients, of both sexes with periodontal health and presence of anterior teeth, were examined using the same OCT system employed to the animal study, SS-OCT at 1325nm and computer controlled periodontal probing (Florida Probe Corporation, Florida, USA).

In each patient, only 3 buccal sites anterior teeth were evaluated (mesiobuccal, midbuccal, distobuccal), which resulted in 445 sites available for the study. To guarantee the sulcus depth records in a standardized position, an individually manufactured acrylic stent was used. Three grooves were made to determine mesiobuccal, midbuccal and distobuccal sites for imaging and probing.
To perform the OCT examination, the patients remained seated, with their head resting on specific positioner, perpendicular to focus laser light emitter. The

acquisition of images relating to the sites was performed using the OCT and the information stored in format jpeg. Subsequently, the images were analyzed for each site and probing depths were obtained through the Image J (Imaging Processing and Analysis in Java, National Institutes of Health, Bethesda, MD). Immediately after image capture by the OCT, the patient was submitted to the examination of periodontal probing of the vestibular sites used controlled pressure probe Florida Probe.

3. RESULTS AND DISCUSSION

An efficient diagnostic method able to identify early periodontal changes is fundamental for clinical success and keeping periodontal health. The diagnostic method most widely used for periodontal evaluation is the probing, due to the higher reproducibility in healthy and sick patients[13,14]. However the clinical probing is considered an invasive method because it leads to a mechanical disruption of the epithelial attachment and this fact can induce errors in diagnosis[15]. Difficulties become the Optical Coherence Tomography a promising method for periodontal clinical evaluation.

In this research, OCT was efficient to identify periodontal structures: gingiva, cementum-enamel junction and the gingival sulcus in humans and animal models due to its spatial resolution, as seen in figure 1. In addition, other structures have been observed, such as dental enamel layer which was identified overlapped to dentin by dentinoenamel junction and free gingiva portions and inserted, the gingival margin, the regions of oral, sulcular and junctional epithelium, and adjacent connective tissue. The images allowed the qualitative and quantitative analysis of the gingiva and gingival sulcus, similar to the results obtained by Colston *et al*.[16].

The presence of supra and subgingival dental calculus was observed in some images of periodontal area of animal teeth, as also observed by Hsieh *et al*.[17], but in humans it was only possible to observe the presence of supragingival calculus. This is probably due to the dehydration caused by formaline solution in porcine soft tissues, allowing higher light scattering into porcine gingiva than human gingiva. The presence of calculus in the area leads to disruption of the existing intimate contact between the tooth and the sulcular epithelium, increasing the distance between

them, and change the propagation of light through enamel and dentin due to the standard features and intensity of
scattering by calculations on the tooth surface. It was not possible to distinguish the structures as cementum and alveolar bone, both belonging to the periodontal support, differing from the results of Baek *et al*.[18]

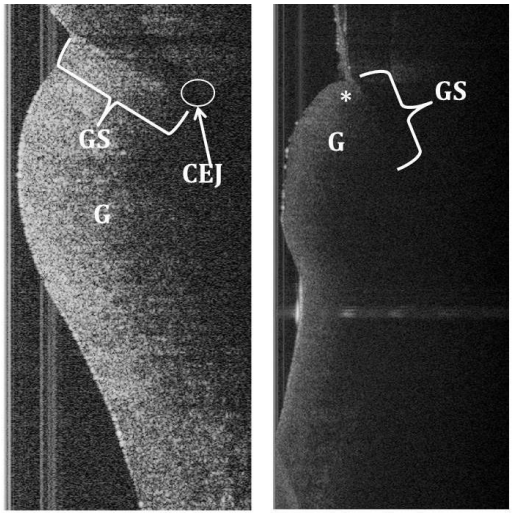

Figure 1 – Images obtained by Swept Source Optical Coherence Tomography at 1325nm showing the distinction between periodontal structures of healthy individuals (a) and porcine (b): G - gingiva; E - enamel; D - dentin; DEJ – dentino enamel junction; CEJ - cementum enamel junction; GS – gingival sulcus; C – calculus; * - subgingival calculus.

As for the sulcus measurement and phenotype, histological gingival sulcus measurement is around 0.69 mm[19], but clinically it ranges from 1 to 3 mm, for healthy pacients[20]. Using Image J software, the thickness and depth of the gingival sulcus have been measured for the periodontal region of the animal model, since it presented severe periodontal disease, in order to validate the OCT as an evaluation method of the parameters. The average value for gingival thickness was 1.18±0.10 mm, whilst a measurement of gingival sulcus depth is 3.33±0.17 mm, consistent with

the results of the stereomicroscopy measurements of the model animal, as seen in figure 2(a).

Monitoring of clinical measures of periodontal probing of patients is critical to the clinical evaluation of periodontal tissues[21]. This study used the OCT technique as an alternative method in the relevant parameter view used in periodontal diagnosis, as sulcus depth and gingival phenotype. The comparison of the average periodontal probing values in healthy individuals obtained by OCT and Florida Probe showed higher values when the computer controlled periodontal probing was used, 0,86±0,27 and 1,25±0,58, respectively, probably due to technical limitations inherent to the probing, such as the extent of penetration, the epithelial attachment and reproduction of probing[12,22]. Furthermore, the OCT enables the measurement and analysis of periodontal tissue preservation region, therefore optical properties do not require direct contact with the tissues and, and no pressure. The technique provides an assessment of healthy tissue without damaging those[12]. The obtained images can be analyzed in different moments, allowing monitoring the evolution of the disease, even before its clinical manifestations[18].

In healthy subjects analyzed were identified gingival phenotypes from the measurement of the thickness of the gum in OCT images, the measure was bounded across from the base of the sulcus to the gingival surface (figure 2b). A mean value of 1.37 ± 0.29 was obtained and according to Esfahrood *et al*[7] characterized them as thin phenotype. This fact demonstrates the ability of the OCT in quantitatively assess the phenotype value, and we suggest the use of OCT should be used as a standard method in evaluating the human gingival phenotype.

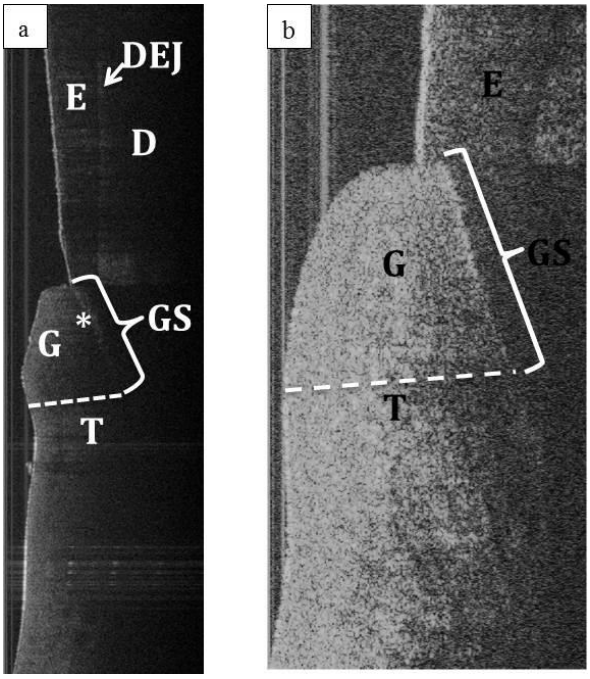

Figure 2- Measurement of the thickness of the gingival sulcus and in pig (a) and healthy individuals (b): GS- gingival sulcus; T- gingival thickness.

4. CONCLUSION

This study demonstrated that OCT is able to investigate and identify non-invasively and with good spatial resolution, structures located in periodontal region, such as gingiva and cementum-enamel junction. The acquired image analysis of tooth/gingiva interface proved to be sufficient to make quantitative measurements of the sulcus and identification of phenotype. Thus it was proposed to use the OCT as standard technique for analysis of periodontal tissues and evaluation and determination of the gingival phenotype.

ACKNOWLEDGEMENTS

The authors are thankful to FACEPE (Foundation for Science and Technology of Pernambuco State), CNPq (National Council of Technological and Scientific Development) and MCT (Ministry of Science and Technology) for financial support. This study was carried out under the PRONEX FACEPE/CNPq (Center of Excelence on Biphotonics and Nanophotonics) program and INCT (National Institutes of Science and Technology) of Photonics program, sponsored by CNPq/MCT.

REFERENCES

[1] Barendregt, D. S., Van der Velden, U., Timmerman, M. F., Van der Weijden, G. A., “Comparison of two automated periodontal probes and two probes with a conventional readout in periodontal maintenance patients,” J. Clin. Periodontol. 33(4), 276-282 (2006).

[2] Van der Zee, E., Davies, E. H., Newman, H. N., “Marking width, calibration from tip and tine diameter of periodontal probes,” J. Clin. Periodontol. 18(7), 516-520 (1991).

[3] Rocha, E. F., Campanelli, V., Crivelenti, L. A. M., Joaquim, A. M. C., “Variability of the probing depth between conventional and controlled-force periodontal probes,” Salusvita 22(2), 219-227 (2003).

[4] Garnick, J. J., Silverstein, L., “Periodontal probing: probe tip diameter”. J. Periodontol. 71(1), 96-103 (2000).

[5] De Rouck, T., Eghbali, R., Collys, K., De Bruyn H., Cosyn J., “The gingival biotype revisited: transparency of the periodontal probe through the gingival margin as a method to discriminate thin from thick gingiva,” J Clin Periodontol 36(5), 428-433 (2009).

[6] Anderegg, C. R., Metzler, D. G., Nicoll, B. K., “Gingiva thickness in guided tissue regeneration and associated recession at facial furcation defects,” J. Periodontol. 66(5), 397-402 (1995).

[7] Esfahrood, Z. R., Kadkhodazadeh, M., Talebi Ardakani, M. R. “Gingival biotype: a review,” Gen. Dent. 61(4), 14-17 (2013).

[8] Kolte, R., Kolte, A., Mahajan, A., “Assessment of gingival thickness with regards to age, gender and arch location,” J. Indian. Soc. Periodontol. 18(4), 478-481 (2014).

[9] Kan, J. Y., Morimoto, T., Rungcharassaeng, K., Roe, P., Smith, D. H., “Gingival biotype assessment in the esthetic zone: visual versus direct measurement,” Int. J. Periodontics Restorative Dent. 30(3), 237-243 (2010).

[10] Wojtkowski, M. “High-speed optical coherence tomography: basics and applications,” Appl. Opt. 49(16), 30-61 (2010).

[11] Gimbel, C. “Optical coherence tomography diagnostic imaging,” Gen. Dent. 56(7), 750-757 (2008).

[12] Xiang, X., Sowa, M. G., Iacopino, A. M., Maev, R. G., Hewko, M. D., Man, A., Liu, K. Z. “An update on novel non-invasive approaches for periodontal diagnosis,” J. Periodontol. 81(2), 186-198 (2010).

[13] Khan, S., Cabanilla, L. L., “Periodontal Probing Depth Measurement: A Review,” Compend. Contin. Educ. Dent.
30(1), 12-14 (2009).

[14] Andrade, R., Espinoza, M., Gómez, E. M., Espinoza J. R., Cruz, E., “Intra-and inter-examiner reproducibility of manual probing depth,” Braz. Oral Res. 26(1), 57-63 (2012).

[15] Lang, N. P., Nyman, S., Senn, C., Joss, A., “Bleeding on probing as it relates to probing pressure and gingival health,” J. Clin. Periodontol. 18(4), 257-261 (1991).

[16] Colston Jr, B. W., Everett, M. J., Da Silva, L. B., Otis, L. L., Stroeve, P., Nathel, H., “Imaging of hard-and soft- tissue structure in the oral cavity by optical coherence tomography,” Appl. Opt. 37(16), 3582-3585 (1998).

[17] Hsieh, Y. S., Ho, Y. C., Lee, S. Y., Lu, C. W., Jiang, C. P., Chuang, C. C., Wang, C. Y., Sun, C. W., “Subgingival calculus imaging based on swept-source optical coherence tomography,” J. Biomed. Opt. 16(7), 071409 (2011).

[18] Baek, J. H., Na, J., Lee, B. H., Choi, E., Son, W. S., “Optical approach to the periodontal ligament under orthodontic tooth movement: a preliminary study with optical coherence tomography,” Am. J. Orthod. Dentofac. Orthop.135(2), 252-259 (2009).

[19] Gargiulo, A. W., Wentz, F. M., Orban, B., “Dimensions and relations of the dentogingival junction in humans,” J. Periodontol. 32(3), 261-267 (1961).

[20] Nanci, A., Bosshardt, D. D., “Structure of periodontal tissues in health and disease,” Periodontol. 2000, 40(1), 11-28 (2006).

[21] Huang, Y., Zhang, K., Yi, W., Kang, J. U., “In-vivo gingival sulcus imaging using full-range, complex-conjugate- free, endoscopic spectral domain optical coherence tomography,” Proc. SPIE 8208, 820804-820810 (2012).
[22] Susin, C., Kingman, A., Albandar, J. M., “Effect of partial recording protocols on estimates of prevalence of periodontal disease,” J. Periodontol. 76(2), 262-2

APÊNDICE B - ARTIGO JOURNAL OF BIOPHOTONICS

OPTICAL COHERENCE TOMOGRAPHY FOLLOW-UP OF PATIENTS TREATED FROM PERIODONTAL DISEASE

Luana O. Fernandes[1] | Cláudia C. B. de O. Mota[2] | Hugo O. Oliveira[2] | José K. Neves[2] | Leógenes M. Santiago[2] | Anderson S. L. Gomes[1,3]*

[1]Graduate Program in Dentistry, Universidade Federal de Pernambuco, Recife, Brazil
[2]Faculty of Dentistry, Associação Caruaruense de Ensino Superior e Técnico, Caruaru, Brazil
[3]Department of Physics, Universidade Federal de Pernambuco, Recife, Brazil
*Correspondence: Anderson S. L. Gomes, Department of Physics, Universidade Federal de Pernambuco, Av. Professor Luiz Freire s/n, 50670-901, Recife, Brazil. Email: anderson@df.ufpe.br

Optical coherence tomography (OCT) is one of the most important imaging modalities for biophotonics applications. In this work, an important step towards the clinical use of OCT in dental practice is reported, by following-up patients treated from periodontal disease (PD). A total of 147 vestibular dental sites from 14 patients diagnosed with PD were evaluated prior and after treatment, using a swept-source OCT and two periodontal probes (Florida probe and North Carolina) for comparison. The evaluation was performed at four stages: day 0, day 30, day 60 and day 90. Exceptionally one patient was evaluated 1-year after treatment. It was possible to visualize in the two-dimensional images the architectural components that compose the periodontal anatomy, and identify the improvements in biofilm and dental calculus upon treatment. In the follow-up after the treatment, it was observed in some cases decrease of the gingival thickness associated with extinction of gingival calculus. In some cases, the improvement of both depth of probing with the traditional probes and the evidence in the images of the region was emphasized. The study evidenced the ability of OCT in the identification of periodontal structures and alterations, being an important noninvasive complement or even alternative for periodontal probes for treatment follow-up. OCT system being used in a clinical environment. Above OCT image (left) prior treatment and (right) 30 days after treatment.

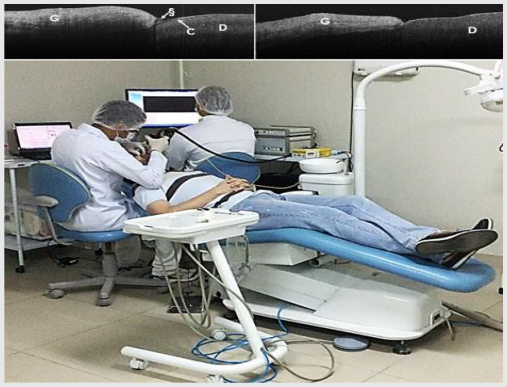

KEYWORDS diagnostic imaging, gingiva, optical coherence tomography, periodontal disease.

1 INTRODUCTION

Periodontal diseases (PD) are chronic multifactorial con- ditions, characterized by the destruction of periodontal tissues and causes 5% to 15% of dental losses in suscepti- ble individuals [1, 2]. Periodontal health depends on the balanced relationship between the dental biofilm and the immunoinflammatory response of the host [3]. Tradition- ally, PD diagnosis is performed through clinical examina- tion by the insertion of periodontal probing, which can be prone to errors [4], or periapical radiographs can be required [5].

Optical coherence tomography (OCT) is recognized as one of the most important imaging modalities in Biopho- tonics [6], providing optical biopsies with micrometer spatial resolution and few millimeters penetration depth (tissue dependent), with 10^7-10^9 voxels/s imaging speed, besides its capability of multimodality integration [7]. The recent review in Ref. [6] shows the fantastic scientific, clinical and commercial advances of OCT in several biomedical areas. The OCT technique, initially used to evaluate the transparent tissues of the eye [8], has come out of age [6] and is now widely used for investigations in other medical areas [6, 7, 9], besides non-medical subjects [10, 11]. It is also recog- nized as an optical biopsy method [12].

Despite being a promising method for optical diagnosis in dental practice, as reviewed in [13–15], there are few reports of its applications in periodontics [16–20], including one of the pioneer applications of OCT in dentistry [21], and to the best of our knowledge none in clinical practice for treatment follow-up.

Reported here is the result of a sequence of studies which first exploited OCT characterization of the tooth/gin- giva interface in an animal model [16], then to clinical evalu- ation of the periodontal structure in healthy patients in a clinical environment [19], and arriving at the present results demonstrating that OCT is a very effective method for clinical follow-up of the treatment progression of PD.

2 METHODS

2.1 Study design and population screening

This observational in vivo study was approved by the Ethics Committee of ASCES-UNITA (CAAE: 43293715.1.0000.5203). A total of the 147 vestibular dental sites from 49 teeth in 14 patients aged 18-65 years old (six males with 46 years old average and eight females with 36 years old average age) were selected from the anterior teeth, three sites

per tooth (mesiobuccal, midbuccal and distobuccal) of the participants with periodontal disease, from the Center of Dental Specialties at the Faculty of Dentistry, ASCES-UNITA (Centro Universitário Tabosa de Almeida), Pernambuco, Brazil. All patients underwent basic peri- odontal therapy and were evaluated at four stages: day 0, day 30, day 60 and day 90 using the OCT imaging, manual probe and automated probe. Exceptionally one patient was evaluated 1 year after treatment. Excluding criteria were smoking; pregnancy; gin- gival recession, prosthesis, composite restoration or fixed ortho- dontic appliance in anterior teeth.

2.2 Periodontal pocket measurements

Periodontal pocket depth was comparatively measured by 3 instruments: (1) Swept Source OCT at 1325 nm (SS-OCT, Thorlabs, New Jersey); (2) computerized probe (Florida probe, Florida Probe Corporation, Gainsvile, Florida); and (3) manual probe (North Carolina probe, Golgran Millen- nium, São Caetano do Sul, SP, Brazil). The OCT technique is based on the reflectometry of a light beam of low coherence, which crosses the different structures of the tissue, forming the image. Each fixed point traveled by the light, in depth, generates information in graph form, called A-scan. The set of them results in a two-dimensional (2D) image (B-scan) [9]. The analysis was performed by the visual interpretation of B-scan, since they contribute more in terms of information than the isolated A-scan.

The image acquisition was performed using the Swept Source OCT at 1325 nm (SS-OCT, Thorlabs, New Jersey), which operates in the Fourier Domain, with axial resolution of 12 μm and lateral resolution of 25 μm, spectral bandwidth of >100 nm and instantaneous bandwidth of 0.13 nm (0.5 GHz), axial scan rate is 16 kHz, average output power up to 10 mW, and 100 dB sensitivity (Figure 1A). The coherent and narrow- band light source is divided into sample and reference arms. The backscattered light from the sample, according to the different refractive indices within it, is redirected to the sample arm fiber and then combined with light that has traveled a fixed optical path length along the reference arm, interfere and detected in the balanced detectors whose signals are sent to the data acquisition card to form the image through appropriate software. The system captures 25 frames per second. To perform the OCT examina- tion, the patients remained seated in a dental chair, with their head supported perpendicular to the focus of the laser guide light emitter (Figure 1B,C). In addition, a lip retractor was used for better exposure of the anterior teeth (Figure 1B-D). In order to standardize the location of the OCT images and probing, customized silicon trays were prepared for each patient, containing niches

performed with a 15-scalpel blade at the three sites on the vestibular surface of the anterior teeth: mesiobuccal, midbuccal, distobuccal (Figure 1E). At the moment of image acquisition, the patient was instructed to temporarily pause the breath, so that there was no change in the angle of incidence of the central beam and the focal length. The lens placed in the handpiece has 36 mm of focal length, and 25.1 mm of working distance. The probing depths obtained through tools of the equipment software and the images were stored in BITMAP format. The 2D OCT images obtained from each site constitute numerical arrays, com- posed by 2000 columns and 512 lines, distributed along 6-mm transversal scanning. Aiming to suppress the signal saturation due to specular reflections the area of interest was air-dried previ- ous to scanning, and the OCT handpiece should be positioned perpendicular to the surface during scanning. The same system and procedure was employed to demonstrate, in healthy patients, the measurements of pocket depth and other periodontal struc- tures, therefore validating its use in the present work. All mea- surements obtained were corrected considering the gingival refractive index of 1.41 0.06 [19].

A reference standard to measure the depth of the peri- odontal pocket was considered, corresponding to the dis- tance between the enamel dentinal junction as the upper limit and the region where the backscattering changes (as seen in Figure 2). The images obtained in gray scale were evaluated by two calibrated operators using Image J software (processing and image analysis in Java, National Institutes of Health, Bethesda, Maryland). Then sulcus depth records were also obtained by computerized and manual probes. The same examiner performed the records with 20 minutes' inter- val, with the OCT image being performed first. Periodontal pocket depth for both instruments was considered as the dis- tance between gingival margin or enamel dentin junction and the base of periodontal pocket.

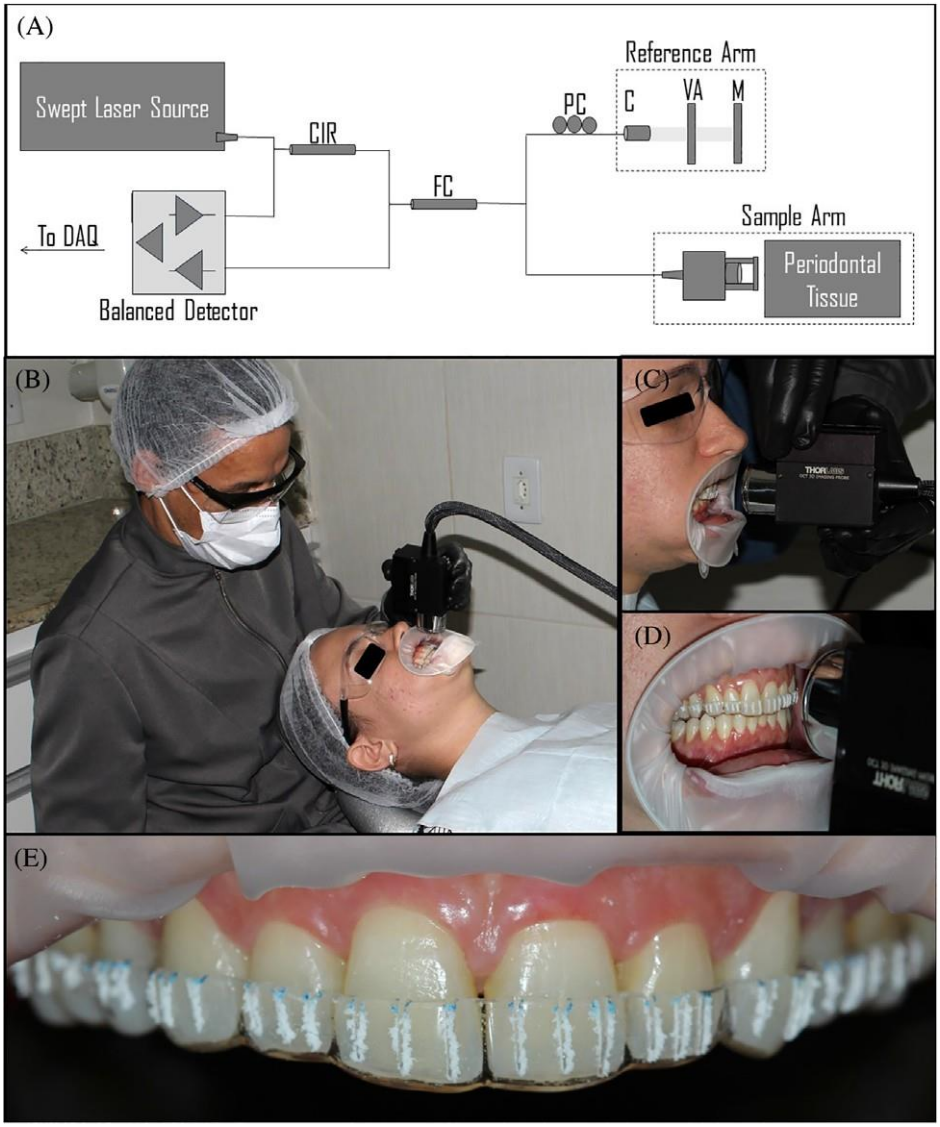

FIGURE 1 (A) The Swept Source OCT (SS-OCT) system simplified scheme. DAQ: data acquisition card; PC: polarization control; FC: fiber connector; CIR: circulator. (B) Patient positioned in a dental chair for OCT images scanning. The tooth surface is positioned perpendicularly to the incident beam, at the appropriate focal distance as shown in (C). To allow the images capture, a lip retractor was used (D), and a silicon plate containing three niches in each tooth (mesiobuccal, midbuccal and distobuccal) standardizes the point of data collection at each session (E)

2.3 Data analysis

The data were analyzed through the interpretation of the images and comparison with the values of the depths of sounding. The depth of survey data collected by two calibrated evaluators, using two manual probing techniques, was used as reference to aid in the interpretation of the find- ings in the images. This qualitative analysis helped in the interpretation and understanding of the images, providing a

unique approach. The images were used as they are provided by the OCT system, without further digital treatment.

3 RESULTS

Figure 2 shows an illustrative OCT image of a healthy indi- vidual (A) and a patient with periodontal disease (B). In the 2D images, it is possible to visualize the architectural com- ponents of the periodontal anatomy, both in healthy and unhealthy region.

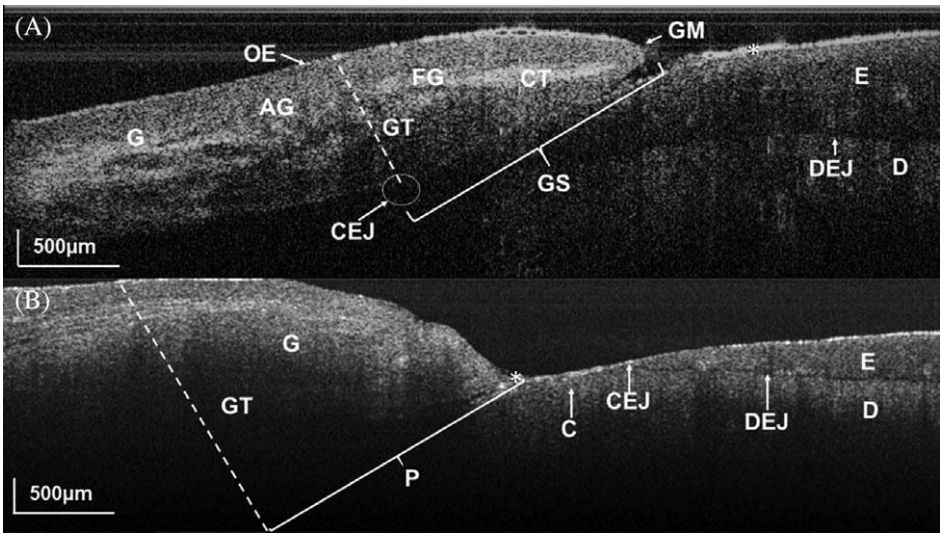

FIGURE 2 Images of the periodontal region of a lower incisor and its anatomical constituents obtained from a healthy (A) and an unhealthy (B) patient. (A) Corresponding to a healthy periodontium, it is possible to identify: gingiva (G), enamel (E); dentin (D); gingival thickness (GT); dentin-enamel junction (DEJ); gingival sulcus (GS), connective tissue (CT); biofilm / dental plaque (*); cement-enamel junction (CEJ); gingival margin (GM); oral epithelium (OE); free gingiva (FG) and attached (AG). (b) Shows some of the same structures visualized in (A), the cement (C) and part of the periodontal pocket (P). The horizontal and vertical scale bars represent 500 µm.

The following images are representative examples of data clinically obtained using the OCT. In Figure 3, it is possible to observe alterations in the periodontal tissue, such as the increase of biofilm thickness and deposition of sub- gingival plaque when comparing before (day 0) and 30-days after the treatment be carried out (Figure 3A,C, respectively). Comparative images allowed visualizing indicative characteristics of the disease regression 30-days after treat- ment, such as the decrease of gingival thickness (Figure 3A, C). Conversely, images in Figure 3B,D show an increase of

thickness observed, indicating that the periodontal therapy was not efficient. A dentin exposure area (Figure 3B,D) is also visualized with a decrease in the area of dentin exposure possibly associated with gingival thickness increasing. It is still possible to notice the presence of vacuolar alterations, suggestive of inflammation (Figure 3D).

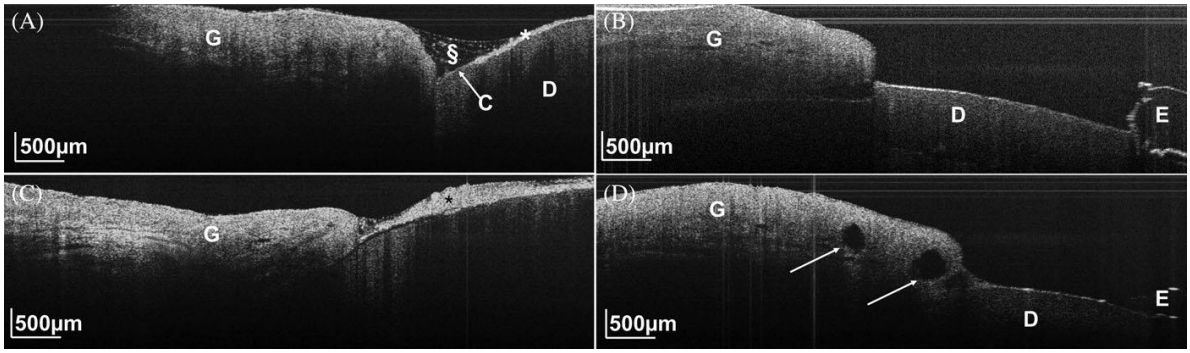

FIGURE 3 OCT images showing changes in periodontal tissues, observed at the initial evaluation (A, B) and after 30 days of periodontal therapy (C, D). (A) and (C) show the reduction of gingival thickness and possible reduction of gingival edema in the region, which may indicate involution of the disease. In (A), it is noted the presence of gingival anatomy components, besides the presence of saliva in the gingival margin region (§) and plaque/biofilm deposition (*). However, it can be observed that in the second assessment (C) there is a greater deposit of supragingival plaque (*), indicating the patient's lack of collaboration with the periodontal therapy. (B) and (D) Correspond to a second patient; in these images the area of exposure of the root dentin (D) can be observed. It is still possible to observe a change in depth periodontal, increasing from 4.32 mm (B) to 6.20 mm (D). After 30 days (D), suggestive areas of vacuolar zones (arrows) may be observed, indicating a sign of active inflammation. All images are in 500 µm scale.

Comparative images of the periodontal region at day 0 and day 60 are shown in Figure 4, exhibiting an increase in subgingival calculus deposition 60-days after periodontal therapy and it is possible to verify the increment in the dis- tance between the cemento-enamel junction and the gingival margin, indicating an increase in gingival recession (Figure 4A,D). Figure 4A,B show initial images obtained which, at 60th day after therapy (Figure 4D,E, respectively) is possible to visualize an increase in gingival thickness, indicating a possible reactivation of the inflammatory pro- cess: 1.51 mm (Figure 4A) to 1.92 mm (Figure 4D) and 1.32 mm (Figure 4B) to 2.68 mm (Figure 4E). In the Figure 4C,F note the decrease of the gingival thickness vary- ing from 2.03 mm (Figure 4C) to 1.24 mm (Figure 4F).

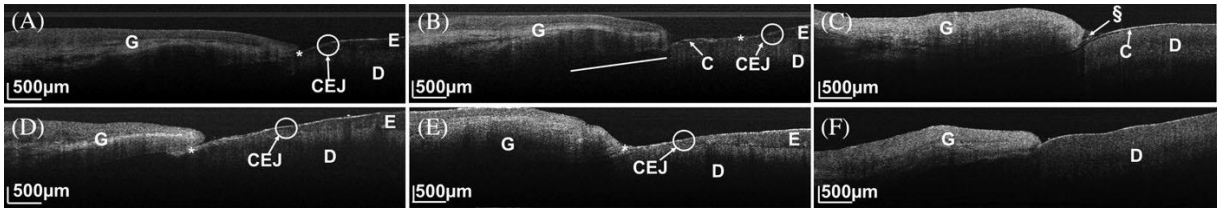

FIGURE 4 OCT images obtained from different patients at day 0 (A-C) and the corresponding images obtained at day 60 (D-F), respectively. By comparing and (D), it is possible to verify in day-60 the increase of: subgingival plaque deposition evaluation, in the distance between the cemento-enamel junction and in the gingival margin, indicating gingival recession. It is still possible to observe a change in gingival thickness, increasing from 1.32 mm (B) to 2.68 mm (E) and decreasing from 2.03 mm (C) to 1.24 mm (F). The presence of saliva in the gingival margin region (§). All images are in 500 µm scale.

The disintegration of the cement layer, probably removed during periodontal scaling (Figure 4B) and the presence of a small amount of supragingival plaque (*), is initially observed in (Figure 4B) and (Figure 4E). In addi- tion, areas of exposed dentin (D) reduced in the images cap- tured at day 60 (Figure 4E), if compared to those at day 0. In the Figure 4C the cement layer is evident (C), whereas in Figure 4F it is observed the loss of this structure and conse- quent dentin exposure.

The images of Figure 5 show an increase in the exposure of dentin after period of 90 days (Figure 5A). Additionally, it was possible to identify the dentin-enamel junction in all images (Figure 5A,B), as well as the presence of supragingival plaque.

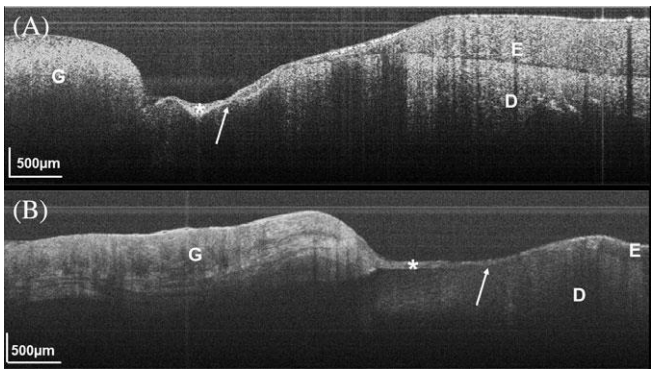

FIGURE 5 OCT images obtained from a lower incisor, evidencing the changes observed initially in the periodontal tissue (A) and 90 days after the initial evaluation (B). Arrows point the area of exposed dentin, which increases after a period of 90 days (B). Increased enamel loss in the region is visible after 90 days. In addition, it was possible to identify the presence of supragingival plaque (*) at both moments. All images are in 500 µm scale.

Figure 6 shows images of a single patient followed up until 1 year after treatment. We can observe the absence of supragingival plaque in Figure 6A and its presence in Figure 6B,C in this last one it is still possible to visualize an increase of biofilm deposition, if compared to Figure 6B. It is clear the variation visualization of the gingival thickness, with moments of increase (Figure 6B) or decrease (Figure 6C), according to the moment evaluated.

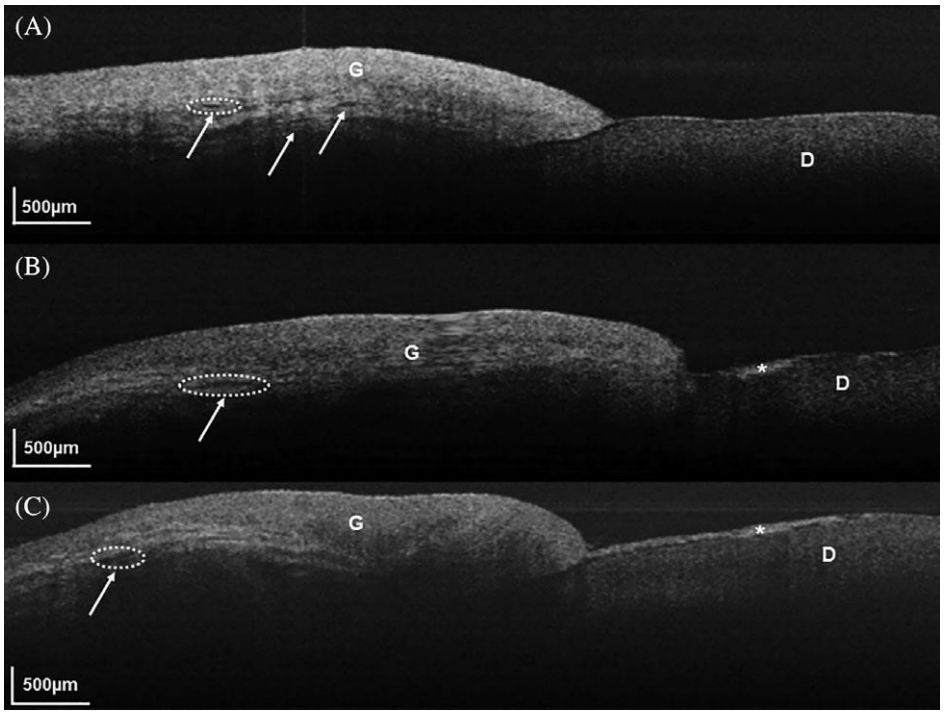

FIGURE 6 Sequence of images obtained from a lower canine and followed up until 1 year after periodontal therapy. The images show the changes observed in periodontal tissue on day 0 (A), day 60 (B) and year after the initial evaluation (C). It is interesting to note that gingival thickness varied by increasing and decreasing (C), according to the moment evaluated. Supragingival plaque (*) can still be observed. It is possible to identify gingival changes (A) suggestive of vacuolar zones (arrows), increasing (B) or decreasing (C) as gingival thickness also varies in this proportion. All images are in 500 µm scale.

From the images of each patient, data of pocket depth can be quantified in millimeters for further analysis. Table 1 shows the mean of the quantitative information from images to 6 obtained using the probe manual instruments (NC/North Carolina; FP/Florida Probe) and OCT. Two evaluators were used for each technique to assure the reliability of the evaluators.

TABLE 1 Mean of the measurements equivalent to the images of Figures 3–6 obtained by two evaluators (1 and 2) using two traditional probe manual instruments (NC/North Carolina; FP/Florida Probe) and OCT.

Periodontal probe	Pocket depth (mm)
NC	3.1 ±1.03
FP	3.6±1.21
OCT	3.3±1.09

4 DISCUSSION

The identification of alterations in periodontium in the subclinical phase, and monitoring of the progression of the peri- odontal disease are still a great challenge in the dental clinic. The measurements obtained with the periodontal probes are essential for the distinction between the depth of healthy areas and regions affected by PD [22]. Measurement errors associated with the instrument and/or technique induced the evolution of the periodontal probes, which is currently in the fifth generation [23]. According to this evolution, OCT could be the sixth generation of periodontal probes, the first using photonics, because it captures bi and three- dimensional images, obtaining transverse images with high resolution in micrometric scale in situ, without physical con- tact or excision, allowing analysis in places where a biopsy could be nonfeasible. The technique can still be used to determine the profiles of in vivo periodontal tissue, such as gingival, epithelial and connective tissue thickness and the position of the alveolar bone crest [20].

Although previous studies have also used the technique for assessing periodontal disease in animal models [16–18, 24], this is the first study that longitudinally evaluates the evolution of periodontal disease in patients. Through OCT images the following structures can be identified, as shown in Figure 2: gingiva; enamel; dentin; dentin-enamel junction; cement bonding; free gingiva; portions of inserted gingiva; gingival margin; oral epithelium; sulcular epithelium; part of the gingival sulcus/periodontal pocket; junctional epithe- lium; connective tissue; calculus deposition; cement; biofilm / plaque deposition. These findings corroborate the results of previous animal model studies [16–18] and healthy individuals [19] in identifying the dental anatomical regions and the periodontal images obtained by the OCT. In addition, it is still possible to see the dentin-enamel junction in all images obtained,

unlike the cemento-enamel junction, which was visualized in most, but not all, of the images.

When evaluating each patient individually, it was possi- ble to observe changes and variations in the regression, maintenance or progression of the periodontal disease in the period evaluated. It is important to notice that not all patients reacted positively to the treatment, which is a common fact in treating periodontal disease since the therapy is very patient dependent, requiring strict oral individual hygiene to be followed. That does not mean that the treatment was not efficient, but clearly shows that it is not being properly followed by the patient and the results are not adequate. For patients following good oral hygiene, the data shows that the treatment is adequate.

Concerning the measurements obtained by the conventional inspection techniques, difference between the moments of the inspection were observed, as well as between the evaluators. This can be illustrated by the mea- surements obtained in patient 1, the depth of probing detected by the evaluator 1 using the hand probe was 6, 2 and 4 mm at the initial evaluation, and 5, 1 and 5 mm after 60 days, to the distal sites, central and mesial, respectively. For evaluator 2, using the same evaluation tool, the values of 5, 2 and 3 mm were initially identified, and after 60 days 4, 1 and 4 mm, respectively, for the same distal, central and mesial sites.

Using an OCT miniature endoscope probe, Meng-Chun et al [25] performed the insertion and visualization of the periodontal pocket and could identify dental calculus in the subgingival region and stated that it is possible to follow the dental surface after periodontal treatment. In our experi- ment, regions with calculus were observed, and identified the increase in supragingival plaque thickness, as can be seen in Figure 3. When comparing the values of depth of probing and the images with 30 days of follow-up, it is possible to affirm that Figure 3B shows a periodontium in regenera- tion, whilst Figure 3D could represent a progression of the disease, justified by the presence of a vacuolar zone.

Hsieh et al [26] demonstrated that OCT images could be used for the detection of subgingival calculus in dentistry. The calculus can be easily distinguished from carious lesions, indicating that OCT is a valuable technique in its detection. In the images obtained, the presence of salivary calculi and biofilm deposition was observed on the surfaces of the elements in the initial image or even in their worsen- ing or improvement after periodontal therapy, as observed in Figure 4A,D and Figure 4B,E,

which shows the biofilm/cal- culus deposition on the images collected 60 days after the periodontal therapy is noted.

After the 60 days' period, areas with dental exposure are probably noticed due to the removal of the cement layer during the periodontal scaling (Figure 4). Figure 4E shows the increase in gingival thickness and may indicate the reactivation of the inflammatory process, a fact evidenced by the depth of the pocket obtained by FP. Possibly the manual probe has not been able to iden- tify the change related to the transition between subclinical and clinical manifestations.

The images obtained after a period of 90 days showed the presence of dentin, dentin-enamel junction and presence of supragingival biofilm/plaque. Some images showed areas of dentin exposure, with increase after 90 days. In Figure 5, it is still possible to observe the evolution of tooth mineral loss, characterizing a non-carious cervical lesion in progres- sion, corroborating the findings of Sugita et al [27], which investigated the progression of non-carious cervical lesions using SS-OCT, and observed that the technique can morphologically differentiate the types of lesions as well as the vari- ations of the disease progression.

Figure 6 allowed to analyze the changes over the course of 1 year; the gingival thickness varied according to the moment of evaluation, showing that the periodontal disease oscillated between the clinical stages, identified by the value of probing (Table 1) and subclinical characteristics seen exclusively in OCT images. In addition, regarding the gingi- val thickness, another notable fact is the presence of vacuo- lar structures (identified by the arrows), which increased (Figure 6B) or decreased (Figure 6C) in the same proportion as the gingival thickness.

It is important to notice that, regardless of the evaluated moment, plaques and calculus were identified in the OCT images, even if they were not clinically evident, reinforcing the importance of the technique for periodontics.

It should be emphasized in this study that the periodontal evaluation was carried out by OCT, computed-controlled and manual probing, from three sites in buccal surface, similar to that recommended in the conventional periogram exam.

It was evident that, although the technique could not sweep the entire extension of the periodontal tissue into a single imaging, OCT was able to identify their anatomical characteristics, such as the extension of pockets to the visu- alization of early biofilm deposits, as well as early tissue changes subclinical level. Park et al [18] observed that the measurements obtained with OCT were smaller than the his-

tological measurements, but the images showed details that allowed the early detection of periodontal disease.

The storage of the captured images at the different moments of evaluation will allow the comparison with future periodontal examinations, to detect changes or inflammatory response in regions of interest. The images can also be easily made available online and even in real time for evaluation at a distance by experts.

5 CONCLUSION

In conclusion, this longitudinal study evidenced the impor- tance of using OCT in the identification of periodontal structures in follow-up of PD treatments. Despite the present limitations, depth of light penetration and scan window lower than the size of the pockets, the technique is efficient in monitoring the periodontal disease. Further studies are certainly necessary to overcome the limitations of the tech- nique. The advances in the development of low cost OCT systems will be of great importance to push its use in not yet exploited clinical environment [28].

ACKNOWLEDGMENTS

This study was carried out under the PRONEX program (Center of Excellence on Biophotonics and Nanophotonics— APQ-0504-1.05/14) supported by FACEPE/CNPq (Foundation for Science and Technology of Pernambuco State and National Council of Technological and Scientific Development) and INCT-INFO (National Institutes of Science and Technology, Institute of Photonics—465.763/2014-6), sponsored by CNPq/ MCT (National Council of Technological and Scientific Devel- opment and Ministry of Science and Technology). The authors are thankful to Golgran Millennium for the donation of manual probes. The authors report no conflict of interest related to this study.

ORCID *Anderson S. L. Gomes* https://orcid.org/0000-0001-6536-6570

REFERENCES

1. WHO—World Health Organization. Oral health: fact sheet, 2012. [WWW document]. http://www.who.int/oral_health/publications/factsheet/en/ (accessed: September 2017).

2. J. Meyle, I. Chapple, *Periodontology 2000* 2015, *69*, 7.

3. I. L. Chapple, P. Bouchard, M. G. G. Campus, M. C. Carra, F. Cocco, L. Nibali, P. Hujoel, M. L. Laine, P. Lingstrom, D. J. Manton, E. Montero, N. Pitts, E. Range, N.

Schlueter, W. Teughels, S. Twetman, C. V. Loveren, F. V. der Weijden, A. R. Vieira, A. G. Schulte, *J. Clin. Periodontol.* 2017, *44*, S18.

4. L. B. Pihlstrom, *J. Periodontol.* 1992, *63*, 1072.

5. G. C. Armitage, *J. Periodontol.* 2003, *74*, 1237.

6. E. A. Swanson, J. G. Fujimoto, *Biomed. Opt. Express* 2017, *8*, 1638.

7. N. Vogler, S. Heuke, T. W. Bocklitz, M. Schmitt, J. Popp, *Annu. Rev. Anal. Chem.* 2015, *8*, 359.

8. D. Huang, E. A. Swanson, C. P. Lin, J. S. Schuman, W. G. Stinson, W. Chang, M. R. Hee, T. Flotte, K. Gregory, C. A. Puliafito, J. G. Fujimoto, *Science* 1991, *254*, 1178.

9. W. Drexler, J. G. Fujimoto, *Optical Coherence Tomography: Technology and Applications*, Springer, Switzerland 2015, p. 2571.

10. H. Liang, B. Peric, M. Hughes, A. Podoleanu, M. Spring and D. Saunders, in: *Proceedings of SPIE: Optics for Arts, Architecture, and Archaeology,* San Francisco, SPIE 2007, 6618, 661605-1.

11. S. L. Campello, W. P. dos Santos, V. F. Machado, C. C. B. O. Mota, S. L. Gomes, R. E. de Souza, *Microporous Mesoporous Mater.* 2014, *198*, 50.

12. J. G. Fujimoto, M. E. Brezinski, G. J. Tearney, S. A. Boppart, B. Bouma, M. R. Hee, J. F. Southern, E. A. Swanson, *Nat. Med.* 1995, *1*, 970.

13. Y. S. Hsieh, Y. C. Ho, S. Y. Lee, C. C. Chuang, J. C. Tsai, K. F. Lin, C. W. Sun, *Sensors* 2013, *13*, 8928.

14. M. Machoy, J. Seeliger, L. Szyszka-Sommerfeld, R. Koprowski, T. Gedrange, K. Woźniak, *J. Healthc. Eng.* 2017, *2017*, 7560645.

15. M. Singh, S. Singh, A. Nagpal, S. Laller, *Int. J. Oral. Maxillofac. Res.*2015, *1*, 22.

16. C. C. B. O. Mota, L. O. Fernandes, R. Cimões, A. S. L. Gomes, *J. Periodontol.* 2015, *86*, 1087.

17. S. H. Kim, S. R. Kang, H. J. Park, J. M. Kim, W. J. Yi, T. I. Kim, *J. Periodontal. Implant. Sci.* 2017, *47*, 13.

18. J. Y. Park, J. H. Chung, J. S. Lee, H. J. Kim, S. H. Choi, U. W. Jung, *J. Periodontal. Implant. Sci.* 2017, *47*, 30.

19. L. O. Fernandes, C. C. B. O. Mota, L. S. A. Melo, M. U. S. C. Soares, D. Silva Feitosa, A. S. L. Gomes, *J. Biophotonics* 2017, *10*, 862.

20. S. Kakizaki, A. Aoki, M. Tsubokawa, T. Lin, K. Mizutani, G. Koshy, Sadr, S. Oda, Y. Sumi, Y. Izumi, *J. Periodontal Res.* 2018, *53*, 188.

21. B. W. Colston, M. J. Everett, L. B. da Silva, L. L. Otis, H. Nathel, *Proceed- ings of SPIE: Lasers in Dentistry III*, San Francisco, SPIE Vol. 2973 1997, p. 216.
22. M. A. Listgarten, *J. Clin. Periodontol.* 1980, *7*, 165.
23. M. Gupta, A. Nirola, S. J. Bhardwaj, *Indian J. Dent. Sci.* 2012, *4*, 114.
24. B. W. Colston, M. J. Everett, L. D. da Silva, L. L. Otis, P. Stroeve, H. Nathel, *Appl. Optics* 1998, *37*, 3582.
25. M. C. Kao, C. L. Lin, C. Y. Kung, Y. F. Huang, W. C. Kuo, *Appl. Optics* 2015, *54*, 7419.
26. Y. S. Hsieh, Y. C. Ho, S. Y. Lee, C. W. Lu, C.P. Jiang, C. C. Chuang, C. Y. Wang, C. W. Sun, *J. Biomed. Opt.* 2011, *16*, 071409.
27. I. Sugita, S. Nakashima, A. Ikeda, M. F. Burrow, T. Nikaido, S. Kubo, J. Tagami, Y. Sumi, *J. Dent.* 2017, *57*, 51.
28. S. Kim, M. Crose, W. J. Eldridge, B. Cox, W. J. Brown, A. Wax, *Biomed. Opt. Express* 2018, *9*, 1232.

APÊNDICE C - ARTIGO JOURNAL OF DENTISTRY AND ORAL BIOLOGY

CAN OPTICAL COHERENCE TOMOGRAPHY TECHNIQUE BECOME THE 6th GENERATION OF PERIODONTAL PROBE?

Luana Osório Fernandes[1], Cláudia Cristina Brainer de Oliveira Mota[2], Anderson Stevens Leônidas Gomes[1,3]

[1] Graduate Program in Dentistry, Universidade Federal de Pernambuco, Recife, PE, Brazil, 50670-901.
[2] Faculty of Dentistry, Associação Caruaruense de Ensino Superior e Técnico, Caruaru, PE, Brazil, 55016-400.
[3] Department of Physics, Universidade Federal de Pernambuco, Recife, PE, Brazil, 50670-901.

Optical coherence tomography (OCT) is already one of the most important imaging modalities in biophotonics [1], widely used in Ophtalmology, providing optical biopsies with micrometer spatial resolution. Penetration depth of up to 3mm is typical and tissue dependent. Imaging speed of 10^7-10^9 voxels/s can be achieved, and OCT is capable of multimodality integration [2]. Although the recent review in ref. [1] shows the fantastic advances of OCT in several biomedical areas, in Dentistry a lot more research is required before clinical/commercial impact becomes beneficial for the society.

Among oral cavity diseases, periodontal diseases (PD) are chronic multifactorial conditions, characterized by the destruction of periodontal tissues. Periodontal health depends on the balanced relationship between the dental biofilm and the immunoinflammatory response of the host [3].

Traditionally, PD diagnosis is performed through clinical examination to detect signs of inflammation, calculus and supra and subgingival presence, as well as evaluation of clinical insertion and loss of bone through periodontal probing. Despite the low cost, wide use and acceptance in the scientific and clinical environment, traditional periodontal probing is prone to errors during its execution, in addition to not identifying PD in the subclinical phase [4].

The search for an early diagnosis method, as well as the monitoring of periodontal tissues with greater precision and sensitivity allied to noninvasiveness, has triggered interest in the use of alternative techniques such as OCT [5,6 and refs therein].

Following the work of [5,6], besides other literature studies, our group has performed a clinical study by following-up patients treated from periodontal disease with OCT, and comparing the results with traditional periodontal probes. 14 patients aged 18-65 years old diagnosed with periodontal disease were evaluated prior and after treatment, and a total of 147 vestibular dental sites from 49 anterior teeth were analyzed. Preliminary results were already reported [7]. Our conclusions from the longitudinal study clearly point out to the importance of using Optical Coherence Tomography in the identification of periodontal structures in follow-up of treatments. Despite some present technical limitations, such as light penetration depth and scan window lower than the size of the pockets, OCT presents advantages as noninvasiveness, possibility of 2D and 3D images in real time, which can be assessed at distance by experts, providing a real case for telemedicine. The technique is efficient in monitoring not only, periodontal disease but has also applications in other niches in dentistry, both in soft and hard tissue, as well as dental materials. In the particular case of PD, manual periodontal probes have evolved to minimize errors and operator manipulation, and are currently in their fifth generation [8]. When one associate the advantages of OCT as a noninvasive method associated to appearance of low cost OCT systems [9], we as the question whether it would not be the ideal tool for the next – 6th - generation of periodontal probes, the first one to exploit photonics.

[1] Swanson, E. A., and Fujimoto, J. G. (2017) The ecosystem that powered the translation of OCT from fundamental research to clinical and commercial impact. *Biomedical Optics Express* **8**, 1638.

[2] Vogler, N.,et al (2015). Multimodal imaging spectroscopy of tissue. *Annual Review of Analytical Chemistry* **8**, 359-387.

[3] Chapple, I. L., et al (2017). Interaction of lifestyle, behaviour or systemic diseases with dental caries and periodontal diseases: consensus report of group 2 of the joint EFP/ORCA workshop on the boundaries between caries and periodontal diseases. *Journal of Clinical Periodontology*, **44**, S18.

[4] Pihlstrom, B. L. (1992). Measurement of attachment level in clinical trials: probing methods. *Journal of periodontology* **63**(12s), 1072-1077.
[5] Mota, C. C., et al (2015). Non-invasive periodontal probing through fourier-domain optical coherence tomography. *Journal of Periodontology* **86**(9), 1087-1094.
[6] Fernandes, L. O., et al (2017). In vivo assessment of periodontal structures and measurement of gingival sulcus with optical coherence tomography: a pilot study. *Journal of Biophotonics*, **10**(6-7), 862-869.
[7] Mota, C. C., et al (2017). Non-invasive diagnostic and monitoring of periodontal disease through optical coherence tomography: validation of the technique with animal model and patients. In *CLEO: QELS_Fundamental Science* (pp. JW2A-50). Optical Society of America.
[8] Gupta, M., Nirola, A., & Bhardwaj, S. J. (2012). Advances In Clinical Diagnosis In Periodontics. *Indian Journal of Dental Sciences*, **4**.
[9] Kim, S., Crose, M., Eldridge, W. J., Cox, B., Brown, W. J., & Wax, A. (2018). Design and implementation of a low-cost, portable OCT system. Biomedical Optics Express, 9(3), 1232-1243.

APÊNDICE D - MONITORING THE GINGIVAL REGENERATION AFTER AESTHETIC SURGERY WITH OPTICAL COHERENCE TOMOGRAPHY

Luana O. Fernandes[b], Nathalia D.R.L. Graça[b], Luciana S.A. Melo [a], Claudio H.V Silva[b], Anderson S.L.Gomes[a]

[a]Dept. of Physics, University Federal of Pernambuco, Av. Prof. MoraesRego, 1235 - CidadeUniversitária, Recife, PE Brazil 50670-901; [b]Graduate Program in Dentistry, University Federal of Pernambuco, Av. Prof. MoraesRego, 1235 - CidadeUniversitária, Recife, PE ,Brazil 50670-901

ABSTRACT

The aim of this study was to use the Optical Coherence Tomography (OCT) technique working in spectral domain (Swept Source OCT at 1325 nm, Thorlabs, New Jersey, USA) to monitor the tissue repair in patients undergoing periodontal plastic surgery. The evaluations were done over a period of 60 days. It was observed that 15 days after periodontal surgery the gum was still in different healing process as compared to the observation after 60 days. Thus it is clear that, despite some technical limitations, the OCT is an efficient method in the evaluation of regeneration gingival.

Keywords: Optical coherence tomography; Investigative Techniques; Gingiva; Clinical Evaluation.

1. INTRODUCTION

The facial aesthetic standard adopted by society is based on a beautiful and harmonious smile, and to supply this need, there is a big search for new treatments. The matching of gum and teeth, especially the front ones, plays an important role in aesthetics, and seeks to meet the current standards of beauty through periodontal surgery.[1-3]

Periodontal plastic surgery presents a high impact on the self-esteem of the patients and, consequently, in their quality of life in society. The gingivoplasty aims to corrector eliminate abnormal gingival anatomy by trauma or development, providing there establishment of gingival aesthetics.[4] Clinically, the recovery of normal gingival appearance is observed 14 days after the surgery, despite the knowledge that this

period is enough just to complete reepithelization and histological healing takes 4 to 5 weeks.[5]

1.1 Imaging by Optical Coherence Tomography

New non-invasive diagnosis methods through image and using the non-ionizing radiation draw attention and great interest of researchers and clinicians. Optical coherence tomography (OCT)[6] is a noninvasive image diagnostic technique, which provides high-resolution in almost real time images.[7] It is considered an optical biopsy because it allows the visualization of cellular and extracellular structures typically up to 3 mm below the surface, depending upon the tissue and wavelength employed, with a spatial resolution ranging from 1 to 20 µm. [8]

The OCT is one of the few instruments that exploit the benefits and the properties of light coherence and is very useful in healthcare.[9] Colston *et al*.[10] were the first to study the oral cavity tissues using the OCT, *in vitro*, identifying the great clinical potential for research the periodontal tissues. Thus, the technique became a good tool for periodontal diagnosis because it is able to penetrate deep enough, keeping a reliable high resolution.[11] It ensures a quick view of the superficial structure of the gingival tissue, reproducing their specific characteristics, in different sections of the oral cavity, and also the study of the gingival morphology.[12]

The aim of this study was to use the Optical Coherence Tomography (OCT) technique, working in spectral domain, to monitor the process of tissue reparation in patient undergoing periodontal plastic surgery, observing the gingival behavior over a period of 60 days from 42 sites on the vestibular face of the anterior teeth.

2. METHODOLOGY

2.1 The patient

A young female patient went to the Integral Clinic of the Dentistry course, at the Federal University of Pernambuco (UFPE) dissatisfied with the aesthetics of her smile. During clinical examination, it was possible to observe diastemas widespread in the upper and lower arch plus a gum disharmony (Figure 1).

Figure 1. Initial appearance of the patient smile (from the authors archive).

The patient was submitted to clinical and radiographic examinations. After that, it was suggested that gingival esthetics correction should be performed on the upper (from 14 to 24) and lower (from 33 to 43) elements. After the written consent of the patient, the treatment was properly planned and started.

2.2 The gingival surgery

The periodontal flap surgery was the technique chosen for the upper arch. An acetate tray was used as guide, for marking the new measure of the gingival margin (Figure 2 A).

First, the slices of keratinized soft tissue were carefully removed, aiming to provide the aesthetic contour of the gingival rgin (Figure 2 B).

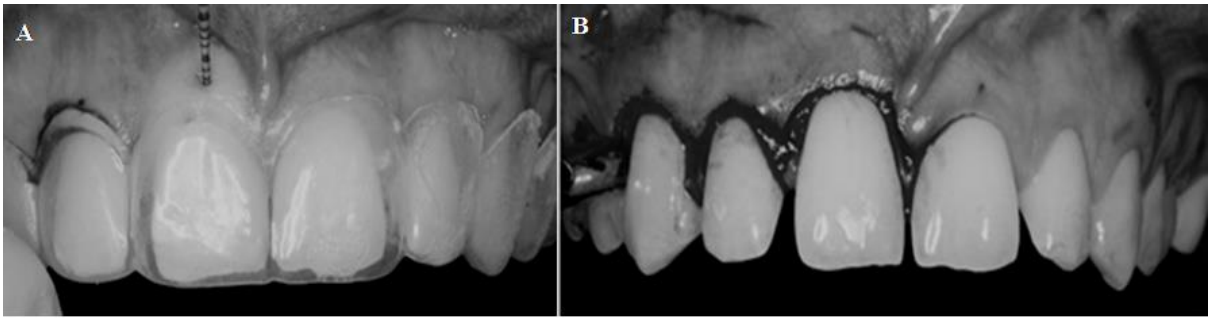

Figure 2. A, the use of acetate tray as guide for the marking of bleeding points; B, Removal of keratinized soft tissue (from the authors archive).

After that, it was performed the gingival flap surgery, osteotomy and osteoplasty, accurately, for recovering the periodontal biological width and smoothing the bone structure. The surgical proceeding was concluded after the flap replacement.

2.3 Optical Coherence Tomography evaluation

In applying the OCT technique, sagittal images of the cervical third of the element 11, 12, 21 and 22 were obtained before surgery, as a control image of the healthy gingiva and periodontal region. Images were acquired again 15 and 60 days after periodontal surgery to monitor the recovery of tissues.

The OCT Swept Source 1325 nm (SS-OCT, Thorlabs, New Jersey, USA) with 12 µm depth resolution and 25 µm lateral resolution which operates in the spectral domain, was used for the acquisition of images. During the examination, the patient was kept sat with her head resting on specific positioner, perpendicular to the focus emitting laser light, in order to standardize the capture of images. In addition, lip retractor was used for better viewing of the area being studied. Figure 3 shows a sagittal image of the middle third of the element 21 obtained through OCT in which it is possible to observe the enamel (E), the dentin (D), the dentino-enamel junction (DEJ), the gingival (G) and gingival sulcus (GS).

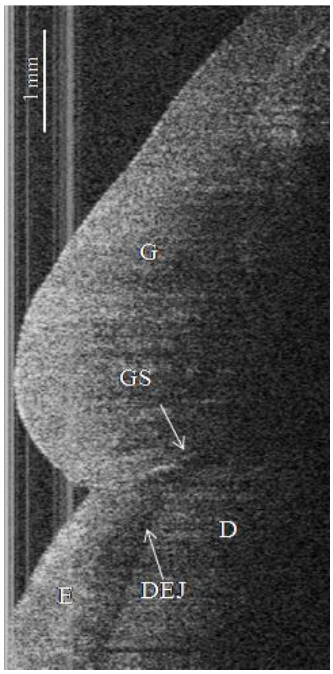

Figure 3. The sagittal image of the element 21, middle third, showing structures such as: E-enamel, D - dentin, DEJ-dentino-enamel joint, G-gum and S - gingival sulcus.

3. RESULTS AND DISCUSSION

As pointed out before, the smile is one of the most important facial expressions and it is essential in expressing friendliness, agreement, and appreciation. A pleasing smile clearly enhances the acceptance of an individual in our society by improving the initial impression in interpersonal relationships. However, a defective smile might be considered properly as a physical handicap.[2] For this reason, aesthetics has motivated the patients to seek dental treatment.

Currently, patients are aware that the aesthetic appearance of the smile is determined not only by the shape and color of the teeth, but also by the harmony and health of the gingival tissue. In many cases, the blend of periodontal cosmetic surgery with other restorative procedures can create a synergistic result, which would not be obtained with the single treatments.

In the present case, plastic surgery for leveling periodontal gingival margin is previously indicated to the aesthetic restorative treatment. For this reason, the treatment proposed in this clinical case associated periodontal surgery prior to placing lumineers.

To assess the tissue recovery after surgery, the Optical Coherence Tomography technique was chosen. OCT is an imaging technology that produces high-resolution cross-sectional images of the internal microstructure of living tissue. It is already in use since 1991.[6] OCT was initially applied for imaging in ophthalmology.[6,14] However, it is now being widely used in dentistry,[9,15]including dental materials.[16,17] Regarding soft oral tissues, *in vitro* evaluation of periodontal morphology in animal has been recently reported[18] as well as phenotype evaluation in animal and human patients.[19]

During the healing process of the present case, the tissue recovery was accompanied. For this, OCT images were acquired in three moments: before the surgery when the tissues had suffered no damage, 15 and 60 days after the surgery, always at the cervical region of the upper anterior teeth, as shown in Figures 4 (A), (B) and (C), respectively.

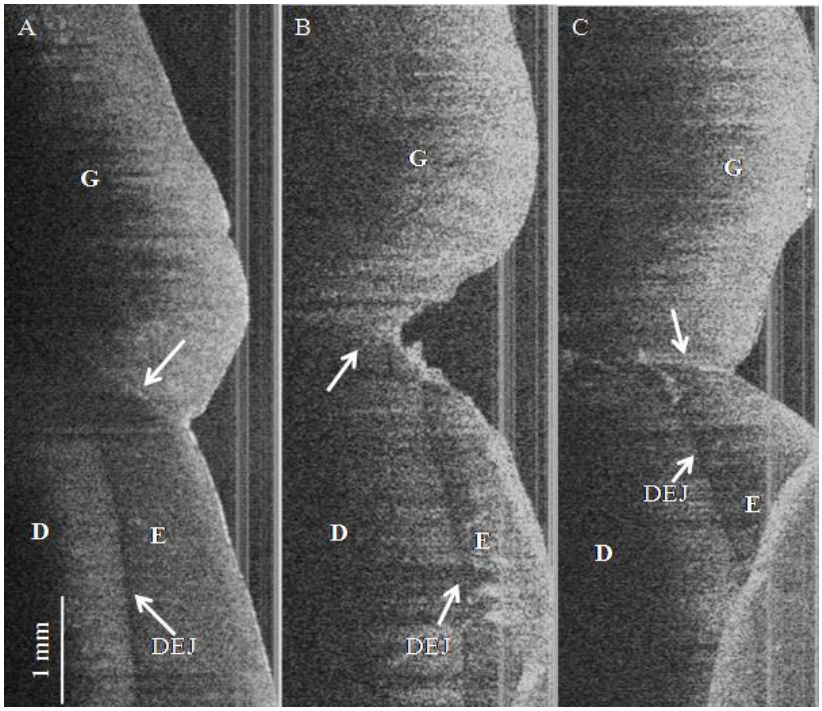

Figure 4. Sagittal images of the element 11 cervical third: A, before surgery, B, 15 days and C, 60 days after periodontal surgery. E-enamel, D - dentin, DEJ- dentino-enamel joint, and G-gum. Arrows indicates the area of tooth-gum interface.

In analyzing Figure 4, attention should be paid to the gingival sulcus indicated by the arrows in Figures 4A, 4B and 4C. In Figure 4A it is possible to visualize the gingival sulcus close to tooth surface, and with its natural inclination; in Figure 4B, 15 days after the gingivoplasty, there is no continuity between the free gingiva and tooth surface, due to the surgery incision. It can also be seen the dentin exposure and possibly some biofilm. 60 days post-operative procedure (Fig. 4C) it is possible to observe the reinsertion of gingival epithelium over the tooth, indicating the healing of the surgical procedure. Notice that the gingival sulcus position is rather horizontal, if compared to the pre-operative procedure image of Figure 4A.

Another important information observed after Figure 4 analysis is about the dentino-enamel joint. It is wholly covered by the gingiva before the surgery (Figure 4A). After that, it is exposed to oral environment, as observed in Figure 4B. Its exposition to salivary fluid and its pH and temperature variations can be uncomfortable and even painful to the patient. This problem was solved after the tissue reepithelization, as shown in Figure 4C, which shows this area cover again.

The aspect presented by the OCT images after the 60 days period showed full recovery of periodontal tissues, as well as the presence of new periodontal sulcus. The clinical aspect in Figure 5 confirms the fact. Only after the period, the restorative treatment has started.

Figure 5. Gingival clinical aspect 2 months after the periodontal surgery (from the authors archive).

4. CONCLUSION

After using OCT images to evaluate periodontal structures, it is possible to assure that this technique is promising method to follow up the tissues recovery after a surgical procedure, adding to the clinical visual observation. The images obtained were consistent with the clinical inspection of the region under went to surgery, confirming the OCT efficacy without the patient to undergo invasive tests, as the use of dental probes, or ionizing radiation. Quantitative measurements of the tissue recovery can also be implemented using the OCT.

ACKNOWLEDEGEMENTS

The authors are thankful to FACEPE (Foundation for Science and Technology of Pernambuco State), CNPq (National Council of Technological and Scientific Development) and MCT (Ministry of Science and Technology) for financial support. This study was carried out under the PRONEX FACEPE/CNPq (Center of Excelence on Biphotonics and Nanophotonics) program and INCT (National Institute of Science and Technology) of Photonics program, sponsored by CNPq/MCT.

REFERENCES

[1] Ahmad, I. “Geometric considerations in anterior dental aesthetics: restorative principles,” Pract Periodontic Aesthetic Dent. 10, 813-23 (1998).

[2] Tjan, A. L., Gary, D. M. and Josephine, G.P. "Some esthetic factors in a smile," J Prosthet Dent 51(1), 24-28 (1984).

[3] Touati, B. “Defining form and position,” Pract Periodonttics Aesthet Dent. 10, 800-7 (1998).

[4] Levine, R.A., McGuire, M.“The diagnosis and treatment of the gum my smile,”Compend Contin Educ Dent 18, 757-64 (1997).

[5] Lindhe, J., Lang, N.P. andKarring, T.,[Tratado de Periodontologia Clínica e Implantologia Oral], Editora Guanabara Koogan, Rio de Janeiro(2010).

[6] Huang, D., Swanson, E. A., Lin, C. P., Schuman, J. S., Stinson, W. G. W., Chang, M., Hee, R. T., Flotte, T., Gregory, K., Puliafito, C. A., and Fujimoto, J. G., “Optical coherence tomography,” Science 254, 1178–1181 (1991).

[7] Wojtkowski, M. “High-speed optical coherence tomography: basics and applications,“ Appl Opt 49(16),D30-D61(2010).

[8] Podoleanu, A. G. “Optical coherence tomography,” Br J Radiol 78(935), 976-88 (2005).

[9] Hsieh, Y. S., Ho, Y. C., Lee, S. Y., Chuang, C. C., Tsai, J. C., Lin, K. F., and Sun, C. W. “Dental optical coherence tomography,” Sensors 13(7), 8928-8949 (2013).

[10] Colston Jr, B. W., Everett, M. J., Da Silva, L. B., Otis, L. L., Stroeve, P., Nathel, H. “Imaging of hard-and soft-tissue structure in the oral cavity by optical coherence tomography,”. Appl Opt 37(16), 3582-3585 (1998).

[11] Schmitt, J. M., Knüttel, A., Yadlowsky, M. and Eckhaus, M. A. “Optical-coherence tomography of a dense tissue: statistics of attenuation and backscattering,” Phys Med Biol 39(10), 1705-1720 (1994).

[12] Feldchtein, F., Gelikonov, V., Iksanov, R., Gelikonov, G., Kuranov, R., Sergeev, A., and Warren, J., “*In vivo* OCT imaging of hard and soft tissue of the oral cavity,” Opt Express 3(6), 239-250 (1998).

[13] Xiang, X., Sowa, M. G., Iacopino, A. M., Maev, R. G., Hewko, M. D., Man, A., and Liu, K. Z.,“An updateon novel non-invasive approaches for periodontal diagnosis,” J Periodontol 81(2), 186-198 (2010).

[14] Swanson, E. A., Izatt, J. A., Hee, M. R., Huang, D., Lin, C. P., Schuman, J. S., Puliafit, C. A. and Fujimoto, J. G. “*In vivo* retinal imaging by optical coherence tomography,” Opt. Lett. 18(21), 1864–1866 (1993).

[15] Mota, C. C. B. O., Gueiros, L. A., Maia, A. M., Santos-Silva, A. R., Gomes, A. S., Alves, F. de A., Leão, J. C., de Freitas, A. Z., Goes, M. and Lopes, M. A. "Optical coherence tomography as an auxiliary tool for the screening of radiation-related caries," Photomed Laser Surg 31(7), 301-306 (2013).

[16] Monteiro, G. Q. M., Montes, M. A., Rolim, T. V., de Oliveira Mota, C. C., Kyotoku, B. B. C., Gomes, A. S. and de Freitas, A. Z. "Alternative methods for determining shrinkage in restorative resin composites," Dent Mat 27(8), e176-e185 (2011).

[17] Monteiro, G. Q. M., Montes, M. A., Gomes, A. S., Mota, C. C., Campello, S. L. and Freitas, A. Z. "Marginal analysis of resin composite restorative systems using optical coherence tomography." Dent Mat 27(12), e213-e223 (2011).

[18] Mota, C. C. B. O., Fernandes, L. O., Cimões, R. and, Gomes, A. S. "Non-Invasive Periodontal Probing Through Fourier Domain Optical Coherence Tomography," J Periodontol 86, 1087-1094 (2015).

[19] Mota, C. C. B. O., Fernandes, L. O., de Melo, L. S. A, Feitosa, D. S., Cimões, R. and Gomes, A. S. L. "Comparative analysis of gingival phenotype in animal and human experimental models using optical coherence tomography in a non-invasive approach," Proc. of SPIE 9531 95313S-1 (2015).

APÊNDICE E - OPTICAL COHERENCE TOMOGRAPHY INVESTIGATIONS OF CERAMIC LUMINEERS

Luana O. Fernandes[b], Nathalia D.R.L. Graça[b], Luciana S.A. Melo [a], Claudio H.V Silva[b], Anderson S.L.Gomes[a]

[a]Dept. of Physics, University Federal of Pernambuco, Av. Prof. Moraes Rego, 1235 - Cidade Universitária, Recife, PE Brazil 50670-901; [b]Graduate Program in Dentistry, University Federal of Pernambuco, Av. Prof. Moraes Rego, 1235 - Cidade Universitária, Recife, PE ,Brazil 50670-901

ABSTRACT

Lumineers are veneer laminates used as an alternative for aesthetic dental solutions of the highest quality, but the only current means of its performance assessment is visual inspection. The objective of this study was to use the Optical Coherence Tomography (OCT) technique working in spectral domain to analyze *in vivo* in a single patient, 14 lumineers 180 days after cementation. It was possible to observe images in various kinds of changes in the cementing line and the laminate. It was concluded that the OCT is an effective and promising method to clinical evaluation of the cementing line in lumineers.

Keywords: Optical Coherence Tomography, Dental Porcelain; Clinical Evaluation

1 INTRODUCTION

Oral aesthetics is related to social, cultural and psychological factors. Recent studies have provided the development of new dental materials, including ceramic laminates, which are reduced veneer laminates with thickness ranging from 0.2 to 0.8mm. They are a treatment option that ensures a good aesthetic result, allowing a correction for color, shape and teeth position. Its great advantage is that preparation is not required, or at most minimal intervention to the tooth surface. Therefore, this treatment is based on the adhesive dentistry and the cementation is a fundamental procedure for the clinical success of the restorations [1].

To date, the evaluation of lumineers adaptation and of their clinical integrity is limited to visual inspection, which can compromise the success of the treatment and is dependent on the clinician ability only [2].

The aim of this study was to use the Optical Coherence Tomography (OCT) technique, working in spectral domain, to analyze the integrity and adaptation of 14 lumineers, 180 days after cementation, *in vivo*.

1.1 Optical Coherence Tomography

Optical Coherence Tomography (OCT) was proposed in 1991 by Huang et al. [3] who demonstrated its ability to acquire cross-sectional images in high resolution, identifying the internal microstructure of materials and biological systems. The images are obtained by measuring the light that is retro-reflected and scattered, without needing to cut the samples to be studied, or even exposing the patient to ionizing radiation. OCT has a penetration capacity in depth of up to 3 mm, depending upon the tissue, resulting in imaging with resolution 1-20 μm.

Initially OCT was mainly used in Ophthalmology, but nowadays its widespread applications incudes dermatology, dentistry and other medical and non-medical areas are using the technique [4,5]. In dentistry, it can be used to evaluate the tooth-restoration interface [6], which could have positive implications in noninvasive diagnosis for secondary caries, adhesive failures in indirect restorations, as well as fractures and cracks in composite resins[7,8].

2 METHODOLOGY

2.1 Patient recruitment

A young female patient at the Integral Clinic of the Dentistry undergraduate course, at Federal University of Pernambuco (UFPE), dissatisfied with her smile aesthetics, was recruited and formally agreed to participate.

2.2 Clinical examination

During clinical evaluation, it was possible to observe widespread diastemas in the upper and lower arch (Figure 1) of the patient. After clinical and radiographic detailed examination, a clinical planning for lumineers fabrication, involving the upper elements 14 to 24 and the lower elements 33 to 43, was presented to the patient.

Figure 1. Initial appearance of the smile. It is possible to observe the upper and lower diastemas (From the authors archive).

2.3 Treatment

After the patient formally agreeing with the proposed treatment, an alginate impression (Hydrogum, ZHERMACK) was taken to obtain a diagnostic cast for studying. Then, the bite was registered and the casts were fixed at a semi-adjustable articulator to perform the dental diagnostic wax-up.

Before starting the aesthetic treatment, a homemade teeth whitening was accomplished for 15 days by using Carbamide Peroxide 16% (White & Brite Night, 3M/ESPE). After the whitening 15 days finished, dental drill 3131 (KG Sorense) and Sof-Lex Pop-On discs (3M/ESPE) were used for teeth abrasions.

To promote the gingival retraction and provide a more faithful reproduction of cervical thirds, gingival retraction cords (000, Ultrapack / Ultradent) were used. After their localization, molds were acquired by using addition silicone (Express, 3M/ESPE).

Dental models for waxing, digital photographs and informations related to morphology, color and teeth details were sent to prosthesis laboratory, aiming the best aesthetic result. The prosthesis laboratory returned lumineers for test, made by wax and resin (Figure 2 A). They were proved, adjusted and sent off to the laboratory for lumineers manufacturing.

The lumineers were fabricated by using IPS e.max Ceramic system (Ivoclar Vivadent), followed by characterization. The lumineers adaptation was evaluated in the plaster models (Figure 2 B) and, later, in the mouth, with specific material for this procedure (Variolink Veneer Try-in, Ivoclar Vivadent). After the former steps, the ceramic lumineers were fixed according to the manufacturer recommendations.

Figure 2. Manufactured lumineers. A, for test, made by wax and resin. B, final lumineers in ceramic (From the authors archive).

The internal surfaces of the lumineers were etched with hydrofluoric acid (HF) 4% (Ivoclar Vivadent) for 30 seconds. After that, the acid was completely removed. Then the pieces were dried and silane (Monobond Plus, Ivoclar Vivadent) was applied for one minute, followed by drying with compressed air. It was then applied an adhesive (Excite F, Ivoclar Vivadent), followed by mild air stream and cured for 15 seconds.

The dental substrate was prepared by using 37% phosphoric acid (Total Etch, Ivoclar Vivadent) for 15 seconds, washing and drying after that. A layer of adhesive (Excite F, Ivoclar Vivadent) was applied at the teeth surfaces, followed by mild air blow and cured for 15 seconds.

After the preliminary preparation of the facets and the tooth, lumineers were cemented. At this stage, Variolink® veener cement translucent, previously selected, was directly applied on the internal surfaces of the facets with the applicator tip (Variolink® veener). When the facets were placed in the correct position, light pressure was exerted. After, removal of the excess with a brush followed the photopolymerization, for 30 seconds. The process was repeated until the cementing of the laminate was completed (Figure 3). The final adjustments were fulfilled in maximum intercuspation, considering the jaw movements.

Figure 3. Aspect of lumineers immediately after cementation of the teeth in the patient mouth (From the authors archive).

2.4Monitoring the clinical study

The clinical study was evaluated after 6 months. Seeking to evaluate the treated region, sagittal images were obtained by Optical Coherence Tomography. The acquisition of images was performed using the Swept Source OCT at 1325 nm (SS-OCT, Thorlabs, New Jersey, USA), with 12 µm depth resolution and 25 µm lateral resolution, which operates in the spectral domain. To facilitate the acquisition of images, the patient remained sitting with her head resting on specific position, allowing the light focusing perpendicular to the study area. In addition, a lip retractor was used to avoid the study area of any bulkhead. The information was stored in jpeg format.

3 RESULTS AND DISCUSSION

A harmonious and aesthetic smile is generally desirable for any patient. This fact drives the development of new materials and techniques in dentistry, seeking more conservative procedures and better results. Among various treatment options for cosmetic purposes, the lumineers are noted for aesthetic naturally present, appropriate color, morphological stability and acceptability by biological and periodontal tissues, and are also considered as a conservative treatment [9]. Current adhesive systems and resin cements enables an effective interaction between the ceramic and the tooth structure, providing that the techniques of ceramics restorations preserve healthy tooth structure and promote the physical and mechanical retention [10].

Advances in adhesive dentistry optimized the use of veneers and porcelain crowns. Initially conventional ceramics were used, however, they were limited by high failure rates due to the high friability and low flexural strength. They were not able to withstand the mechanical stresses in the buccal environment and could generate more wear on

the opposing tooth. The increased resistance of ceramic veneers was possible with the development of new ceramic systems reinforced by leucite and lithium disilicate. These systems require no metal, providing excellent cosmetic result without compromising the mechanical performance [11, 12].

In this clinical study IPS e.Max system was used because it is a lithium disilicate glass ceramic with optimized translucency, durability and strength for full anatomical restorations. IPS e.Max truly mimics the natural translucency necessary for outstanding aesthetic appearance. It has been the material of choice for minimally invasive aesthetic dentistry.

Because of the new ceramic system, it is possible to use very thin ceramic laminates (0.1 to 0.7 mm thick) on tooth structure, with minimal or no wear. Therefore, the color of the cement used is fundamental on the final aesthetic result, especially when the election of ceramics have high translucency. Variolink Veneer Ivoclar Vivadent was the cement chosen because of its advantages such as ease of excess removal, shades available and high mechanical resistance.

Laminates when fully cemented are extremely resilient. The perfect continuity between the cement and the tooth surface gives superior resistance, required for successful treatment. However, current available cementing techniques are prone to the appearance of bubbles in cement line (due to mixing and handling), difficulting an ideal cementing.

Very recently, an *in vitro* study was performed to evaluate the cementation after aging simulation of 20 lithium disilicate laminates divided into 4 groups, with images made by SD-OCT [13]. From the OCT images, it was readily found – almost real time - that all groups showed various types of failure, such as bubbles, gaps or even interruption of the cementation line. It results in variations in the thickness of cement and certainly contributes to the air bag formation and cracking, which increases over time and culminates in the detachment of the restoration or its fracture as a result of the creation of a weak area resulting from a discontinuity in the adhesion line. The OCT showed to be able to view the cement layer below the ceramic laminate, validating the technique as an accurate method in the investigation of lumineer- cement- tooth [13]. As in that study, the findings visualized corroborate the observation in the *in vivo* case reported here (see Figure 4).

The methods currently available for evaluating failure in the cementing line (clinical and radiographic inspection) often do not allow its correct identification [2]. In the present

study this limitation has been overcome since the OCT allowed *in vivo* imaging of cementing line and identifying defects in the interface laminate- cement- tooth, which can be performed in almost “real-time” and during or after the procedure.

The case reported was evaluated after 6 months, when a color change, between the middle and incisal thirds, was detected at element 11, as pointed out in Figure 4A.

By analyzing the tomographic images, it was observed that the cement line is clearly visible and homogeneous between the enamel dental and the lumineer, as can be seen in the cervical third image (fig. 4B). In the medium and incisal thirds, faults have been clearly identified in the cementing line in the form of bubbles at the location where the color change was clinically detected (Figures 4C and D). We propose that this observation of bubble formation (as as example of failure), which can be detected in very early stages, right after the cementation procedure, see [13], can be the cause for further failures, including color changes.

It is important to draw attention to the fact that in the present case, the failure appeared externally in the color change, which induced our OCT study. The ideal situation is to employ the OCT to evaluate the cementation procedure immediately after the lumineer placement, to verify the presence of bubbles or other undesirable artifacts.

As far as we know, OCT is presently the only way to verify and even quantify the presence of undesirable artifacts and failures in the particular case of lumineers placement, providing *in vivo* noninvasive observation.

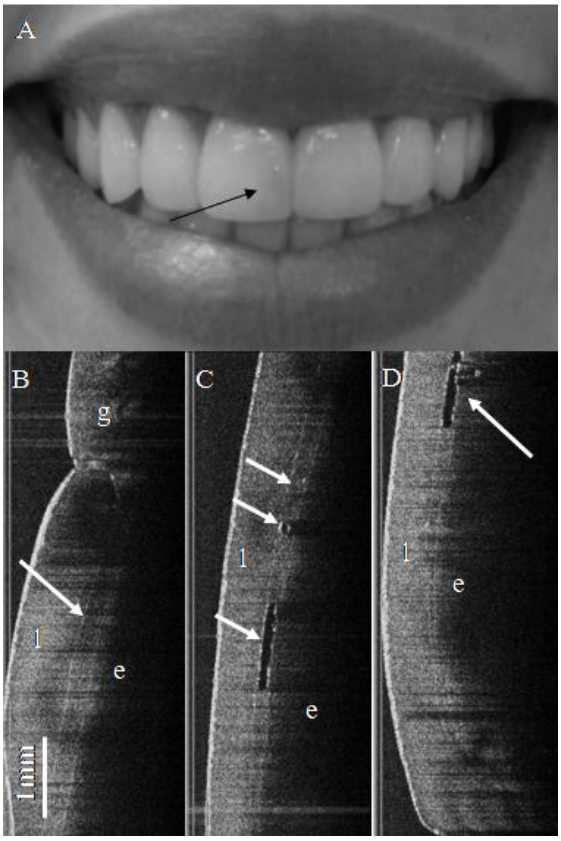

Figure 4. A, photograph of the patient after 6 months of lumineers placement. The arrow indicates the site of the color change. B, image acquired by Optical Coherence Tomography from the cervical third. The arrow indicates the cement layer located between the lumineer (l) and the dental enamel (e); C, OCT image from the middle third and D, from the incisal third. The arrows in both indicate the detected failure (bubble). (From the authors archive).

4 CONCLUSIONS

We have demonstrated, for the first time, the use of OCT in a clinical environment for evaluation by imaging of lumineers placed in a female patient. The evaluation was triggered by the observation of failure (color change) in one of the 14 laminates placed in the patient teeth (upper elements 14 to 24 and the lower elements 33 to 43).

OCT was employed as a new and efficient method to evaluate the cement line and proved to be efficient by acquiring tomography images. The images made possible monitoring the cement line in both areas: where it has remained intact, and where failures were observed, showing that the OCT technique was an effective method to evaluate lumineers. We believe that this result opens up yet another clinical application of optical coherence tomography in dentistry.

ACKNOWLEDEGEMENTS

The authors are thankful to FACEPE (Foundation for Science and Technology of Pernambuco State), CNPq (National Council of Technological and Scientific Development) and MCT (Ministry of Science and Technology) for financial support. This study was carried out under the PRONEX FACEPE/CNPq (Center of Excelence on Biphotonics and Nanophotonics) program and INCT (National Institute of Science and Technology) of Photonics program, sponsored by CNPq/MCT.

REFERENCES

[1] Lin, C. L., Kuo, W. C., Chang, Y. H., Yu, J .J. and Lin, Y. C., “Examination of ceramic/enamel interfacial debonding using acoustic emission and optical coherence tomography,” Dent Mater 30(8), 910–916 (2014).

[2] D’arcangelo, C., De Angelis, F., Vadini, M. and D’Amario, M. “Clinical evaluation on porcelain laminate veneers bonded with light-cured composite: results up to 7 years,” Clin Oral Investig 16(4), 1071-1079 (2012).

[3] Huang, D., Swanson, E.A, Lin, C.P., Schuman, J. S., Stinson, W. G., Chang, W., Hee, M. R., Flotte, T., Gregory, K., Puliafito, C. A. and Fujimoto, J. G, “Optical coherence tomography,” *Science* 254(5035), 1178-1181 (1991).

[4] Zysk, A. M., Nguyen, F. T., Oldenburg, A. L., Marks, D. L., and Boppart, S. A., “Optical coherence tomography: a review of clinical development from bench to bedside,” J Biomed Opt. *12*(5), 051403-051403 (2007).

[5] Hsieh, Y. S., Ho, Y. C., Lee, S. Y., Chuang, C. C., Tsai, J. C., Lin, K. F., and Sun, C. W. “Dental optical coherence tomography,” Sensors 13(7), 8928-8949 (2013).

[6] Melo, L.S.A., Araujo, R.E., Freitas, A.Z., Zezell, A.D., Vieira, Jr. N.D; Girkin, J., *et al*. “Evaluation of enamel dental restoration interface by optical coherence tomography,” J Biomed Opt. 10(6), 064027 (2005).

[7] Monteiro, G.Q.M., Montes, M.A.J.R., Rolim, T.V., Mota, C.C.B.O., Kyotoku, B.B.C., Gomes, A.S.L. and Freitas, A.Z. “Alternative methods to determine shrinkage in restorative resin composites,” Dent Mat. 27(e), e176-e185 (2011).

[8] Braz, A.K.S., Kyotoku, B.B.C., Braz, R. and Gomes, A.S.L. “Evaluation of crack propagation in dental composites by optical coherence tomography,” Dent Mat 25(1), 74-79 (2008).

[9] Layton, D.M. Clarke, M. and Walton, T.R. “A systematic review and meta-analysis of the survival of feldspathic porcelain veneers over 5 and 10 years,” Int J Prosthodont 25, 590–603 (2012).

[10] Friedman, M.J. “Porcelain Veneer Restorations: A Clinician´s Opinion About a Disturbing Trend,” J Esthet Restorative Dent 13, 318 – 327 (2001).

[11] Kelly, J.R. and Benetti, P. “Ceramic materials in dentistry: historical evolution and current practice,” Aust Dent J 56(1), 84-96 (2011).

[12] Conrad, H.J., Seong, W.J. and Pesun, I.J. “Current ceramic materials and systems with clinical recommendations: A systematic review,” J Prosthet Dent. 98(5), 389-404 (2007).

[13] de Andrade Borges, E., Cassimiro-Silva, P. F., Fernandes, L. O. and Gomes, A. S. L. “Study of lumineers' interfaces by means of optical coherence tomography,” Proc. SPIE 953147-953147 (2015).

APÊNDICE F – ARTIGO A SER SUBMETIDO NO JOURNAL OF DENTISTRY

IN VIVO EVALUATION OF THE INTEGRITY AND ADAPTATION OF LAMINATES USING OPTICAL COHERENCE TOMOGRAPHY: A PRELIMINARY STUDY

Short title: *In vivo* appraisal of laminates with OCT

Luana Osório Fernandes[a], Anderson Stevens Leonidas Gomes[b]

[a]Graduate Program in Dentistry, University Federal of Pernambuco, Av. Prof. Moraes Rego, 1235 - Cidade Universitária, Recife, PE, Brazil

[b]Deptartment of Physics, University Federal of Pernambuco, Av. Prof. Moraes Rego, 1235 – Cidade Universitária, Recife, PE, Brazil

Corresponding author: e-mail: anderson@df.ufpe.br, Phone: +55 81 2126-7636, Fax: +55 81 2126-8450

ABSTRACT

Objectives: The aim of this study was to verify the ability of OCT in the in vivo assessment of the integrity of dental laminates fixed in anterior teeth.

Materials and Methods: A total of 84 sites were evaluated in 28 ceramic laminates (Ivoclar Vivadent, Lichtenstein), and 18 sites in 6 prefabricated facets of prepolymerized nanohybrid composite resin (Componeer Brilliant, Coltene), fixed to the anterior superior teeth. The analysis was done using images obtained with Optical Coherence Tomography (SS-OCT 1325nm, Thorlabs). The perpendicular scan of three vestibular sites (mesial, central and distal) was performed in the three thirds of the teeth (cervical, middle and incisal). In one patient, the imageology was performed for a period of one year, capturing the images using an acrylic plate with markings to standardize the longitudinal analysis. Two-dimensional images were acquired and analyzed qualitatively and quantitatively.

Results: The images obtained allowed to carry out the inspection of the body and surface of the laminate and the fixing layer, in all cases. In the ceramic laminates, there was presence of areas indicative of tension in the laminate body (15%), disadaptation (38%), spaces not filled by cement (28%) and areas of probable inclusion of air (10%) in the cementing line. In resin laminates, the type of defect visualized was the presence of bubbles in the body in 16% of the images and in the fixation layer in 15%.

Conclusions: OCT images allowed *in vivo* monitoring of defects in laminates before they even become clinically perceptible, but still require further studies to be used in the dental clinic.
Clinical Significance: The Optical Coherence Tomography allows the *in vivo* and non-invasive evaluation of the integrity and adaptation of ceramic laminates as well as of the cement line in real time and non-destructive way.

Key words: Cementation, Ceramic, Laminate, Gap, Diagnostic imaging, tomography, optical coherence.

1. Introduction

The evolution of adhesive technique and dental ceramics allowed more conservative treatments to be applied in dentistry. The laminates are used in modern Dentistry because it is a minimally invasive procedure, but they need good planning for the treatment to be successful [1].

Prefabricated resin laminates stand out clinically because they require only one session for finalization, with minimal or no wear and a lower cost than ceramics [2]. Prefabricated composite resin laminates currently used are of nanohybrid composition, with a laser surface vitrification that provides a hard and shiny surface similar to enamel [3]. However, composites may have limitations such as shrinkage, limited toughness, color instability and susceptibility to wear [4].

Ceramic laminates are one of the most conservative ceramic restorations and have an excellent esthetic-longevity ratio [5, 6]. They have excellent color stability, wear resistance, biocompatibility and durability [7, 8]. However, this type of restoration requires a greater technical ability, is more time consuming, has a high cost, susceptible to detachment, fracture, chipping, marginal defects and microleakage. [9, 10].

The preparation and cementation are similar for the two types of restorations, but the resin laminate restorations usually require an individualization of the cervical, proximal and incisal regions [3]. Another important point is the cementing technique, which is made with resin cement for the ceramic and composite resin for the prefabricated laminate, allowing an easy alignment of the part to the tooth [11].

The evaluation of the laminate, the adaptation on the dental substrate and the survival time of these restorations is still a challenge in dentistry. Therefore, Optical Coherence Tomography (OCT) emerged as a diagnostic method in the identification and evaluation of the strata that make up the restoration (laminate-cement-tooth layer) [12, 13]. This technology was first used in ophthalmology, and since then has had its applicability extended to several specialties in the area of health [14]. The OCT is based on low coherence interferometry with a micrometric resolution, non-invasive penetration of millimetric order [15], with high acquisition speed and better sensitivity when compared to other imaging techniques [16].

The objective of this study was to evaluate *in vivo* the integrity and adaptation of dental laminates of different materials (ceramic and resin) fixed to the anterior teeth in order to identify and describe possible defects in the adhesive layer through inspection with Optical Coherence Tomography (OCT).

2. Materials and Methods

2.1 Ethical aspects

All study participants were informed in writing of the research content and signed the study term before inclusion in the evaluation. The study was carried out in accordance with the Declaration of Helsinki and approved by the Ethics Committee of the University of Pernambuco (protocol number 30543914.0.0000.5207).

2.2 Characterization of the study

The participants were aged between 18 and 65 years, of both sexes, taken at the Integral Clinic I, of the Dentistry course of the Federal University of Pernambuco, Pernambuco, Brazil. The following exclusion criteria were used: poor oral hygiene; absence of anterosuperior teeth; prosthesis and composite restoration or fixed orthodontic appliance in the evaluated region.

An *in vivo* observational study of 84 sites in 28 ceramic laminates (IPS e.max Ceramic, Ivoclar Vivadent, Schaan, Liechtenstein) and 18 sites in 6 prefabricated facets of prepolymerized composite nanohybrid resin (Componeer Brilliant, Coltene, Whaledent, Switzerland), fixed to the anterior superior teeth, was performed.

The resin laminates were cemented to the teeth according to the manufacturer's recommendations, indicating the use of a high-load nanohybrid composite resin as a

fixing agent (Brilliant NG, Coltene Whaledent, Switzerland) on the previously conditioned dental substrate (Magic Acid 37%, Coltene, Whaledent, Switzerland) and covered with adhesive layer (One Coat Bond SL, Coltene Whaledent, Switzerland). The teeth submitted to this treatment did not require any type of dental preparation, only adjustment of the edges of the laminate with discs of coarse granulation (Sof-Lex, 3M ESPE, São Paulo, Brazil).

For ceramic laminates, ultraconservative preparations were performed on all teeth with diamond tips (KG Sorense, São Paulo, Brazil), only to adjust the insertion axis of the ceramic restorations. The internal surface of veneers was treated with 4% hydrofluoridric acid (Ivoclar Vivadent, Schaan, Liechtenstein) for 30s, silane (Monobond Plus, Ivoclar Vivadent, Schaan, Liechtenstein) for 1 min and bonding agent (Excite F, Ivoclar Vivadent, Schaan, Liechtenstein). The teeth were etched (37 % phosphoric acid gel), rinsed, dried, and treated with dentin bonding agent (Excite F, Ivoclar Vivadent, Schaan, Liechtenstein). The ceramic laminates were fixed to the dental substrate with the aid of light-curing veneer luting resin cement (Variolink Veneer, Ivoclar Vivadent, Schaan, Liechtenstein) and removing the excess of luting agent with a brush and dental floss the restorations were light polymerized according to the manufacturer's recommendations.

All patients were clinically evaluated for color, presence of marginal gap and fracture, before image collection [17].

2.3 OCT system, imaging and analysis

Optical Coherence Tomography (OCT) imaging was performed to investigate the vestibular face of each element, evaluating the three sites (mesial, central and distal) in the three thirds of the teeth (cervical, middle and incisal). The images were captured up to one year in a single patient and for a standardized longitudinal analysis, an acetate guiding plate was made, with markings delimiting the sites (mesial, central and distal).

The OCT system used was the SS-OCT 1325nm (Thorlabs) with a spectral bandwidth of ~100nm, axial scan rate of 16kHz/25fps, lateral resolution ~25μm and axial resolution of 12/9μm (air/ water). The buccal surfaces of the teeth were swept perpendicularly by a light beam and the two-dimensional (2D) images acquired were stored in bitmap format. Aiming at the longitudinal monitoring of some regions, three -

dimensional images were captured with a volume of 512 pixels in the X - Y - Z directions, within 1 minute.

The images were evaluated for the presence of changes within the laminate body and in the fixation line to the dental substrate. In addition to the qualitative analysis of the images, the measurement of the defects presented in each reevaluation period was performed in order to correlate the size of the defect with the identification of clinical signs of change in the region. All two-dimensional (2D) measurements were taken in the equipment software, without any other image treatment, and clinically visible defect volume measurement was obtained with ImageJ (Imaging Processing and Analysis in Java, National Institutes of Health, Bethesda, MD) software.

3 Results

All the patients evaluated did not present any clinically visible changes in the laminates. A total of 54 images were obtained for the resin laminates and 252 images for the ceramic laminates.

By analyzing the adaptation of the laminates, regardless of the material, it was possible to visualize areas of marginal adaptation, defects within the layer of resin adhesive cementation and resin cement. In some sites of the cervical third the biofilm deposit in the region were visualized, while in others there was cementing material, even after the period of one year. The presence of a large distance between the gingival margin and the laminate was observed in some elements with resin laminate, a fact that served as a niche for biofilm deposition (fig 1).

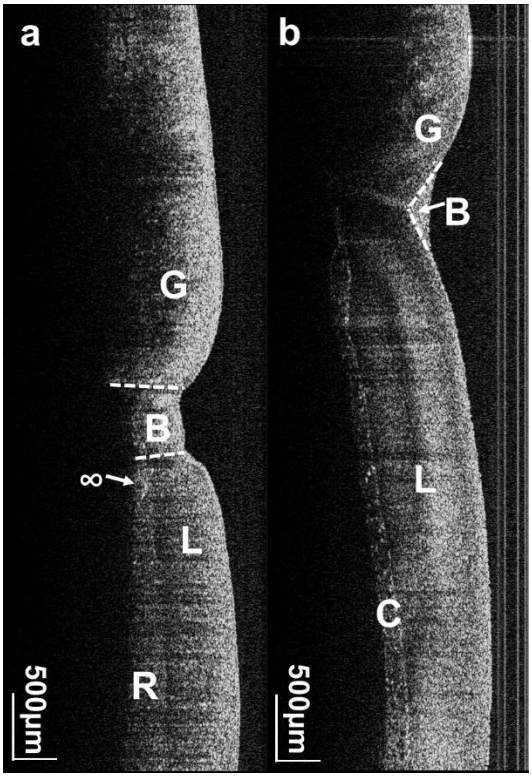

Figure 1- The OCT images show biofilm deposition (B) in the cervical region of teeth with resin laminate (a) and ceramic (b). The figure a shows the presence of a great distance between the gingival margin and the resin laminate. G-gingiva, B - biofilm, L-laminate, C- cementing line, R- resin, ∞- bubbles. All images are in 500 µm scale.

In some images obtained in the ceramic laminates we can notice the presence in the body of a wider bright area followed by a darker area (15%), which is indicative of stress or tension in the laminate (fig 2a). In relation to the cementing line, only 25% of the images showed total marginal adaptation. Marginal maladaptation was observed of the cervical third (17%) and incisal third (21%), corresponding of the 38% the failures (fig 2d). 28% images evidenced probable areas with presence of space, not filled by cement, between the laminate and the dental surface, with several dimensions. The investigations revealed areas of probable aerial inclusion (10%).

In the evaluation of resin laminates, it was possible to identify the presence of bubbles in the body, limited to the incisal third (central site) in 16% of the images, with a mean diameter of 0.11 mm and a surface depression in 5% of the images (fig. 2e-h). In relation to the resin laminate fixation layer, the only type of defect visualized was the presence of bubbles, in 15% of the images, with the greater part (60%) located in the central portion of the cervical and middle thirds.

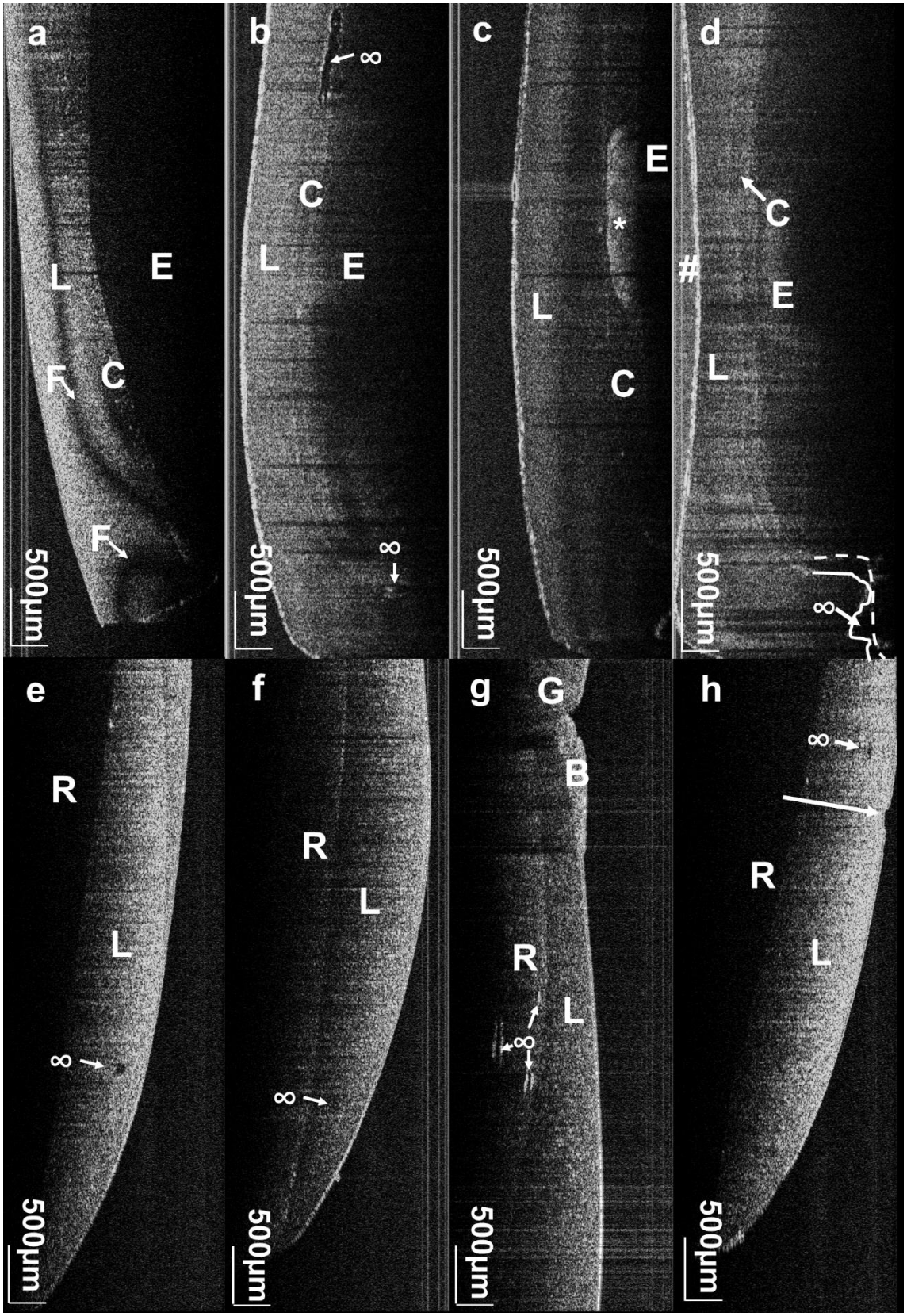

Figure 2- The images allow to identify the integrity and adaptation of ceramic (a-d) and resin (e-h) laminates. In the ceramic laminates we can notice the presence of area marginal maladjustment (∞), presence of space not filled by cement, besides an area of probable inclusion of air and area of stress concentration (*). In resin laminates, the

presence of depression in the incisal (arrow) and bubble regions can be observed in both the laminate body and the cementation line (∞). E-enamel, G-gingiva, B - biofilm, L- laminate, C- cementing line, F- defect in the body of the ceramic laminate, R- resin, , * - area of stress concentration area with increased reflectivity of ceramics , ∞- bubbles and , #- inversion of images. All images are in 500 µm scale.

In the areas accompanied for one year in the ceramic laminates, it was possible to observe the progression of the finding until it became clinically perceptible. The mean initial volume of the defect located in the middle third was 1.05mm^3, and evolved to 13mm^3 when clinically visible. It is worth mentioning that the clinical identification occurred through the color change present in the middle third, after 6 months of fixation to the tooth (fig 3).

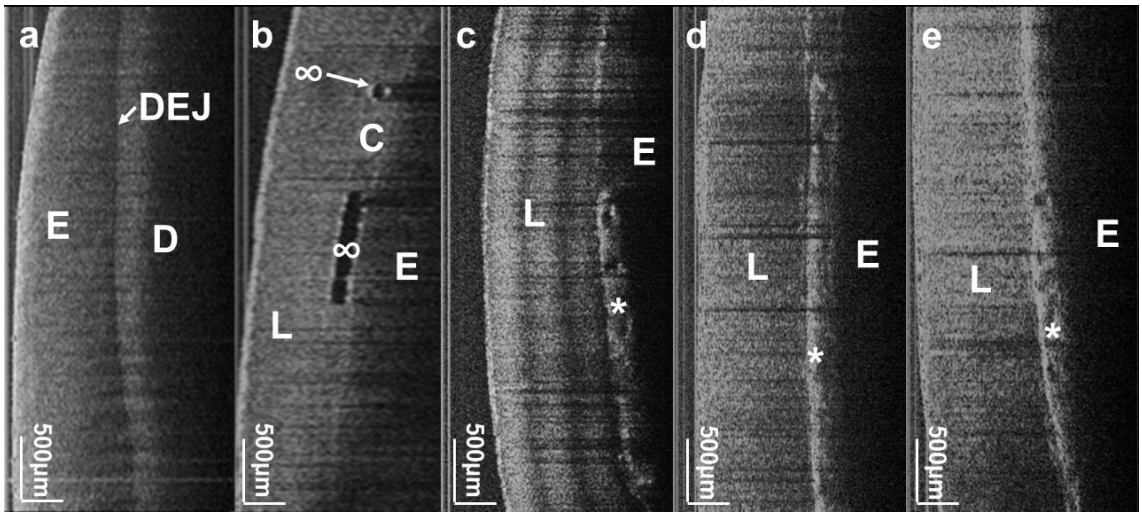

Figure 3- The images show the longitudinal follow-up of the middle third of the element 11: prior to the installation of the ceramic laminate (a), immediately after (b), 3 months (c), 6 months (d) and one year after cementation (e). E-enamel, D - dentin, DEJ- dentin-enamel junction, L- laminate, C- cementing line, * - area of stress concentration , ∞- bubbles. All images are in 500 µm scale.

It should be noted that the manufactured ceramic laminates did not present any defects such as bubbles or cracks, only the presence of wide bright/darker stripes characteristics of stress on tension in the laminates.

4 Discussion

The success of laminated restorations is mainly related to color stability and cementation made with resinous composite [18, 19]. The appearance and propagation of defects such as fatigue microcracks in the adhesive layer is difficult to monitor because they require sectioning or dissolution of the samples to confirm failure paths [20]. The OCT allows direct and real-time evaluation [21], through the noninvasive acquisition of images of the structures, providing important information [22]. The optical differences allow to identify the presence of secondary caries, distinguish the tooth-restoration interface [23], tooth-laminate [13] and marginal adaptation [24].

Marginal adaptations are important factors for the longevity of restorations, impacting on the prevention of secondary caries and microleakage [25]. A uniform cementation layer determines the internal adaptation and durability of the restoration [26]. In our study, we observed the marginal adaptation, the fixation layer, as well as the laminate body. The technique allowed the identification of areas without adaptation, fixation layer defects, biofilm accumulation and excess resin cement (fig 1). Another point observed was the position of the margin of the laminates, independent of the material and technique of cementation, since if it is in the gingival supra will have aesthetic consequences and if subgingival can cause periodontal damages. Excess cement or resin in the marginal region of the gingiva requires careful removal so as not to induce gingival trauma in the region and a good polishing, avoiding plaque accumulation and induction of periodontal disease.

Prefabricated resin laminates have advantages over direct resins, such as reduction of polymerization stress, less formation of gaps, post-operation hypersensitivity, microleakage and optimum marginal adaptation [27, 28]. We can observe the presence of bubble in the body of the resin laminates and the layer of cementation, besides a superficial depression. Erickson *et al* [28], states that the presence of defects or imperfections can accelerate the development of cracking and microleakage. Perdigão *et al* [30] claims that if the resin laminate is damaged, it can be easily restored with composite resin, a fact that may extend to the laminate body that already presents defect prior to cementation.

Using ceramic laminates are one of the methods of reestablishing the smile aesthetics. In the images captured, the presence of areas of marginal maladaptation in the cervical and incisal regions was observed. Insufficient sealing between restorations and preparations can lead to oral fluid leaks along the interfaces between

blades and teeth, and may result in cement dissolution, postoperative sensitivity, marginal discoloration, and recurrent caries [31, 32].

We can note that the evident changes in the images had a location closer to the tooth-line interface of cementation, especially when located in the cervical region. Haralur [33] evaluated the presence of microinfiltrations in ceramic laminates of lithium disilacate and observed that the cervical region had a higher microleakage index, and that the tooth-cement interface was the most affected.

Todor *et al*. [34] evaluated the behavior of sintered dental ceramics at different temperatures with the aid of the OCT and identified that the elevation of temperature above the ideal can increase the reflectivity of the ceramic, indicating stress that could induce ceramic defects. Some of the obtained images observed a pattern similar to those observed here, but without the identification of any type of defect in the body of the ceramic laminate. At this point, during the laminates fabrication process, regular monitoring using the OCT would be interesting, since the technique allows the identification of changes in micrometric scale.

Lack of cement and / or the presence of a bubble may lead to laminate take-off, color change or secondary caries. The growth of defects due to stress, such as microcracks in the cement layer, is difficult to monitor from in vitro studies that require sectioning or dissolving the sample tissues to confirm failure paths [20]. We highlight that the OCT allowed the identification of spaces not filled by cement, areas of tension and bubbles of various sizes and location. Li *et al*. [35] evaluated OCT as a marginal gap identification method and proved their efficacy in the noninvasive diagnosis of ceramic restorations.

Some authors state that most frequent failures in the first year are related to adhesive failure in the cementation, occur mainly in the first 6 months after the end of the work, after the problems tend to decrease or stabilize at low rates [17,36]. Ge *et al*. [37] state that porcelain thickness, enamel thickness, and their combination influenced all the loads required to produce catastrophic failure. In our experiment, we noticed the coalescence of defects reported previously, after the period of one year. We observed that the clear majority of changes identified in OCT images were not clinically visible. This fact may be due to the technique's ability to acquire images with high resolution power.

In longitudinal monitoring, the clinical identification of defects in ceramic laminates was due to color change. Probably, this finding was due to a set of factors,

such as: stress concentrations; dissolution of the cementing agent [5]; marginal and internal maladaptation [38]; and oral fluid leaks along the cementation interface [32]. Interface failures are still a challenge for Dentistry and in an attempt to repair the area with color change, the repair was performed using a fluid resin. The images show that the fluidity of the composite resin incorporated a large amount of micrometric bubbles in the bonding interface, when compared to the image of the cementation with nanohybrid resin (fig. 4). Authors such as Gresnigt, Magne and Magne [39] advocate this type of intervention, but argue that highly filled composite resins should be used because they are less prone to discoloration than fluids. According to our evaluation, we can assume that the increase in the number of bubbles in the region repaired with fluid resin negatively affects the stability of the cementation line through biomechanical stress.

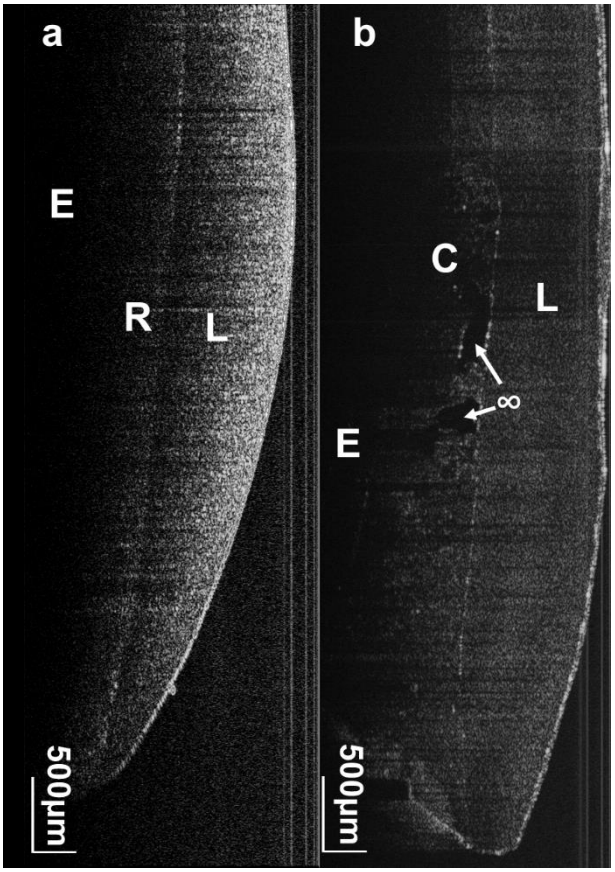

Figure 4- The images show the behavior of the laminate cementation layer using nanohybrid resin (a) and fluid resin repair area (b). In picture b it is possible to see large amount of bubbles of varied size in the union interface. All images are in 500 µm scale.

5 Conclusions

The studies that explore the images associated with the OCT aim to try to provide a tool to go beyond the current clinical parameters. We can conclude that the technique allows the identification and follow-up of defects *in vivo* before they become clinically perceptible and may become a modern diagnostic method in the evaluation of laminated restorations.

Future studies should be conducted to determine the best time to capture OCT images, whether before or after cement polymerization. In addition, it should be investigated whether the images can determine the best time for intervention in laminated restorations.

Acknowledgements

The authors are thankful to all the participants of the research. This study was carried out under the PRONEX FACEPE/ CNPq (Center of Excellence on Biophotonics and Nanophotonics– Foundation for Science and Technology of Pernambuco State and National Council of Technological and Scientific Development – APQ-0504-1.05/14) program and INCT-INFO (National Institutes of Science and Technology) of Photonics program, sponsored by CNPq/MCT (National Council of Technological and Scientific Development and Ministry of Science and Technology- 573.916/ 08).

REFERENCES

[1] M.A. Vargas, C. Bergeron, A. Diaz-Arnold. **Cementing all-ceramic restorations: recommendations for success**. J Am Dent Assoc., 142 (2011), pp 20S-4S.

[2] H.P. Beddis, P.J. Nixon. **Layering composites for ultimate aesthetics in direct restorations**. Dent Update., 39 (2012), pp 630-6.

[3] D. Dietschi, A. Devigus. **Prefabricated composite veneers Historical perspectives, indications and clinical application**. Eur J Esthet Dent., 6 (2011), pp 178–187.

[4] N. B. Cramer, J. W. Stansbury, C. N. Bowman. **Recent advances and developments in composite dental restorative materials**. J Dent Res., 90 (2011), pp 402-16.

[5] M. Peumans, M.B. Van, P. Lambrechts, G Vanherle**. Porcelain veneers: a review of the literature**. J Dent., 28 (2000), pp 163-77.

[6] F. Zarone, R. Leone, M. I. Di Mauro, M. Ferrari, R. Sorrentino. **No-preparation ceramic veneers: a systematic review**. Journal of Osseointegration, 10 (1) (2018), pp 17-22.

[7] A.S. Kassem, O. Atta, O. El-Mowafy. **Fatigue resistance and microleakage of CAD/CAM ceramic and composite molar crowns**. J Prosthodont. 21 (2012), pp 28-32.

[8] B. Stawarczyk, R. Egli, M. Roos. **The impact of in vitro aging on the mechanical and optical properties of indirect veneering composite resins**. J Prosthetic Dent 106 (2011), pp 386-398.

[9] M. Peumans, J. De Munck, S. Fieuws, P. Lambrechts, G. Vanherle, B. Van Meerbeek. **A prospective ten-year clinical trial of porcelain veneers**. J Adhes Dent., 6 (1) (2004), pp 6576.

[10] F. J. Burke. **Survival rates for porcelain laminate veneers with special reference to the effect of preparation in dentin: a literature review**. J Esthet Restor Dent. 24(2012), pp 257-65.

[11] G. Gomes, J. Perdigão. **Prefabricated composite resin veneers: a clinical review**. J Esthet Restor Dent., 26 (5) (2014), pp 302-13.

[12] E. de Andrade Borges, P. F. Cassimiro-Silva, L. O. Fernandes, A. S. L. Gomes. **Study of lumineers' interfaces by means of optical coherence tomography**. International Society for Optics and Photonics In: Biophotonics South America, 9531 (2015), p. 953147.

[13] L. O. Fernandes, N. D. Graça, L. S. Melo, C. H. Silva, A. S. L. Gomes. **Optical coherence tomography investigations of ceramic lumineers**. International Society for Optics and Photonics In: Lasers in Dentistry XXII, 9692 (2016), pp 96920P.

[14] M. Machoy, J. Seeliger, L. Szyszka-Sommerfeld, R. Koprowski, T. Gedrange, K. Woźniak. **The use of optical coherence tomography in dental diagnostics: a state-of-the-art review**. Journal of healthcare engineering, 2017 (2017).

[15] A. G. Podoleanu. **Optical coherence tomography**. Journal of Microscopy, 247(3) (2012), pp 209-219.

[16] M. Wojtkowski. **High-speed optical coherence tomography: basics and applications**. Applied optics, 49(16) (2010), pp D30-D61.

[17] G. Gurel, S. Marimoto, M. A. Calamita, C. Coachman, N. Sesma. **Clinical performance of porcelain laminate veneers: outcomes of the aesthetic pre-evaluative temporary (APT) technique.** The International Journal of Periodontics & Restorative Dentistry, 32 (2012)., 32, pp. 625-635.

[18] D. S. Smith, K. S. Vandewalle, G. Whisler. **Color stability of composite resin cements**. General dentistry, 59(5) (2011), pp 390-394.

[19] E. Öztürk, R. Hickel, Ş. Bolay, N. Ilie. **Micromechanical properties of veneer luting resins after curing through ceramics.** Clinical oral investigations, 16(1) (2012), pp 139-146.

[20] C. L. Lin, W. C. Kuo, J. J. Yu, S. F. Huang. **Examination of ceramic restorative material interfacial debonding using acoustic emission and optical coherence tomography**. Dental Materials, 29(4) (2013), pp 382-388.

[21] G. Q. Monteiro, M. A. Montes, A. S. Gomes, C. C. Mota, S. L. Campello, A. Z. Freitas. **Marginal analysis of resin composite restorative systems using optical coherence tomography**. Dent Mater., 27(12) (2011), pp e213-23.

[22] T. Minamino, A. Mine, K. Omiya, M. Matsumoto, H. Nakatani, T. Iwashita, M. Ohmi, H. Yatani. **Nondestructive observation of teeth post core space using optical coherence tomography: a pilot study**. J Biomed Opt., 19(4) (2014), pp 046004.

[23] P. Lenton, J. Rudney, R. Chen, A. Fok, C. Aparicio, R. S. Jones. **Imaging *in vivo* secondary caries and ex vivo dental biofilms using cross-polarization optical coherence tomography**. Dent Mater., 28(7) (2012), pp 792-800.

[24] A. G. Turk, M. Sabuncu, M. Ulusoy. **Evaluation of adaptation of ceramic inlays using optical coherence tomography and replica technique**. Brazilian oral research, 32 (2018).

[25] R. Uzgur, E. Ercan, Z. Uzgur, H. Çolak, M. Yalçın, M. Özcan. **Cement thickness of inlay restorations made of lithium disilicate, polymer-infiltrated ceramic and nano-ceramic CAD/CAM materials evaluated using 3D X-ray micro-computed tomography**. J Prosthodont., (2016).

[26] N. K. Alajaji, D. Bardwell, M. Finkelman, A. Ali. **Micro-CT evaluation of ceramic inlays: comparison of the marginal and internal fit of five and three axis CAM systems with a heat press technique**. J Esthet Restor Dent., 29(1) (2017), pp 49-58.

[27] A. A. El Zohairy, A. J. De Gee, M. M. Mohsen, A. J. Feilzer. **Microtensile bond strength testing of luting cements to prefabricated CAD/CAM ceramic and composite blocks**. Dent Mater., 19 (7) (2003), pp 575–83.

[28] S. Batalha-Silva, M. A. Andrada, H. P. Maia, P. Magne. **Fatigue resistance and crack propensity of large MOD composite resin restorations: Direct versus CAD/CAM inlays**. Dent Mater., 29 (2013), pp 324-331.

[29] R. L. Erickson, A. J. De Gee, A. J. Feilzer. **Fatigue testing of enamel bonds with self-etch and total-etch adhesive systems**. Dental Mater., 22(11) (2006), pp 981–7.

[30] J. Perdigão, A. Sezinando, M. A. Muñoz, I. V. Luque-Martinez, A. D. Loguercio. **Prefabricated veneers — bond strengths and ultra-morphological analyses**. J Adhes Dent., 16(2014), pp 137-146.

[31] S. M. Beschnidt, J. R. Strub. **Evaluation of the marginal accuracy of different all-ceramic crown systems after simulation in the artificial mouth**. J Oral Rehabil., 26 (1999), pp 582-593.

[32] P. Boitelle, B. Mawussi, L. Tapie L, O. Fromentim. **A systematic review of CAD/CAM fit restoration evaluations**. J Oral Rehabil., 41 (2014), pp 853-874.

[33] S. B. Haralur. **Microleakage of porcelain laminate veneers cemented with different bonding techniques**. J Clin Exper Dent., 10(2) (2018), pp e166.

[34] R. Todor, M. L. Negrutiu, C. Sinescu, F. I. Topala, A. Bradu, V. F. Duma, M. Rominu, A. G. Podoleanu. **Investigation of firing temperature variation in ovens for ceramic-fused-to-metal dental prostheses using swept source optical coherence tomography**. International Society for Optics and Photonics. In 2nd Canterbury Conference on OCT with Emphasis on Broadband Optical Sources, 10591 (2018), p. 105910I.

[35] W.Li, J. Liu, Z. Zhang. **Evaluation of marginal gap of lithium disilicate glass ceramic crowns with optical coherence tomography**. Journal of biomedical optics, 23(3) (2018), pp 036001.

[36] S. Morimoto, R.B. Albanesi, N. Sesma, C.M. Agra, M.M. Braga. **Main Clinical Outcomes of Feldspathic Porcelain and Glass-Ceramic Laminate Veneers: A Systematic Review and Meta-Analysis of Survival and Complication Rates.** The International Journal of Prosthodontics, 29 (2016), pp. 38-49.

[37] C. Ge, C. C. Green, D. Sederstrom, E. A. McLaren, S. N. White. **Effect of porcelain and enamel thickness on porcelain veneer failure loads in vitro**. J Prosth Dent., 111(5) (2014), pp 380-387.

[38] A. G. Türk, M. Sabuncu, S. Ünal, B. Önal, M. Ulusoy. **Comparison of the marginal adaptation of direct and indirect composite inlay restorations with optical coherence tomography**. Journal of Applied Oral Science, 24(4) (2016), pp 383-390.

[39] M. Gresnigt, M. Magne, P. Magne. **Porcelain veneer post-bonding crack repair by resin infiltration**. The international journal of esthetic dentistry, 12(2) (2017), pp 156-170.

APÊNDICE G - OPTICAL COHERENCE TOMOGRAPHY AS A METHOD FOR QUANTITATIVE SKIN EVALUATION IN SYSTEMIC SCLEROSIS

Natália Sotero Machado Pires,1
Andréa Tavares Dantas,2
Angela Luzia Branco Pinto Duarte,2
Marcello Magri Amaral,3
Luana Osório Fernandes,1
Tereza Januária Costa Dias,1
Luciana Santos Afonso de Melo,4
Anderson Stevens Leônidas Gomes1,4

1Graduate Program in Dentistry, Federal University of Pernambuco, Recife, Pernambuco, Brazil
2Department of Rheumatology, Federal University of Pernambuco, Recife, Pernambuco, Brazil
3Laboratory of Biophotonics, Center for Lasers and Applications, IPEN—CNEN/SP, São Paulo, São Paulo, Brazil
4Department of Physics, Federal University of Pernambuco, Recife, Pernambuco, Brazil

Correspondence to Dr Andréa Tavares Dantas; Hospital das Clínicas, Rua Prof. Moraes Rego, Recife, PE50740-900, Brazil; andreatdantas@gmail.com

Improved, non-invasive techniques for the diagnosis, classification and monitoring of patients with systemic sclerosis (SSc) are needed. One potential technique for quantifying the extent of cutaneous sclerosis in these patients is optical coherence tomography (OCT).12Recently, Abignano et al3 suggested the use of OCTas a feasible and reliable technique to evaluate skin fibrosis in SSc. Based on that initial work, the aim of this study was to evaluate OCT images and compare the findings with the modified Rodnan skin score (mRSS) in patients with SSc. Thirty-three Brazilian patients with SSc (28 women; mean age 46.1 years; range 19–71 years) were recruited and fulfilled criteria for SSc proposed by American College of Rheumatology (ACR), 19804 or ACR/European League Against Rheumatism, 2013.5 Patients were classified into limited SSc (n=18) and diffuse SSc (n=15) groups. The mean disease duration was 9.7 years (median 8 years, range 2–26 months). Thirty-five healthy control (HC) (28 women, mean age 39.2 years; range 20–68 years) were also included. The OCT scans were performed using a Swept Source-OCT at 1325 nm (Thorlabs,

Newton, New Jersey, USA). All subjects had OCT scans and mRSS performed on specific sites such as proximal third finger and dorsal forearm, both sides. The tissue optical density at 300 μm depth (OD300) from OCT images was obtained using the Matlab programme. The study protocol was approved by the Ethics Committee of the Universidade Federal de Pernambuco and informed consent was obtained from all patients. Spearman's rank correlation coefficient, Mann-Whitney U-test or Kruskal-Wallis test and Dunn test were employed. Values of $p<0.05$ were considered statistically significant. In a descriptive analysis, one can readily see that the air–skin interface in forearm between patients with SSc (figure 1A) and HC (figure 1B) shows a difference in rugosity, as well as in the visual scattering behaviour observed in both images. In the quantitative analysis of the scattering intensity as a function of depth in the skin (figure 1C), a difference is observed especially in the dermal–epidermal junction (indicated by the arrow). At 300 μm depth, the photon attenuation was higher for patients with SSc (figure 1C, dashed line).

Stratifying patients according to mRSS, there was a significant overall difference across the five groups ($p=0.0045$ for finger and $p=0.0145$ for forearm). After Tukey correction for multiple variables, the difference remained significant between HC or patients with mRSS=0 or 1 and patients with mRSS=3 in finger (figure 2A) and between HC or patients with mRSS=0 and patients with mRSS=3 in forearm (figure 2B). However, there was no difference between HC and patients with mRSS=0 or 1, indicating that this measure could not discriminate between HC and these patients and this could be a potential limitation of this technique. Besides, we also found a negative correlation between OD300 values and mRSS groups ($r=-0.66$, $p<0.0001$ in finger; $r=-0.55$, $p=0.0008$ in forearm) (figure 2C, D) and total mRSS ($r=-0.59$, $p=0.0003$ in finger; $r= -0.69$, $p<0.0001$ in forearm) (figure 2E, F). These results corroborate the findings of Abignano et al3 on the usefulness of OCT in evaluating cutaneous fibrosis. In conclusion, the skin appearance of patients with SSc in OCT images is clearly different from HC, and OCTcan provide a unique perspective for objectively assessing skin thickness.

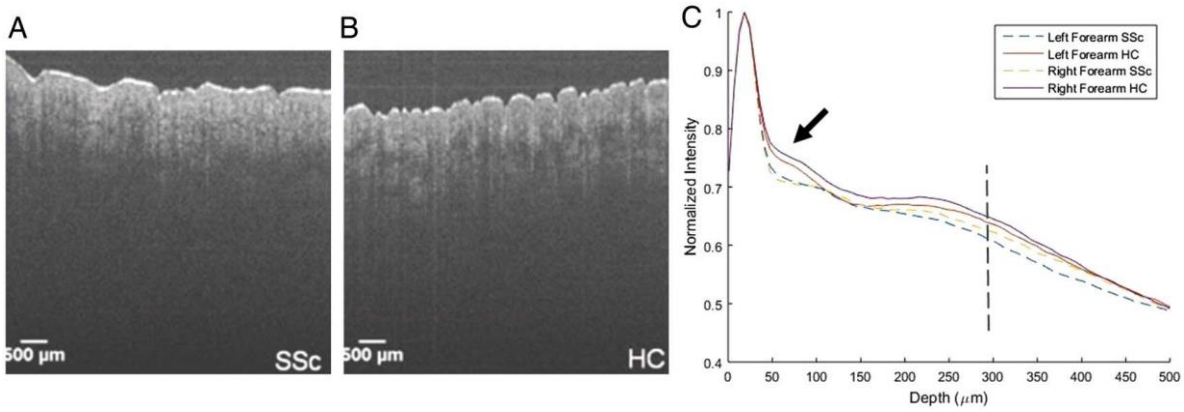

Figure 1 Qualitative analysis of the forearm by optical coherence tomography (OCT). (A) OCT image of the patient with systemic sclerosis (SSc); (B) OCT image of the healthy control (HC); (C) graphical representation of the optical density mean in HC and SSc, where the difference in the dermal–epidermal junction (arrow) and intensity of light penetration at 300 µm depth (dashed line).

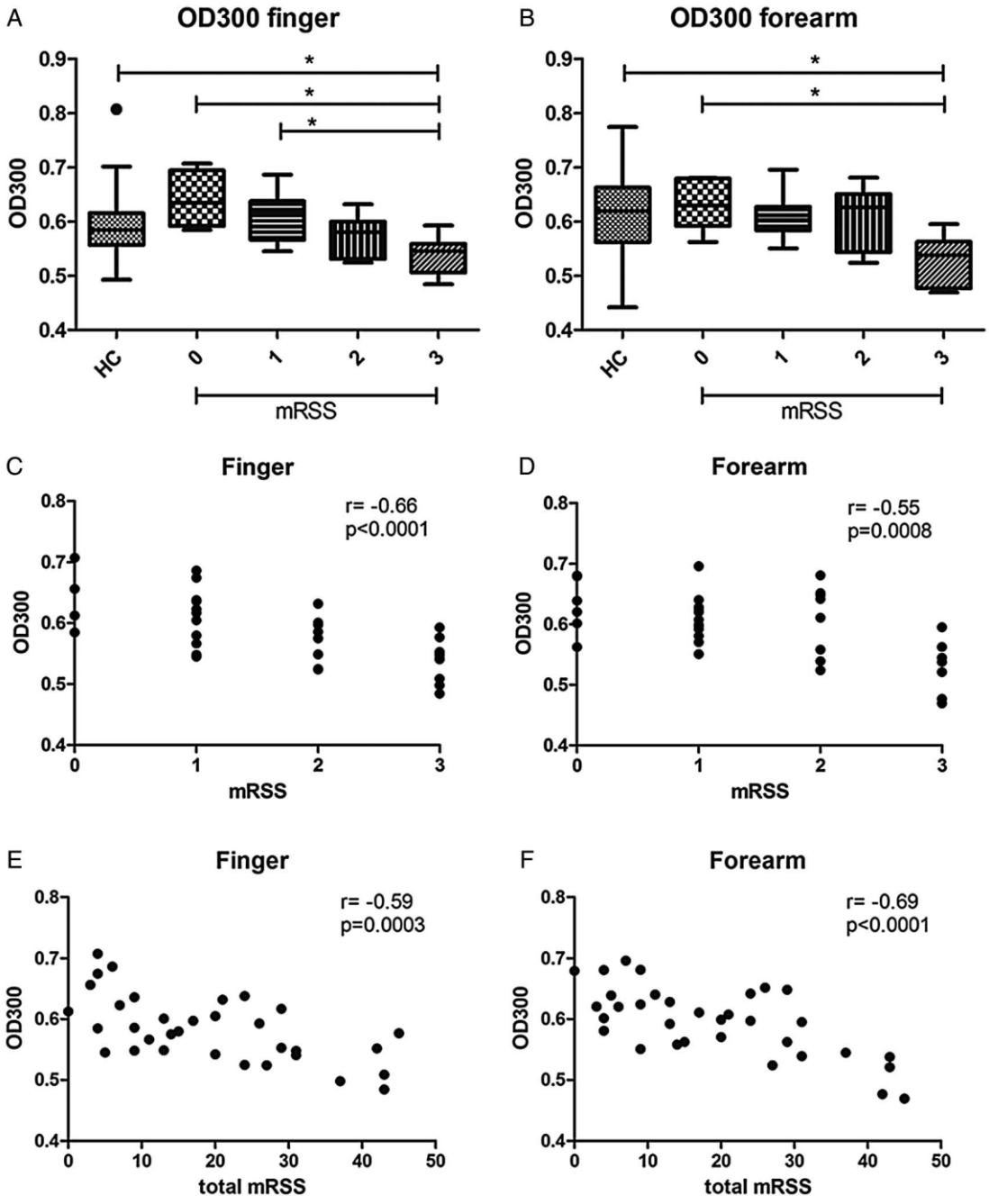

Figure 2 - Graphical representation of the measurements obtained from the optical density at 300 μm depth (OD300). (A) OD300 between healthy control (HC) and the modified Rodnan skin score (mRSS) systemic sclerosis (SSc) patients on the finger and (B) on the forearm; (C) correlation of the OD300 between the mRSS groups on the finger and (D) on the forearm; (E) correlation of the OD300 between mRSS total on the finger and (F) on the forearm. *p<0.05.

REFERENCES

1 Gladkova ND, Petrova GA, Nikulin NK, et al. In vivo optical coherence tomography imaging of human skin: norm and pathology. Skin Res Technol 2000;6:6–16.

2 Fernandes LO, Mota CCBO, Melo LSA, et al. In vivo assessment of periodontal structures and measurement of gingival sulcus with optical coherence tomography: a pilot study. J Biophotonics. 2016. doi:10.1002/jbio.201600082. [Epub ahead of print 8 Aug 2016].

3 Abignano G, Aydin SZ, Castillo-Gallego C, et al. Virtual skin biopsy by optical coherence tomography: the first quantitative imaging biomarker for scleroderma. Ann Rheum Dis 2013;72:1845–51.

4 Masi AT. Preliminary criteria for the classification of systemic sclerosis (scleroderma). Subcommittee for Scleroderma Criteria of the American Rheumatism Association Diagnostic and Therapeutic Criteria Committee (1980). Arthritis Rheum 1980;23:581–90.

5 van den Hoogen F, Khanna D, Fransen J, et al. Classification criteria for systemic sclerosis. Ann Rheum Dis 2013;72:1747–55

APÊNDICE H - OPTICAL COHERENCE TOMOGRAPHY IMAGING OF THE LABIAL MUCOSA: AN ALTERNATIVE BIOMARKER FOR DIAGNOSTIC OF SYSTEMIC SCLEROSIS PATIENTS.

Submetido na ARTHRITIS CARE & RESEARCH (2019).

Running head: Labial mucosa evaluation in scleroderma

Natália Sotero Machado Pires, MD - Universidade Federal de Pernambuco, Brazil
Andréa Tavares Dantas, PhD – Universidade Federal de Pernambuco, Brazil
Angela Luzia Branco Pinto Duarte, PhD - Universidade Federal de Pernambuco, Brazil
Marcelo Magri Amaral, PhD - Instituto de Pesquisas Energéticas e Nucleares, Brazil
Luana Osório Fernandes, MD – Universidade Federal de Pernambuco, Brazil
Tereza Januária Costa Dias, MD – Universidade Federal de Pernambuco, Brazil
Luciana Santos Afonso de Melo, PhD – Universidade Federal de Pernambuco, Brazil
Cláudia Cristina Brainer de Oliveira Mota, PhD – Associação Caruaruense de Ensino Superior e Técnico, Brazil
Patrícia Fernandes Cassimiro da Silva, MD - Universidade Federal de Pernambuco, Brazil
José Antônio Aleixo da Silva, PhD – Universidade Federal Rural de Pernambuco, Brazil
Anderson Stevens Leônidas Gomes, PhD - Universidade Federal de Pernambuco, Brazil

*Corresponding author - Dr Andréa Tavares Dantas; Hospital das Clínicas, Rua Prof. Moraes Rego, Recife- PE- Brazil, 50740-900; e-mail: andreatdantas@gmail.com; Phone/Fax: +55 81 34540155.

Word count: 2059 words

This study was carried out under the support of PRONEX program (Center of Excellence on Biophotonics and Nanophotonics – APQ-0504-1.05/14) supported by FACEPE/CNPq (Foundation for Science and Technology of Pernambuco State and National Council of Technological and Scientific Development) and INCT-INFO (National Institutes of Science and Technology, Institute of Photonics – 465.763/2014-6 sponsored by CNPq/MCT (National Council of Technological and Scientific

Development and Ministry of Science and Technology). The authors also thank financial support from CAPES and CNPq, Brazilian Agencies. The authors report no conflict of interest related to this study.

ABSTRACT

Objective: to evaluate the applicability of Optical Coherence Tomography (OCT) in the oral cavity as an alternative biomarker for diagnostic of patients with systemic sclerosis (SSc).

Methods: An observational clinical study was developed with 33 SSc patients: 18 of the limited cutaneous and 15 of the diffuse cutaneous forms. The healthy control (HC) consisted of 35 individuals. All of them underwent evaluation of the inferior labial mucosa by OCT.

Results: It was observed that the OCT optical density measured at 300 μm depth was higher in SSc patients when compared to the HC ($p=0.016$). The thickness (μm) of the labial mucosa epithelium ($p<0.0001$) was lower than those observed in the HC. There was no statistically significant difference between the early and established phases in the lcSSc ($p=0.9$) and dcSSc ($p=0.4$). No statistical difference was found in the correlations with the following parameters: disease time, clinical form, modified Rodnan score, Raynaud's phenomenon, digital ulcers, interstitial lung disease, pulmonary arterial hypertension, esophageal dysfunction and musculoskeletal involvement.

Conclusion: As labial mucosa evaluation with OCT in SSc patients showed a clear distinct pattern with respect to the controls, even in the early stage, it is proposed as an alternative biomarker with potential use in SSc diagnosis and follow up.

Keywords: Scleroderma. Optical Coherence Tomography. Oral Mucosa. Oral health. Diagnosis.

SIGNIFICANCE AND INNOVATIONS

- Oral abnormalities are usually seen in patients with systemic sclerosis but have not been adequately exploited as a clinical marker.
- Optical coherence tomography (OCT) has been shown to be a promising method in evaluating skin and mucosal tissue in various clinical conditions.

- In this cross-sectional study, we evaluated the qualitative and quantitative characteristics of the labial mucosa in patients with systemic sclerosis and healthy controls using OCT and we found significant differences between the two groups.
- Significant changes were identified even in patients with early disease, suggesting the use of OCT as an instrument for the evaluation of systemic sclerosis patients.

INTRODUCTION

Systemic Sclerosis (SSc) is frequently an insidious disease, clinically heterogeneous, of unknown cause. It is characterized by inflammation and hyper-reactivity of micro and macro vascular circulation associated with excessive collagen deposition in tissues, resulting in fibrosis of the skin and/or internal organs, with varying severity and prognosis (1-4).

Oral abnormalities are usually seen in SSc patients. The most common oral changes, resulting from altered collagen deposition, are: microstomia, xerostomia, periodontal disease and teeth loss (5-9). These changes in the oral region have been somehow neglected when compared to evaluation in other parts of the human body (10-12), and therefore deserve further investigation. Evaluation of the patient's oral biological structure have not been exploited as a correlation clinical marker, even though it is already known that structural tissue modifications are highly prevalent in patients with SSc.

Optical imaging techniques have been widely employed in several medical areas, and are contemplated to be introduced in primary care, because in the early stages of many diseases, it is difficult to see abnormalities with limited tools currently available to medical doctors in such service sector (13, 14). Among the several optical imaging methods, Optical Coherence Tomography (OCT) is presented as an established clinical method in ophthalmology (15). It is a technique of particular importance for providing *in vivo*, noninvasive real time diagnostics. The generated images are regarded as an optical biopsy due to its ability to expose micro structural details of living tissue, allowing the verification of structures which could often be assessed only by histopathology, without excision and processing of the samples and without producing known harmful effects, as recently reviewed by Swanson et al (16).

Abignano et al (17) were the first to apply OCT to SSc and demonstrated that this imaging technique can visualize the skin subsurface with high spatial definition, proposing it as a potential sensitive image biomarker to evaluate and quantify skin fibrosis in SSc. This method was subsequently reproduced by our group, also in arm and hand skin tissue, reinforcing the role of OCT in the non-invasive evaluation of SSc patients (18). More recently, Abignano's group demonstrated the potential of OCT as biomarkers for nail disease in psoriasis and psoriatic arthritis (19), expanding the scope of OCT use in autoimmune diseases evaluation.

In this work, we explore for the first time the applicability of OCT in the oral cavity, namely the lower lip mucosa, as an alternative biomarker for diagnostic of patients with SSc, as a complementary method prior further patient examination. When compared to the evaluation in the arm and forearm skin regions, the labial mucosa presented improved sensitivity to the OCT measurement.

PATIENTS AND METHODS

Study design and population

The study was carried out in accordance to the Declaration of Helsinki, and approved by the Ethics Committee of Universidade Federal of Pernambuco (protocol number 54101316.1.0000.5208). Written informed consent was obtained from each patient and health control before participation in the study. All patients were properly informed of the nature, benefits and possible risks of the study.

An observational clinical study was developed and carried out at the Rheumatology Department of Hospital das Clínicas, Universidade Federal of Pernambuco, Brazil, where the collection of rheumatologic clinical data and imaging procedure was performed.

Thirty-three Brazilian patients with SSc were recruited. All patients were ≥ 18 years of age and fulfilled criteria for SSc proposed by the American College of Rheumatology (ACR) (20) or criteria of the American College of Rheumatology/European League Against Rheumatism (ACR/EULAR, 2013) (21) and were classified into limited cutaneous SSc (lcSSc; n=18) or diffuse cutaneous SSc (dcSSc; n=15) groups. Up to 03 years (diffuse) and 05 years (limited) of disease onset, it was considered at an early stage (20). Patients answered a clinical questionnaire from which demographic and clinical data were collected and additional information was obtained from hospital records and reviewed by experienced physicians (Table 1).

Table 1. Demographic and clinical characteristics of the systemic sclerosis patients (n=33).

Characteristics	
Age (years) - mean ± SD (range)	46.1 ± 11.4 (19-71)
Female gender n (%)	28 (84.8)
Disease duration (years) median (IQR)	08 (4-14.5)
Clinical subgroups N (%)	
Diffuse cutaneous	15 (45.5)
Early diffuse cutaneous	3/15 (20.0)
Limited cutaneous	18 (54.5)
Early limited cutaneous	5/18 (27.8)
Clinical manifestations N (%)	
Esophageal dysfunction	29 (87.9)
Raynaud phenomenon	26 (78.8)
Interstitial lung disease	18 (54.5)
Digital ulcer	16 (48.5)
Musculoskeletal involvement	9 (27.3)
Pulmonary arterial hypertension	4 (12.1)
Modified Rodnan skin score mean ± SD (range)	19.2 ± 13.2 (0-45)

IQR= interquartile range; SD= standard deviation

Thirty-five healthy control (HC) were also included as a comparison group. Individuals with disorders that compromise the understanding and adherence to the tests, patients with other known autoimmune rheumatic diseases and clinical evidence of any other type of injury in the area being studied were excluded of the study.

Clinical evaluation

All individuals selected for this study underwent a rheumatologic clinical assessment with a professional experienced in the diagnosis of SSc. Lung involvement was observed using high-resolution computed tomography (HRCT) and a pulmonary function test (PFT); esophagus involvement was determined by scintilography and/or

endoscopy; proximal muscle weakness and elevated serum creatine kinase indicated muscle involvement; and pulmonary hypertension was evaluated by Doppler echocardiogram (22). The modified Rodnan total skin score was used to evaluate skin fibrosis (23).

OCT evaluation

The images were acquired with a Swept Source-OCT (SS-OCT, Thorlabs Inc., New Jersey, USA), operating at 1325 nm central wavelength, spectral bandwidth of >100 nm and instantaneous bandwidth of 0.13 nm (0.5 GHz). Acquisition was performed with 512 pixels in the X-axis and Z-axis, using a 6 mm width window in the X axis and 3 mm depth in the Z axis. The axial scan rate is 16 kHz, average output power up to 10 mW, and 100 dB sensitivity. The system captures 25 frames per second, with axial resolution in air/water of 12/9 μm and lateral resolution of 25 μm. All images were stored in BITMAP format. For the measurements, the patients were placed in appropriate chair, with the head resting on a positioner (see fig. 1a), perpendicular to the laser guide light beam from the OCT head. Fig. 1(b) shows an expanded view of the OCT head and the black mark shows the inferior labial position of the beam.

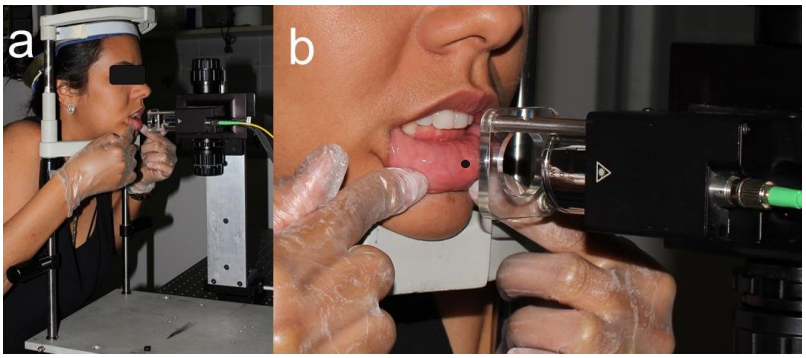

Fig. 1 – (a) Patient position in the adapted head resting positioner and (b) close-up showing the OCT head and the position where the beam is incident on the lower lip.

Data and statistical analysis

A quantitative analysis of the OCT images was obtained from a computational processing, through the calculation of the intensity attenuation as the light beam penetrates the mucosa, which leads to the tissue optical density (OD), represented by

a graph of the normalized intensity as a function of depth, using the MATLAB software (Mathworks Inc., Massachusetts, USA). The images were analyzed using ImageJ (Imaging Processing and Analysis in Java, National Institutes of Health, Bethesda, MD) for measuring the thickness of the epithelium (in µm).

Statistical Analysis

Aiming at statistical comparison of the optical density, the optical density at a depth of 300µm (OD300), to keep the same depth as in (17, 18), and the data were tabulated in Excel (Microsoft Office 2007). Numerical data were expressed as mean ± standard error (SE) if they were in normal distribution or median and interquartile range (IQR) if they were not in Gaussian distribution. The test of Shapiro/Wilks was applied to verify the normality of data set. In order to verify the degree of association between the considered variables, the Pearson correlation coefficient was applied. Later, a variance analysis (ANOVA) was carried out. In the event of significance by F test, then proceeded to the mean comparison tests using Tukey's test. p Value<0.05 was considered statically significant. Data were analyzed employing the SYSTAT 9.0 Version Demo.

RESULTS

Figure 2 (a and b) shows the images obtained by the OCT in the central region of the inferior labial mucosa, where a clear distinction between the two layers representing the epithelium (hypodense) and the lamina propria and submucosa (hyperdense) is observed. It was found a distinct template of epithelial thickness in the image obtained in healthy patients (fig 2a) with SSc patients (fig. 2b). It is also observed a difference in the total thickness of the layers of the mucosa, corresponding to the light penetration behavior, where in the healthy individuals it is deeper (Fig. 2a) compared to the unhealthy (fig. 2b). In the OD graphic, fig 2c, the normalized intensity attenuation curves clearly showed the difference between the HC with respect to those with SSc. When this characteristic curve is compared to the similar ones in (17, 18) for arm/forearm skin, it is clear that the labial mucosa presents a more pronounced difference between healthy and unhealthy patients.

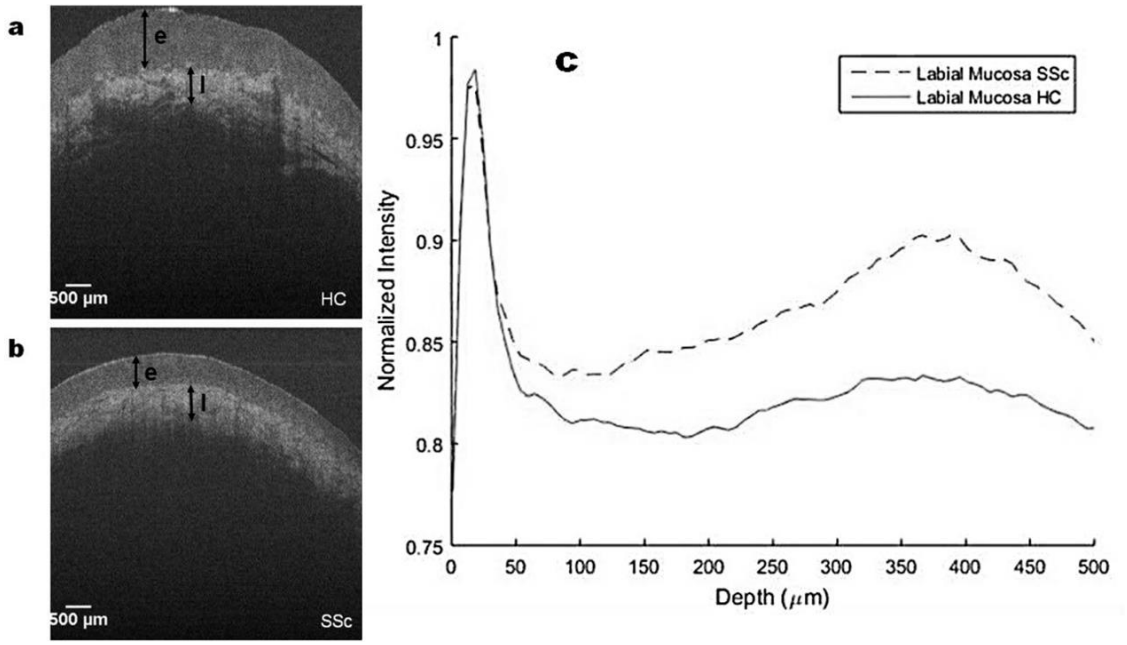

Fig. 2 - a) illustrative image of the healthy control (HC); b) illustrative image of the patient with systemic sclerosis (SSc); c) graphical representation of the optical density mean in HC e SSc. The arrows indicate the thickness of the epithelial layer of the oral mucosa (e) and lamina propria (l).

In the quantitative analysis, the differences between healthy and scleroderma labial mucosa were significant. It was observed that the optical density at 300 µm depth (OD300) was higher in patients with SSc when compared to the control group (0.87 and 0.82, respectively; p=0.016) as shown graphically in fig 3(a) suggesting a marked density of the region analyzed in the SSc group. The thickness of the labial mucosa epithelium was lower in SSc patients compared to HC (290.90µm and 442.63µm, respectively, p<0.0001), figure 3(b).

The analysis of the labial mucosa thickness did not allow differentiating between dcSSc (261.7 µm) and lcSSc (283.2 µm) subsets (p=0.83). Also, there was no difference between early and established forms, both in patients with dcSSc (330 µm and 285 µm, respectively, p=0.4) and lcSSc (291µm and 286 µm, respectively, p=0.9).

Comparisons were also made between mucosa thickness and other clinical parameters such as disease time (p=0.85), modified Rodnan score (p=0.51), Raynaud's phenomenon (p=0.86), presence of digital ulcers (p=0.21), interstitial lung disease (p=0.44), pulmonary arterial hypertension (p=0.90), esophageal dysfunction (p=0.54) and musculoskeletal involvement (p=0.31), where none of them presented significant statistical difference, as seen by the indicated p-values.

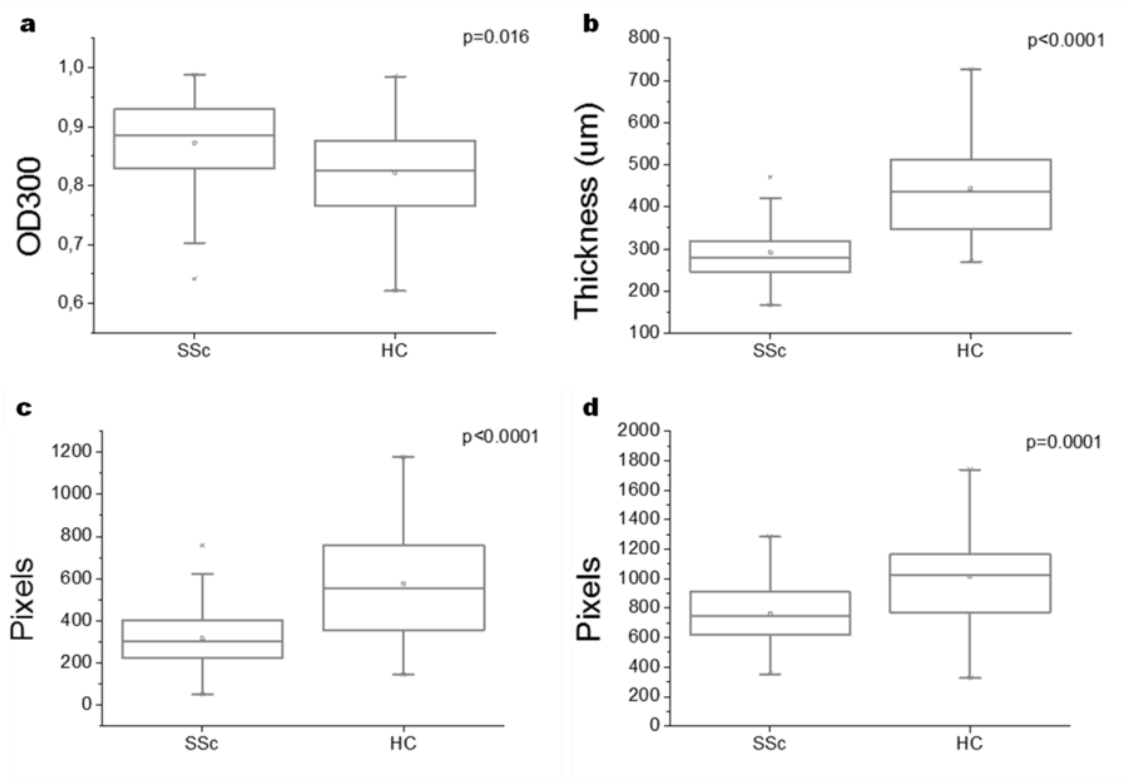

Figure 3. Graphical representation of the average of analyzes made in labial mucosa: a) optical density in 300 µm depth (OD300); b) linear thickness of the epithelium in µm.

DISCUSSION

Labial mucosa evaluation with OCT in SSc patients, discussed here for the first time in the literature as a potential biomarker, showed a distinct pattern with respect to the controls. The OCT is a technological tool that produces images of the skin and mucosa like those obtained by a cross-section of tissue surgical biopsy, with a resolution approaching light microscopy (17, 24-26). It has the potential to serve as a quantitative and non-invasive method to detect changes in the collagen levels of the skin, an important feature in patients with sclerosis systemic and it could help to early diagnosis and track responses for treatment (27). In recent studies using OCT in soft tissues in the oral cavity, we have shown the OCT's ability to follow up clinical treatment of patients with periodontal diseases (28, 29), demonstrating its clinical potential. Systemic sclerosis presents a wide range of oral manifestations. The most frequent problems include dental, periodontal and orofacial (decreased oral opening, decreased saliva production and bone resorption of the mandible) abnormalities (8). Previous

studies showed the importance of OCT in lower labial mucosa assessment (30, 31), but other aspects of mucosal characteristics have not yet been adequately evaluated. Our results for SSc patients demonstrated that the thickness of the layers of the lower lip mucosa is thinner than in the healthy individuals, and we have quantified this parameter. Even in the early stage, patients already present changes in the thickening of the epithelium similar with the established phases.

Further quantitative evaluation was performed for the average attenuation of the intensity decay of the light propagating and being scattered in the tissue, and its values compared at 300μm depth (OD300). There were significant statistical differences between patients with systemic sclerosis (SSc) and healthy control (HC).

As identified drawbacks of the procedure, the analysis of the labial mucosa through OCT did not allow us to differentiate diffuse and limited cutaneous clinical forms. Although there were differences between SSc patients and healthy controls, the findings were similar in patients with early and established disease, both in the limited and diffuse forms. These findings suggest that, even in the early stage, patients already present alterations in the thickening epithelium, similar with the established disease, indicating the labial mucosa as a site of initial impairment. Further studies are required to corroborate this assumption.

Further limitations in this study can also be overcome, such as the cross-sectional design of the study. A longitudinal study would be required to better characterize changes in labial mucosa of SSc patients in disease progression as well as possible response to treatment. Furthermore, the sample size should be increased to detect differences between diffuse and limited clinical forms and early and established disease.

In conclusion, we demonstrated significant differences in labial mucosa of SSc patients and healthy controls when evaluated by OCT. This reinforces the role of this noninvasive optical technique as a potential tool in the management of these patients. Further studies are needed to demonstrate the reliability of OCT as a universally accepted method for clinical evaluation of SSc, complementing existing methods. Recent technological developments have made OCT equipment’s cost more accessible, while it is also foreseen as a clear point-of-care solution. Multidisciplinary training of human resources in using OCT in different health care areas are also required.

REFERENCES

1. Gabrielli A, Avvedimento EV, Krieg T. Scleroderma. N Engl J Med 2009; 360(19): 1989-2003.

2. Jimenez SA, Derk CT. Following the molecular pathways toward an understanding of the pathogenesis of systemic sclerosis. Ann Intern Med 2004;140(1): 37-50.

3. O'Reilly S. Innate immunity in systemic sclerosis pathogenesis. Clin Sci (Lond) 2014; 126(5): 329-37.

4. Fischer DJ, Patton LL. Scleroderma: oral manifestations and treatment challenges. Spec Care Dentist 2000; 20(6): 240-4.

5. Albilia JB, Lam DK, Blanas N, Clokie CM, Sandor GK. Small mouths ... Big problems? A review of scleroderma and its oral health implications. J Can Dent Assoc 2007; 73(9): 831-6.

6. Nagy G, Kovacs J, Zeher M, Czirjak L. Analysis of the oral manifestations of systemic sclerosis. Oral Surg Oral Med Oral Pathol 1994; 77(2): 141-6.

7. Vincent C, Agard C, Barbarot S, N'Guyen J M, Planchon B, Durant C, et al. [Orofacial manifestations of systemic sclerosis: A study of 30 consecutive patients]. Rev Stomatol Chir Maxillofac 2010; 111(3): 128-34.

8. Baron M, Hudson M, Tatibouet S, Steele R, Lo E, Gravel S, et al. The Canadian systemic sclerosis oral health study: orofacial manifestations and oral health-related quality of life in systemic sclerosis compared with the general population. Rheumatology (Oxford) 2014; 53(8): 1386-94.

9. Leung WK, Chu CH, Mok MY, Yeung KW, Ng SK. Periodontal status of adults with systemic sclerosis: case-control study. J Periodontol 2011; 82(8): 1140-5.

10. Co HT, Block JA, Sequeira W. Scleroderma lung: pathogenesis, evaluation, and current therapy. Am J Ther 2000; 7(5): 321-4.

11. Tolle SL. Scleroderma: considerations for dental hygienists. Int J Dent Hyg 2008; 6(2): 77-83.

12. Kowal-Bielecka O. Targeting vascular disease in systemic sclerosis. Endocr Metab Immune Disord Drug Targets 2006; 6(4): 401-7.

13. Shelton RL, Jung W, Sayegh SI, McCormick DT, Kim J, Boppart SA. Optical coherence tomography for advanced screening in the primary care office. J Biophotonics 2014; 7(7): 525-33.

14. Boppart SA, Richards-Kortum R. Point-of-care and point-of-procedure optical imaging technologies for primary care and global health. Sci Transl Med 2014; 6(253): 253rv2.

15. Costa RA, Skaf M, Melo LA, Jr., Calucci D, Cardillo JA, Castro JC, et al. Retinal assessment using optical coherence tomography. Prog Retin Eye Res 2006; 25(3): 325-53.

16. Swanson EA, Fujimoto JG. The ecosystem that powered the translation of OCT from fundamental research to clinical and commercial impact [Invited]. Biomed Opt Express 2017; 8(3): 1638-64.

17. Abignano G, Aydin SZ, Castillo-Gallego C, Liakouli V, Woods D, Meekings A, et al. Virtual skin biopsy by optical coherence tomography: the first quantitative imaging biomarker for scleroderma. Ann Rheum Dis 2013; 72(11): 1845-51.

18. Pires NS, Dantas AT, Duarte AL, Amaral MM, Fernandes LO, Dias TJ, et al. Optical coherence tomography as a method for quantitative skin evaluation in systemic sclerosis. Ann Rheum Dis 2018; 77(3): 465-66.

19. Abignano G, Laws P, Del Galdo F, Marzo-Ortega H, McGonagle D. Three-dimensional nail imaging by optical coherence tomography: a novel biomarker of response to therapy for nail disease in psoriasis and psoriatic arthritis. Clin Exp Dermatol 2018 Sep 23. doi: 10.1111/ced.13786. [Epub ahead of print]

20. Preliminary criteria for the classification of systemic sclerosis (scleroderma). Subcommittee for scleroderma criteria of the American Rheumatism Association Diagnostic and Therapeutic Criteria Committee. Arthritis Rheum 1980; 23(5): 581-90.

21. van den Hoogen F, Khanna D, Fransen J, Johnson SR, Baron M, Tyndall A, et al. 2013 classification criteria for systemic sclerosis: an American College of Rheumatology/European League against Rheumatism collaborative initiative. Arthritis Rheum 2013; 65(11): 2737-47.

22. Dantas AT, Goncalves SM, Pereira MC, Goncalves RS, Marques CD, Rego MJ, et al. Increased IL-35 serum levels in systemic sclerosis and association with pulmonary interstitial involvement. Clin Rheumatol 2015; 34(9): 1621-5.

23. Clements P, Lachenbruch P, Siebold J, White B, Weiner S, Martin R, et al. Inter and intraobserver variability of total skin thickness score (modified Rodnan TSS) in systemic sclerosis. J Rheumatol 1995; 22(7): 1281-5.

24. Gladkova ND, Petrova GA, Nikulin NK, Radenska-Lopovok SG, Snopova LB, Chumakov YP, et al. In vivo optical coherence tomography imaging of human skin: norm and pathology. Skin Res Technol 2000; 6(1): 6-16.

25. Lee CK, Tsai MT, Lee HC, Chen HM, Chiang CP, Wang YM, et al. Diagnosis of oral submucous fibrosis with optical coherence tomography. J Biomed Opt 2009; 14(5): 054008.

26. Adegun OK, Tomlins PH, Hagi-Pavli E, McKenzie G, Piper K, Bader DL, et al. Quantitative analysis of optical coherence tomography and histopathology images of normal and dysplastic oral mucosal tissues. Lasers Med Sci 2012; 27(4): 795-804.

27. Babalola O, Mamalis A, Lev-Tov H, Jagdeo J. Optical coherence tomography (OCT) of collagen in normal skin and skin fibrosis. Arch Dermatol Res 2014; 306(1):1-9.

28. Fernandes LO, Mota CCBO, de Melo LSA, da Costa Soares MUS, da Silva Feitosa D, Gomes ASL. In vivo assessment of periodontal structures and measurement of gingival sulcus with Optical Coherence Tomography: a pilot study. J Biophotonics 2017; 10(6-7): 862-9.

29. Fernandes LO, Mota CCBO, Oliveira HO, Neves JK, Santiago LM, Gomes ASL. Optical coherence tomography follow-up of patients treated from periodontal disease. J Biophotonics 2018: e201800209.

30. Hamdoon Z, Jerjes W, Al-Delayme R, McKenzie G, Jay A, Hopper C. Structural validation of oral mucosal tissue using optical coherence tomography. Head Neck Oncol 2012; 4:29.

31. Garcia-Hernandez A, Roldan-Marin R, Iglesias-Garcia P, Malvehy J. In Vivo Noninvasive Imaging of Healthy Lower Lip Mucosa: A Correlation Study between High-Definition Optical Coherence Tomography, Reflectance Confocal Microscopy, and Histology. Dermatol Res Pract 2013; 2013: 205256.

ANEXO A – AVALIAÇÃO COMPARATIVE DA PROFUNDIDADE DE SONDAGEM POR TOMOGRAFIA POR COERÊNCIA ÓPTICA E SONDAS PERIODONTAIS

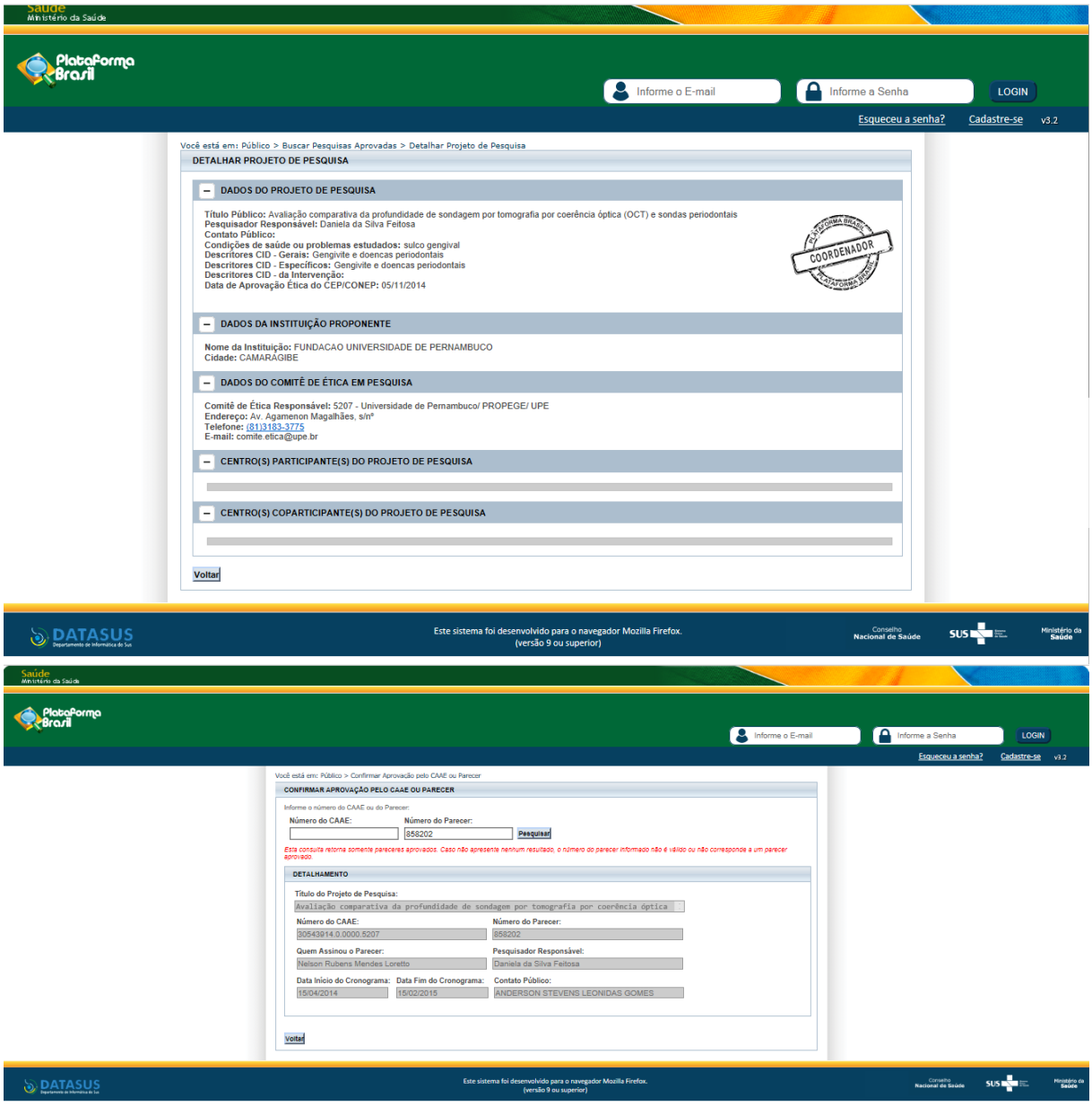

ANEXO B– ANÁLISE COMPARATIVA DA PROFUNDIDADE DE BOLSA PERIODONTAL ATRAVÉS DE TOMOGRAFIA POR COERÊNCIA ÓPTICA, DA SONDA COMPUTADORIZADA FLORIDA PROBE E DA SONDA CAROLINA DO NORTE

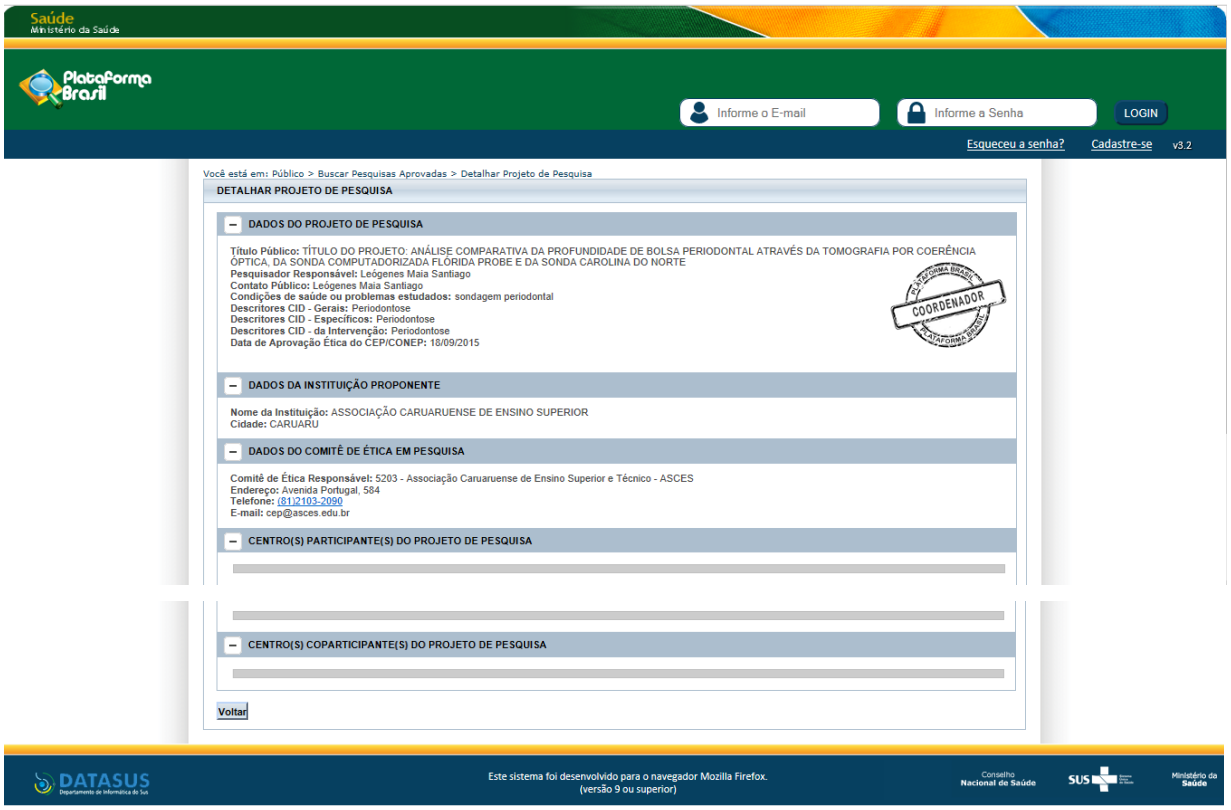

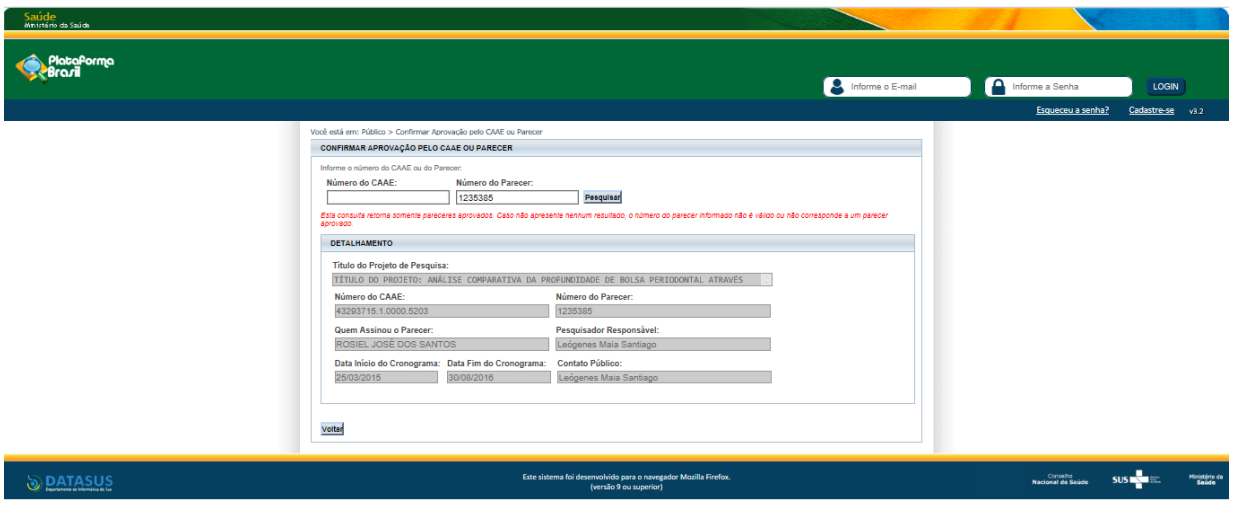

ANEXO C– AVALIAÇÃO DA QUALIDADE DA CIMENTAÇÃO ADESIVA DE MICROLAMINADOS CERÂMICOS